REPUBLIC OF IRAQ
MINISTRY OF HIGHER EDUCATION

AND SCIENTIFIC RESEARCH

AL-FURAT AL-AWSAT TECHNICAL UNIVERSITY

ENGINEERING TECHNICAL COLLEGE- NAJAF

Exergy and Performance Analysis of Combined Double Pass PV/T with PCM, Nano-Fluid and Porous Media

Zainab Mohammad Mahdi

M.TECH.
IN MECHANICAL ENGINEERING TECHNIQUES OF POWER

2022

EXERGY AND PERFORMANCE ANALYSIS OF COMBINED DOUBLE PASS PV/T WITH PCM, NANO-FLUID AND POROUS MEDIA

A THESIS

SUBMITTED TO THE DEPARTMENT OF MECHANICAL ENGINEERING TECHNIQUES OF POWER

AS PARTIAL FULFILLMENT OF THE REQUIREMENTS FOR MASTER OF THERMAL TECHNOLOGIES DEGREE IN MECHANICAL ENGINEERING TECHNIQUES OF POWER (M. TECH.)

BY
Zainab Mohammad Mahdi

(B.Tch. Automobile.Eng.)
2016

Supervised by:

Asst. Prof

Dr. Ali Najah Al-Shamani

2022

بسم الله الرحمن الرحيم

قالوا سبحانك لا علم لنا الا ما علمتنا انك انت
العليم الحكيم

صدق الله العلي العظيم

سورة البقرة **(32)**

DECLARATION

I assure that the work exhibited in this manuscript is my special work and has not been exhibited to other institution or to get another degree.

Signature:

Name: Zainab Mohammad Mahdi

Date: / / 2022

ACKNOWLEDGMENTS

First of all, I thank God for His support, help and guidance for me to prepare this work.

I would like to express my thanks and gratitude to my supervisor Asst. Prof. **Dr. Ali Najah Al-Shamani** and my adviser **Prof. Dr. K. Sopian** for his support and guidance to complete this study.

My gratitude and sincere thanks to the Dean of Technical Engineering College – Najaf **Asst. Prof. Dr. Hassanain Ghani Hameed** and affiliates for their support and assistance during my preparation for this thesis.

My gratitude and sincere thanks to the head of the Department of Power Mechanics Techniques **Prof. Dr. Dhafer Manea Hicham** and affiliates for their support and assistance during my preparation for this thesis.

Thanks are due to: those who were and still holding our hands; those of whom we did not feel suspicious even once, who were safety and refuge if even our souls were narrowed; those who did not leave us in the time of our sorrows even after our desires; those who supported us until we crossed towards our happiness…, I am grateful to you: My Father, My Mother, My Brother, My Sisters.

Zainab Mohammad Mahdi

SUPERVISOR CERTIFICATION

I certify that this thesis which is titled "**Exergy and Performance Analysis of Combined Double Pass PV/T with PCM, Nano-Fluid and Porous Media**", which is presented by

Zainab Mohammad Mahdi, has been prepared under my supervision at the mechanic Techniques Engineering of Power Department, Engineering Technical College - Najaf, AL-Furat Al-Awsat Technical University, as partial fulfillment of the requirements for the Master degree of Technical Thermal Engineering.

Signature:
Name: **Asst. Prof. Dr. Ali Najah Al-Shamani**
(Supervisor)
Date: / /2022

In view of the available recommendation, we forward this thesis for debate by the examining committee.

Signature:
Name: **Prof. Dr. Dhafer Manea Hachim**
Head of Dept. Mechanical Eng. Tech. of Power
Date: / / 2022

Committee Report

We certify that we have read this thesis titled "**Exergy and Performance Analysis of Combined Double Pass PV/T with PCM, Nano-Fluid and Porous Media**" which is being submitted by **Zainab Mohammad Mahdi** and as Examining Committee, examined the student in it is contents. In our opinion, the thesis is adequate for an award of degree of Master of Technical in Thermal Engineering.

Signature:

Name: **Asst. Prof. Dr. Ali Najah Al-Shamani**

(Supervisor)

Date / / 2022

Signature:

Name: **Asst. Prof. Dr. Ameer Abed Jaddoa**

(Member)

Date / / 2022

Signature:

Name: **Lecture. Dr. Salah M. Salih**

(Member)

Date / / 2022

Signature:

Name: **Prof. Dr. Dhafer Manea Hachim**

(Chairman)

Date / / 2022

Approval of the Engineering Technical College – Najaf.

Signature:

Name: **Asst. Prof. Dr. Hassanain Ghani Hameed**

Dean of Technical Engineering College - Najaf

Date: / / 2022

LINGUISTIC CERTIFICATION

This is to certify that this thesis entitled "**Exergy and Performance Analysis of Combined Double Pass PV/T with PCM, Nano-Fluid**

and Porous Media" was reviewed linguistically. Its language was amended to meet the style of the English language.

Signature :

Name : Asst. Prof. Raed Dakhil Kareem

Date:

ABSTRACT

The PV/T combine system produces simultaneously the electrical and thermal energy as a form of hot air and water. This study aims to combine solar PV panels with two types of thermal

solar collectors for air and water which work to increase extracted heat and reduce the temperature of the solar PV panel, in addition to many extras such as PCM, pours media. Nano-fluid was used with 1% concentrations of MWCNT- nanoparticles. Experimental work have been built and inaugurated in the Technical Collage of Najaf, Al-Furat Al-Awsat Technical University, Iraq. Geographically, an investigation on PV/T combine system has been carried out under the weather conditions at Najaf (32° N / 44° E) for selected day of June and July from 7am to 8pm ,the readings were taken and recorded every 15 minutes. A comparison was made for PV/T combine system under two mode of fluids flow air plus water and air plus MWCNT-nanofluid with conventional PV without any cooling system under different mass flow rate for air varies from 0.02 kg/s to 0.05 kg/s and from 0.01kg/s to 0.08 kg/s for both water and MWCNT-nanofluid. The copper pipes with three different inner diameters was tested (8mm, 10mm, 12mm) with different number of pipes arrangement at the bottom of the PV solar panel started from 8 to16 to get the best design for the PV/T water collector. To fulfill numerical computations, a Comsol Multiphysics program has been employed as a computational fluid dynamics (CFD). The numerical study was carried out to determine the optimal design from each configuration. The experimental setup of the system was constructed, using the optimal of copper pipes diameter and number for each configuration and were evaluated using the numerical results. Paraffin wax was used as a PCM, which dictates the content surrounding the copper tubes. A double pass single duct air thermal collector type was used, it was filled with porous media (steel wool) at the back duct of air thermal collector. The practical tests showed that the PV/T combine system with MWCNT-nanofluid and air as

cooling fluid has a higher improvement in electrical efficiency than PV/T combine system with water and air in comparison with traditional PV panel. The amount of improvement in electrical efficiency was 21.667% for PV/T combine with air and water as a cooling fluid when the base temperature (T_b) was lowered from 89.3℃ to 53.5℃ electrical efficiency increased from 10.747% to 13.076%. The rate of improvement in electrical efficiency was 23.529% when the T_b was lowered from 87℃ to 49.3℃ and electrical efficiency increased from 10.815% to 13.359% for PV/T with air and MWCNT-nanofluid as a cooling fluid. Also, the practical tests showed the improvement in the thermal performance of the PV/T combine system with MWCNT-nanofluid and air compared to the thermal performance of the PV/T combine with water and air. Each of the heat power generated, total thermal efficiency ,overall efficiency and exergy efficiency reached to 302.728W, 56.579%, 92.883%, 14.685% respectively for PV/T combine system with MWCNT-nanofluid and air compare with 235.403W, 49.475% 82.966%, 14.492% respectively for PV/T combine system with water and air. Due to the presence of phase changing materials the difference in temperature continued for an hour after sunset for both the air and the outside water.

TABLE OF CONTENTS

LIST OF FIGURE

LIST OF TABLES

NOMENCLATURE

Symbol	Definition	Unit
A	Area	m^2
D	Diameter	m
T	Temperature	℃
I	Current	**A**
R	Resistance	**Ω**
G	Solar radiation	W/m^2
$\dot{E}$	Energy rate	W
$\dot{m}$	Mass flow rate	Kg/s
C_P	Specific heat at constant pressure	J/kg.℃
$\dot{E}x$	Exergy rate	W
FF	Fill factor of the PV module	-
PF	Packing factor of the PV module	-
N_c	Number of the cells	-
Q_u	Rate of the thermal power of the PV/T system	W
V	voltage of PV module	V
S	Absorbed solar energy	W/m^2
U_L	Overall heat loss coefficient	$W/m^2\ ^oC$
F_R	Flow rate factor	-
m	Mass	Kg
k	Thermal conductivity	W/m. K

GREEK SYMBOLS

Symbol	Definition	Unit
α	Transmittance of glass	
τ_{pv}	Transmittance of Photovoltaic PV	
η	efficiency	%
β_R	The temperature coefficient of the cell efficiency (usually 0.004-0.005)	1/ °C
Φ	volume fraction	%
ρ	Density	Kg/m^3
μ	Dynamic viscosity	Pa.s

SUBSCRIP

Symbol	Title
sc	Short circuit
mp	maximum power
Voc	Open Circuit Voltage
in	inlet
out	outlet
loss	losses
elc	Electrical
th	Thermal
OV	Overall
a	Air
w	Water
c	cell
m	module
b	Base
S	Surface
ref	Reference at STC
np	nanoparticles
nf	nanofluid
bf	base fluid

CHAPTER ONE

INTRODUCTION

1.1 RESEARCH BACKGROUND

Any country's economy and prosperity progress are heavily reliant on energy. Fossil fuels provide a large portion of the world's energy [1]. The world continues to use fossil fuels to generate energy and increase energy consumption with increased demand, and the growing concern about environmental issues. It becomes necessary to find alternative sources for generating electrical energy from renewable energy sources [2]. Solar power is an important factor in clean energy and it is a promising solution to energy consumption problems. There are three main applications for solar power, photovoltaic (PV) Panel application, solar thermal collector application and photovoltaic-thermal (PV/T) system application [3], as illustrated in Figure 1-1 .

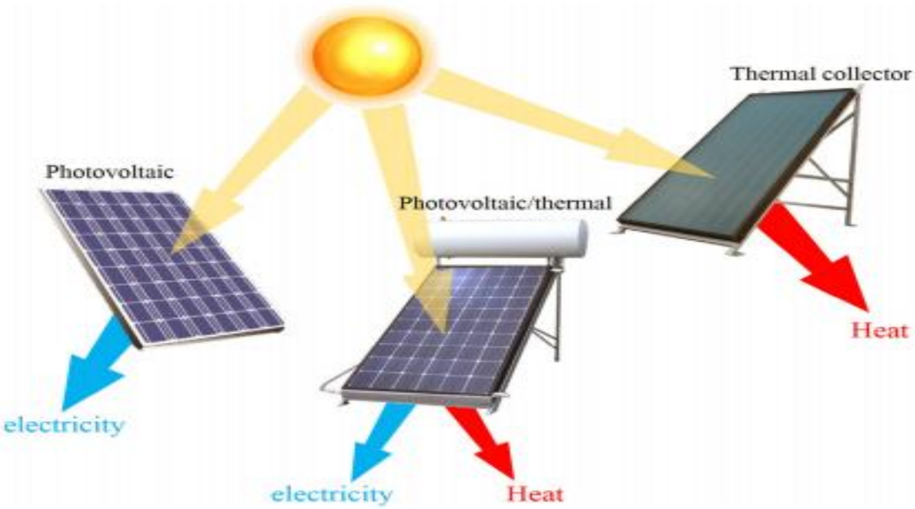

Figure1 -1 solar power applications [3]

Photovoltaic PV panels transfer sunlight to electricity, solar thermal collectors generate heat from sun power and PV/T systems able to production electricity and heat from sunlight by integrating the thermal collector and photovoltaic application.

PV/T systems can be classified into various division attributed: structure or thermal transfer medium. Depending on the structural PV/T systems, they can be classified into: flat plate, concentrating, and building, combined modules, and into: air-based, water- based, heat pipe-based, phase change material (PCM)-based and thermoelectric-based systems according to thermal extraction medium [3], as shown in 1-2.

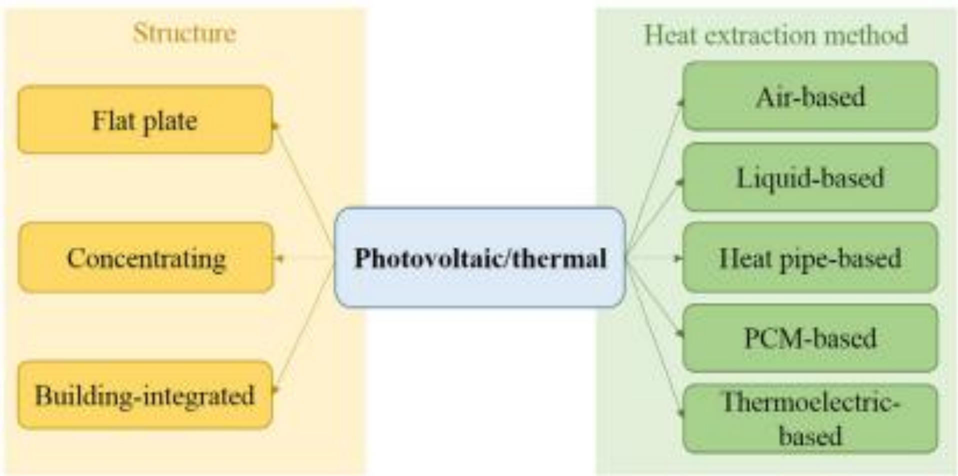

Figure1- 2 Classification of PV/T systems [3]

About 20% of the solar radiation falling on the photovoltaic PV panels is converted into electrical energy, while the remaining part is converted into heat. The temperature of the photovoltaic PV panel rises as a result of the heat created by the module, resulting in a considerable reduction in electrical efficiency. In addition to lowering module electrical efficiency, higher generated temperatures in PV modules can harm the module's structures, resulting in thermal damage stresses [4]. As a result, PV panel cooling is required. This may be accomplished by integrating thermal collectors with photovoltaic PV panel in the same unit which is able to cool down it by extracting their heat [5]. This combining of the photovoltaic PV panel and thermal collectors has the ability to produce both thermal and electrical efficiency from the same unit. This is the most efficient way of using solar energy [6].

1.2 Photovoltaic (PV) Panels

Photovoltaic (PV) panels are parts of a solid nature configured from semi-conductor materials and have ability to transfer solar power, directly to electricity.

They work without sound and without harmful emissions [7]. The electric potential difference is generated as soon as the solar radiation falls on the surface of the PV panels and the electrons move as a result of their absorption of the photon energy as shown in Figure1-3.

PV panels are able to convert (13 - 20) % from solar radiation to electrical output, while the remaining part of the incident radiation is converted into heat leading to an increase in cell temperature. The electrical productivity of the cells decreases when the temperature becomes higher than 25℃ to 27℃. It is estimated that the electrical productivity decreases by (0.4 - 0.65) % when the PV panels temperature increases by 1℃. Continuous rise in temperature affects the internal structure of photoelectric PV panels and increases thermal degradation [7].

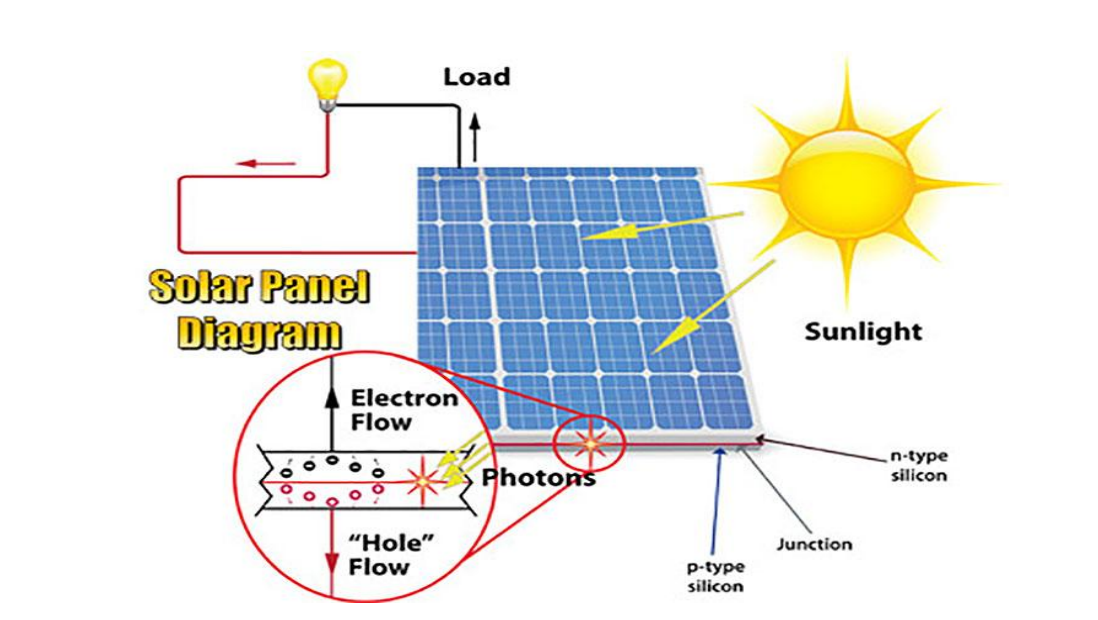

Figure1- 3 Photovoltaic PV panel application [7]

1.3 Photovoltaic Thermal (PV/T) System

The process of combining the solar photovoltaic PV applications with the solar thermal applications in the same module is known as the photovoltaic thermal (PV/T) hybrid system. This combination produces not only electricity but is also capable of producing thermal energy, it reduces manufacturing cost, and it occupies a little space, lowers the temperature of the PV. This contributes to rise its efficiency [8]. PV/T can be categorized into air-based PV/T system, water-based PV/T system and combine (air-water) PV/T system [9], as shown in Figure1-4.

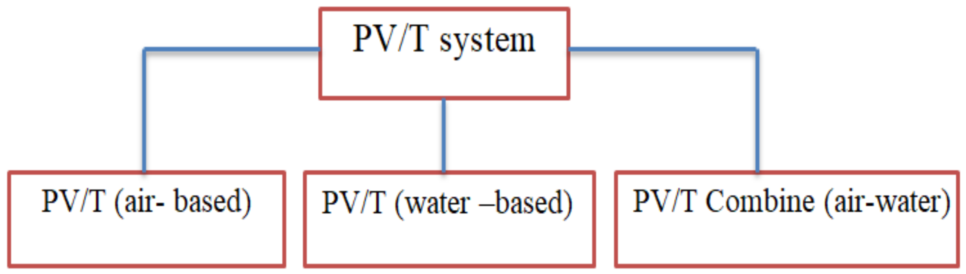

Figure1-4 Categorized of the PV/T system[12]

1.3.1 Air-based PV/T System

It is the result of uniting solar air thermal collector system with PV panel, defined as PV/T air based system. Air acts as a heat transfer medium that absorbs heat from the bottom surface of the PV panels. This contributes to lowering its temperature and raising the electrical energy produced. The useful heat energy is released as hot air that can be used in other thermal applications such as drying purposes as drying grains and heating. For this system, both the thermal and electrical efficiency can be improved by adding modifications to the air duct such as adding porous media and thin sheets from metallic[10].

1.3.2 Water-based (PV/T) System

It is the result of uniting of solar water thermal system with PV panel in the same unite, defined as photovoltaic thermal PV/T water-based system. Compared to PV/T with air employed systems, the PV/T with water employed systems have the ability to extract high thermal attributed to its high conductivity of water. Passing water under the solar panel works to draw heat from and contributes to lowering its temperature, leading to increase in the electrical efficiency. The heat extracted from the bottom surface of the PV panel comes out in the form of hot water that can be used in various thermal applications such as household uses. It is possible to combine PV/T, water with the solar distiller to obtain safe drinking water in addition to thermal and electrical benefits [10].

1.3.3 PV/T Combine System

It is combination of a dual-fluid heat exchanger with a photovoltaic panel, defined as PV/T combine system. Air and water both are employed as heat exchange fluid. This system is not only able to generate electricity but it also can simultaneously produce hot air and hot water by having two types of thermal collector mode in one system. The temperature of PV panel will be decreased and cell efficiency would be of higher enhancement. Depending on the energy needs and applications, the employing of both fluids also generates a higher range of thermal applications. The improvement system by integrating both type of heat transport mode is to be desirable, for the best performance of PV/T technology and for getting higher efficiencies. The integration of two systems is to cover the determinants and weaknesses of separate PV/T water and air thermal collector systems. In terms of cost, the integration as one unit system displays reduction structure cost and shows less payback time period[11].

1.3.4 Phase-Changing Materials Based PV/T System

The temperature of the bottom surface of the photovoltaic PV panels reaches from 20℃ to 70℃. The addition of PCM as energy storage materials, that draw a larger amount of heat during the phase shift, contributes to lowering the temperature, increasing the efficiency of the PV panels, reducing the heat loss to the external environment and working to increase the processing time with thermal energy to the thermal transfer fluid when the sun is setting or not available. PCMs are classified into organic fatty acids, inorganic salt hydrates and eutectics [12].

1.4 Aims of Research

The aims of this study is to enhance the performance of photovoltaic PV panels and increase its productivity of electrical energy by integrating it with two types of thermal collectors (water and air) with mult-additives such as PCM, porous medium and nanofluids. All of these together work to extract the largest amount of heat, which leads to a reduction in the temperature of the PV panel. It is also possible to benefit from the heat energy extracted in the form of hot water and air in thermal applications, such as using hot water for domestic purposes and hot air for drying purposes.

1.5 Objectives of Research

The objectives of this work are:

1- To develop numerical models of the photovoltaic thermal water collectors (PV/T) with various absorber configuration (pipes diameter and number of pipes)

2- To design and assemble the PV/T combine system, with PCM, porous media and nanofluids.

3- To investigate the using MWCNT-nanofluid instead of water with air as cooling fluid on the electrical and thermal performance of the system.

4- To analysis the Exergy and performance for both PV/T combine system with air and water as cooling fluid and PV/T combine system with air and MWCNT-nanofluid

1.6 THESIS OUTLINE

This thesis is outlined in the following order:

Chapter One introduces the study (brief discussion of the importance, potential of solar energy and some solar technologies), aims and objectives.

Chapter Two discusses the background of the stages of development of photo voltage thermal PV/T solar collector system, PV/T air-based system, PV/T water-based system, PV/T-PCM based system and PV/T combine with (air and water) system, and the effect of additives on improving the performance of the system such as phase-changing materials, porous media and nano-fluids.

Chapter Three details the numerical analysis. It mainly concentrates on numerical PV/T water model; CFD analysis, modelling process, energy balance analysis of PV/T collector, physical model, and boundary conditions, exergy and entropy analysis for PV/T combine system and governing equation

Chapter Four will provide an overview experimental setup, the measurements, and data acquisition system and error analysis. Measurements of the thermo-physical properties of the nano-fluids will be provided as well.

Chapter Five presents the research questions, and revisits the aim and objectives of the study, followed by conclusion for the work, suggestions and recommendations for future work which are in Chapter six.

CHAPTER TWO

LITERATURE REVIEW

2.1 INTRODUCTION

The operating temperatures of PV cell raise the conversion efficiency from solar energy to electricity reduced ,combining a solar thermal collectors with PV panels in the same unit known as photovoltaic thermal PV/T system this addition process can reduce the operating temperature and improve the system efficiency.

2.2 PV/T WITH Air-Based System

PV/T air-based systems have a pass of air up or down for exchanging the temperature of the PV panels by permitting convection natural or forced air. Circulation of air is able to exchange heat from the absorber plate of the integrated air pass to the beneath of the PV panels to lower the PV temperature and contribute to its cooling**.**

Srinivas and S. Jayaraj (2013**)**[13]**.** Experiments were carried out on a novel design of double pass hybrid PV/T solar air heater with slats (DPHSAH), where air enters from the top channel and exits from the bottom channel as shown in2-1. It has been discovered that using slats as an essential element of the absorber surface is critical for achieving higher efficiency. In this situation, the hybrid PV/T solar collector's thermal and electrical output improved significantly. The immediately overall exergy and overall energy efficiency of the (PV/T) hybrid with double pass air solar thermal system ranged from14-17% and 29 – 37% respectively

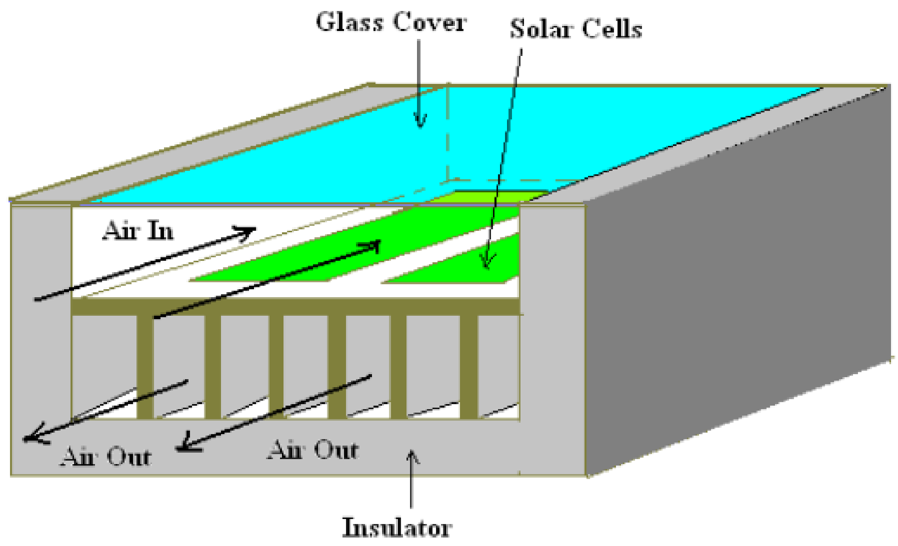

Figure 2-1 Double pass hybrid (PV/T) solar air heater with slats[14]

Mohd Yusof et al (2013**)**[14]**.** They made a comparison between three different designs of heat exchanger for photovoltaic-thermal (PV/T) air-base solar collector, V-groove, honeycomb and stainless steel wool. Heat exchangers were horizontally placed in the PV module's back side channel 2-2. The system was tested at mass flow rate ranging from 0.02 kg/s to 0.13 kg/s at 828 W/m^2 solar irradiance. The highest thermal efficiency of the system was discovered at a mass flow rate of 0.11 kg/s. where it reached to 87% with honeycomb, 86 %with stainless steel wool and 71% with V-groove. The system's electrical efficiency was 7.13%, 6.88% and 7.04% respectively. The results of the experiments revealed that the honeycomb design is the most effective heat exchanger design.

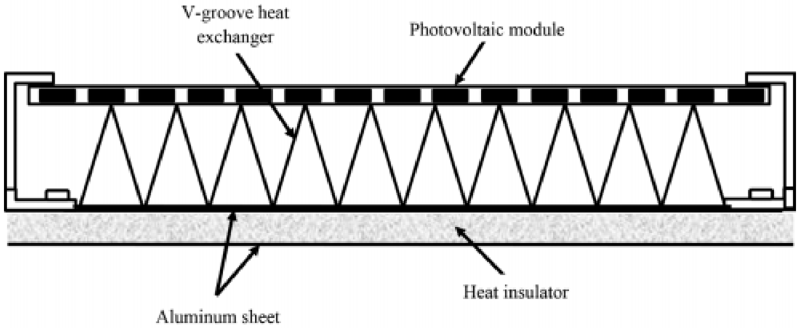

Case1

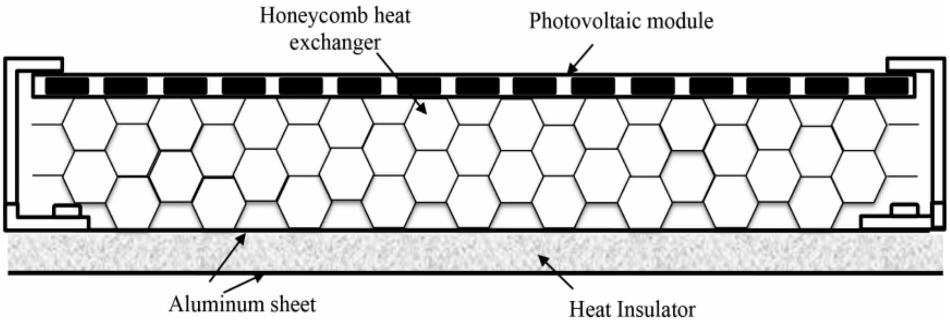

Case2

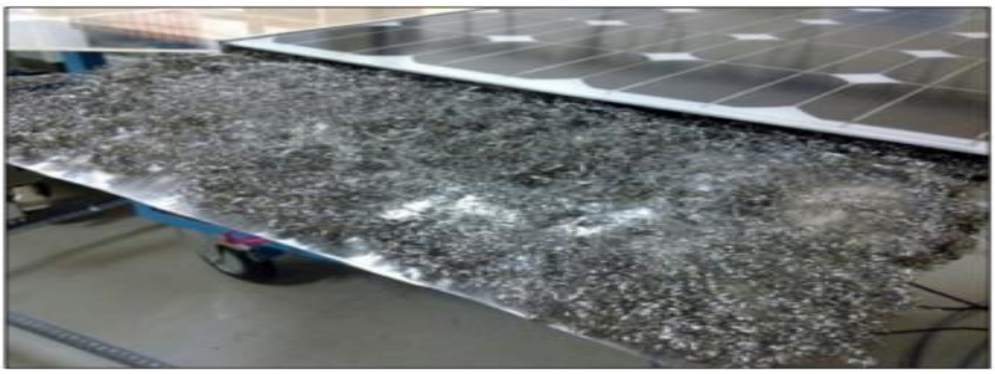

Case3

Figure 2-2 Three varies structure of the (PV/T) air system ,Case1 V-groove, Case2Honeycomb, Case3 Steel wool[15]

Karima and Mustafa (2014)[15]**.** It was a comparative study between three varies structure of hybrid photovoltaic thermal collectors case1 (single pass single duct), case 2 (double pass single duct) and case 3 (single pass double duct) to Iraq weather conditions, as shown in Figure 2-3. The mathematical model has been developed and solved by a Matlab computer program. The overall efficiency of module case 3 from the obtained results indicated larger than that of case 2 and case 1, and case 1 had the best electrical efficiency. The lower pressure reduction was achieved in case 3 as compared to case1 and case 2.

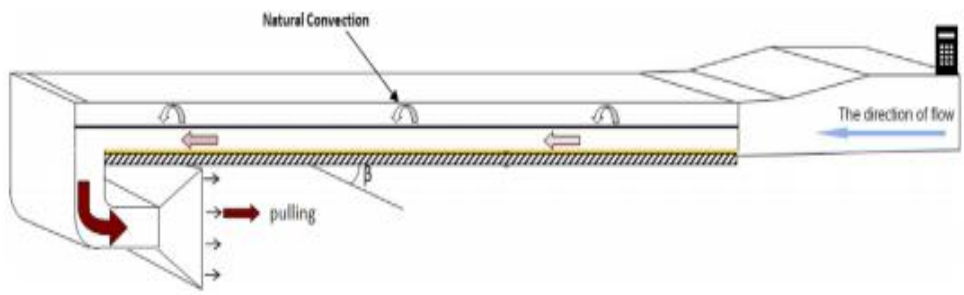

Case 1

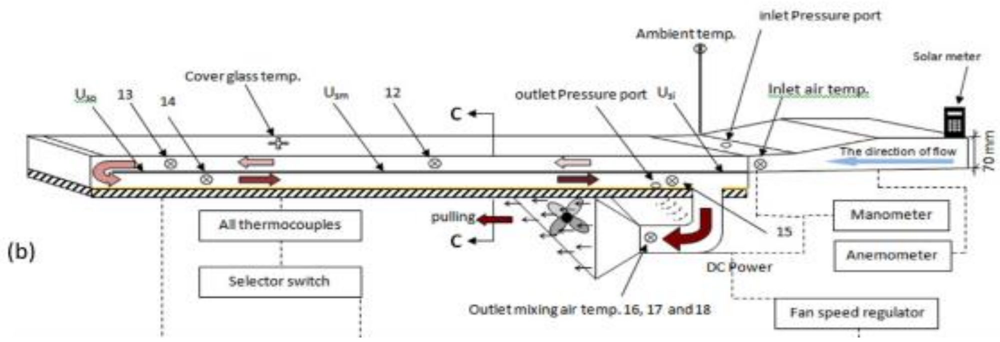

Case 2

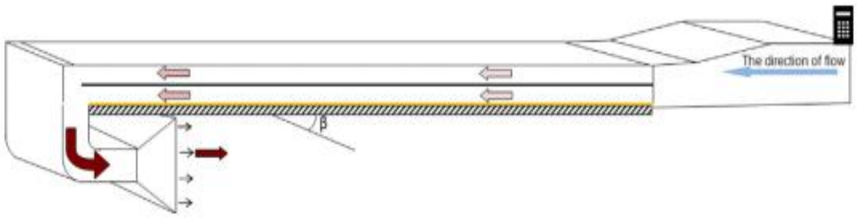

Case 3

Figure 2-3 Three various types for (PV/T) air system [16].

M.Omer and Zala (2017**)**[16]**.** The effect of using porous media was checked on the effectiveness of a hybrid PV/T with a double pass air collector. The hybrid solar air thermal collector has two air path upper and lower the PV panels, and the lower filed with porous media. The performance of the system was compared with another hybrid PV/T system without porous media and class cover. The results showed that the amount of increase in the compound efficiency was 3% for hybrid PV/T with porous media. The maximum value for the daily thermal efficiency was 80.23% for collector with porous media and glass cover, while the maximum amount of thermal efficiency was 51.25% without porous media and glass cover.

Ahmad Fudholi et al (2019**)** [17]**.** They experimentally and theoretically studied a PV/T system with air collector which had absorber plate with ∇-corrugated shape, as shown in Figure 2-4, to predict air outlet and photovoltaic (PV) temperatures performed of the PV/T air collector at steady-state energy analysis. Both the experimental and theoretical results are close to each other; 3.75% and 5.49% represented the percentage errors between the theoretical and experimental study for air outlet and PV temperatures, where 13.36% and 12.89% represented the exergy efficiency for the PV/T with a ∇-corrugated absorber plate air system.

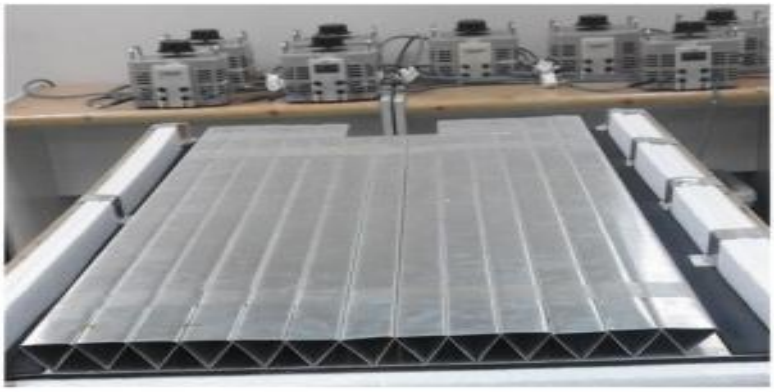

Figure 2-4 ∇-corrugated absorber plate air system [18].

Shuang-Ying Wu(2019**)** [18]**.** They evaluated the properties of thermoelectric and heat exchange efficiency for the cooling channel location of PV/T air-cooled systems which were studied numerically. Two structure locations were considered, case1 cooling duct upper the PV panel and case 2 lower the PV panel, as shown in2-5. The influences of internal, radiation on the system efficiency in the cooling duct is found to be greater in case 1 than in case 2. For two case systems the magnitude and variation pattern of the Nusselt convective number on PV panels are almost the same. The air inlet temperature for case1 and case 2 was obtained to 298.15 K and 295.65 K for maximum overall efficiency for the system. Case1 was preferred from the perspective of the amount of energy supplied.

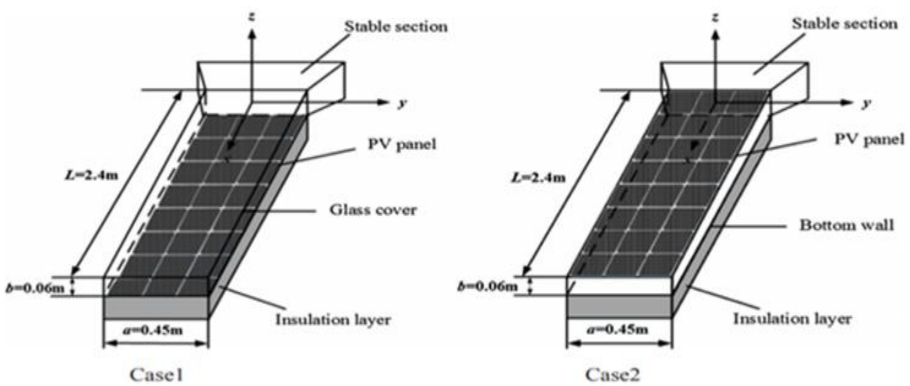

Figure 2-5 Different cooling channel location [19].

Yan Zhao et al (2020) [19]**.** They built and analyzed a PV-driven aluminum honeycomb solar air collector by numerical and experimental study, as shown in 2-6. The structure of a honeycomb progress to the collector to form the large surface area for heat exchange experimentally testing the system with irradiance of 200 W/m^2 to 600 W/m^2 and PV coverage ratio of 15%, 30%, 45%, 60%, 75% and 90%. From the analysis of thermal behavior to the system, it was noticed that the well-designed PV configuration integrated with honeycomb solar air collector would be able to suitable improve of the thermal efficiency with different of experimental conditions, with the 45% PV coverage ratio. The maximum immediate efficiency was reached 64%**.**

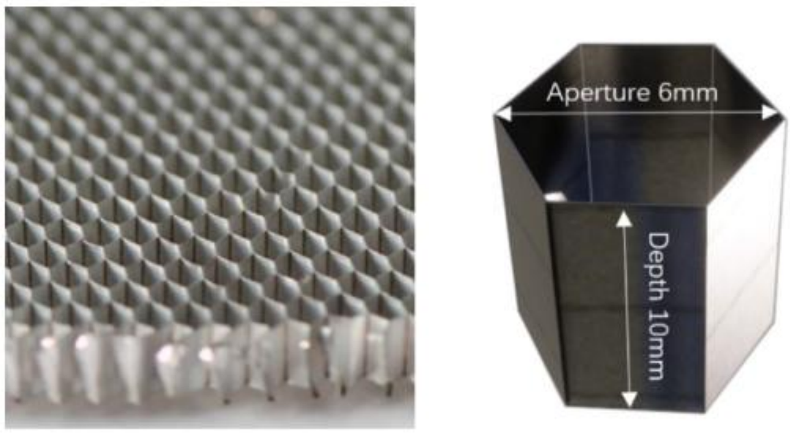

Figure 2-6 Aluminum honey comb [20].

Abdullatif et al (2020)[20]**.** They studied the behavior of a double-flow Photovoltaic-thermal (PV/T) hybrid air system employment for drying application theoretically and experimentally, as well as the module is structured and fabricate as seen in 2-7. The hot air outlet from the PVT collector can be employed as a source of heat for the drying process. The results showed that with lesser mass flow rate of 0.017 kg/s detected the higher production air temperature reached to 63 C. and electrical, thermal and overall maximum efficiencies with higher mass flow of 0.031kg/s was 12.65 %, 56.73% percent and 85 % respectively. Furthermore, at 0.031 kg/s, the optimum electrical power and thermal energy reached to 50.57 W and 389.37 W.

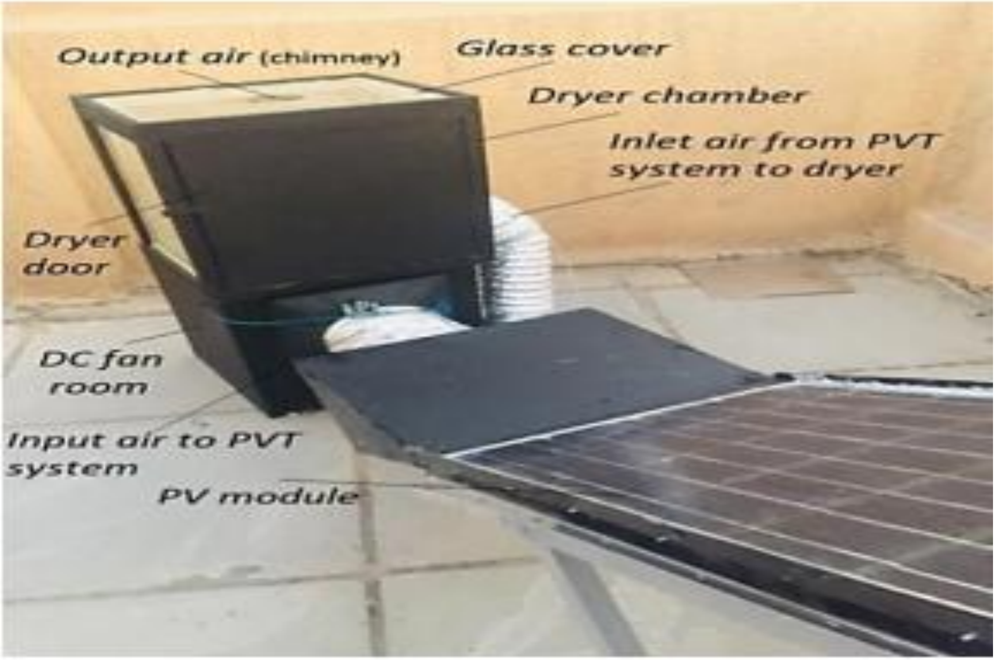

Figure 2-7 PV/T hybrid air system for drying application [21].

2.3 PV/T With Water-Based and Nano-fluid Based System

PV/T water-based systems were the result of an addition of solar water thermal system to PV panel in the same unite, compared to PV/T, air employed systems. The PV/T with water employed system has the ability to extract high thermal attributed to its high conductivity of water.

Afroza Nahar et al (2017**)**[21]**.** They experimentally and numerically evaluated the PV/T module with parallel thermal plate without plate in collector absorber which has been directly connected to the PV backside of module by using thermal paste only, as shown in 2-8. The numerical analysis was validated with experimental results under different operating weather conditions. The result indicated that the PV/T thermal performance without plate in the system absorber was best performance than the system absorber with plate, both inlet and temperatures of ambient kept at the same value about 34℃ and radiation level was 1000 W/m^2. The highest overall, efficiency of PV/T module achieved was 80%, and 84.4% respectively, by numerical and experimental values.

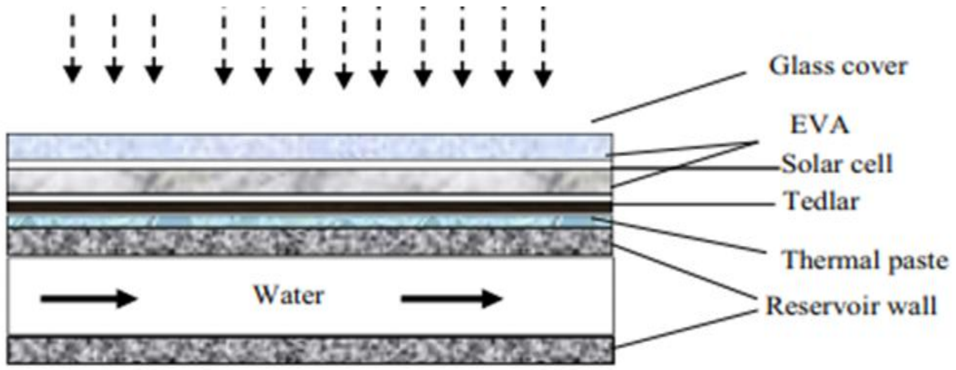

Figure2- 8 PV/T and solar system with flat plate [22].

Arash Kazemia et al (2019**)** [22]**.** They offered experimentally the influences of the glass cover and cooling fluid on photovoltaic thermal PV/T system. To perform the experiments, two similar photovoltaic thermal modules: one with glass cover and one without glass cover. They are structured and constricted, with three different working fluids consisting of ethylene glycol, water and 50% water ethylene glycol (EG)/water combine. Energy and energy analyses are carried out to investigate the thermal and electrical, efficiencies for PV/T system. The results showed that employing combine 50% EG/water as cooling fluid had best combine energy and exergy efficiency and reduction freezing temperature, compared to those of EG employed. For cold climate conditions, 50% EG/ water combine is recommended as a best cooling fluid. Also, for more extensive results, the electrical efficiency of PV/T system, without glaze is larger than that of PV/T system with glaze. The unglazed PV/T is best chosen when electrical energy is only required. But, if a higher overall energy efficiency is required, the glazed PV/T system is preferred.

Hussein A. et al (2020**)** [23]**.** They evaluated three variable collector's types for PV/T module with water cooling system direct, Web and Spiral, as shown in the 2-9.Studied and analyzed in terms of electrical performance relative to conventional PV, with 40 kg/h flow rate of water. The suggested systems have lowered the average temperature of the cells by 3℃. The spiral pass collector achieved the better efficiency, compared to direct, and web, pass collectors**.**

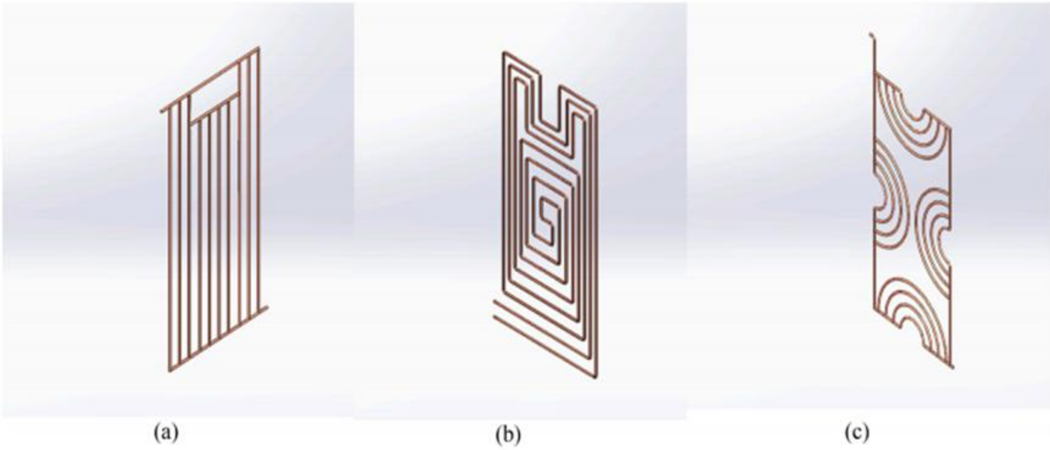

Figure 2-9 (a) PV/T with direct pass,(b) PV/T with spiral pass,(c) PV/T with web pass[24]

Wei Pang et al (2020**)**[24]**.** They studied experimentally the behavior of hybrid sheet-tube PV/T module with two different indoor laboratory conditions, closed and ventilated air circulation, combined with different mass flow rates. The research results have shown that the influence of environmental conditions on PVT module output is more significant than mass flow rates. Every calculated electrical efficiency, thermal efficiency and electrical energy of PV/T module was raised with these two environmental conditions. Also, the electrical efficiency for PV/T module with the conditions for ventilated air circulation were higher than those for closed conditions, as seen in Figure2-10.

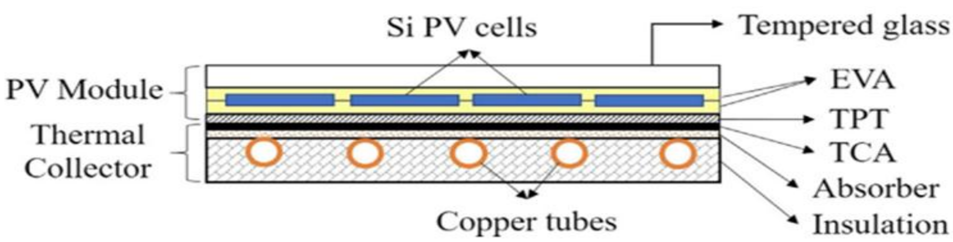

Figure 2-10 PV/T with sheet and tube thermal exchanger[25].

Poor thermal conductivity of the cooling fluids has constantly been the main limitation in the evolution of fluids with high efficient heat transfer energy and higher collector effectiveness. This is to remove this limitation and produce heat transfer fluids with higher thermal conductivity suspended nanoparticles with higher suspension stability, as compared to the micrometer or millimeter size nanoparticles. This new production fluid, called nanofluid, is for heat transfer. Thus, by using nanofluids, the heat transfer characteristics will be improved.

Ali Najah et al (2016**)[6].** They investigated the behavior of photovoltaic thermal PV/T system with specially designed rectangular channel absorber, made from (stainless steel material), with dimension of 15 mm in height , 25 mm in width and 1mm in thickness joined to the pack side of photovoltaic module, as shown in 2-11. PV/T system was tested experimentally with difference types of (SiC, SiO2, and TiO2) nano-fluid. With 0.170 kg/s in flow rate of and 1000 W/m^2 radiation intensity, the results showed that SiC nano-fluid achieved best additions for photovoltaic, thermal, and PV/T efficiency, reaching to 81.73% and 13.52% in electrical efficiency followed by PV/T with TiO2 nanofluids, PVT with SiO2 nanofluids, and PV/T with water based system.

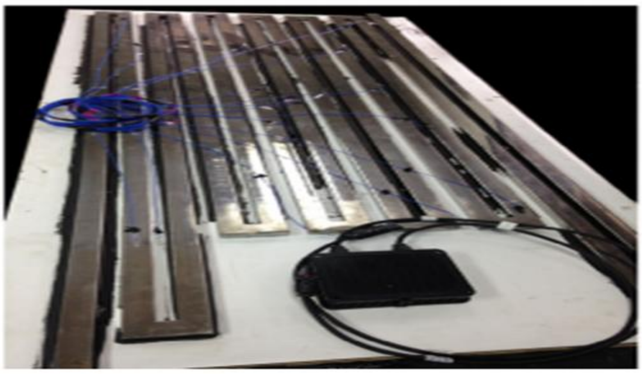

Figure 2-11 PV/T with rectangular channel tube [6]

Mohammad Sardarabadi et al (2017**)** [25]**.** They experimentally analyzed the impact of employing nano-fluids consisting of metal-oxides and water as working fluids on a Photovoltaic thermal PV/T system with sheet and tube heat exchanger. They considered three nanoparticles containing (ZnO, Al_2O_3, and TiO_2) with 0.2 wt%, and water as the working fluid flowing inside the collector with 30 kg/h constant flow rate. The experiments were done at certain days in August and September. The measured information is inspected with energy, exergy points of view and generation of entropy. Compared to the other systems, the experimental result showed that the highest overall, energy and exergy, efficiencies for PV/T with ZnO and PV/T with TiO_2 systems, and the overall exergy efficiencies for the systems of PV/T with water, PV/T withTiO_2, PV/T with Al_2O_3, and PV/T with ZnO were improved by 12.34%, 15.93%, 18.27% and 15.45%. Also, the PV/T with Al_2O_3 system with respect to the PV panels with no collector, has better improvement in entropy, production, as shown in 2-12.

Figure 2-12 PV/T with sheet and tube thermal collector [26].

Ali Najah et al (2018**)**[26]**.** They performed three rounds of tests. Firstly, the best structure of sheet - tube thermal collector has been specified employ water as the thermal exchange fluid; secondly, comparing the behavior of PV/T from the portion of difference types of Nano-Fluids ZnO, CuO and SiO2 combination with water. The results discovered that the NF-SiO2 showed significantly an improvement as a compared to other types of NFs and water. In addition, using NF- SiO_2 in the PV/T collector decreased the PV module temperature from 65°C to 45°C and raised the outlet fluid temperature from 35°C to 44°C, leading to an improvement in both the electrical and thermal efficiency by 12.70% and 5.76% respectively with solar irradiance of 1000 W/m^2.

R. Nasrin et al (2018**)[1].** They investigated the performance of PVT system with Water-MWCNT nano-fluid as cooling fluid by experimental and numerical testing at various irradiation levels from 200W/m^2 to 1000W/m2, weight fraction from 0 to 1% with constant mass flow rate of 0.5 L/min and inlet temperature32 C, by using water cooling system. The enhanced percentage of PV performance is found as 9.2% by using nano-fluid than water. The enhanced thermal performance is gained as 4 and 3.67% in numerical and experimental studies, respectively. In the PV/T system employ the nano-fluid at 1000 W/ m^2 irradiation. The numerical and experimental overall efficiency has been found to be 89.2% and 87.65% respectively as seen in 2-13.

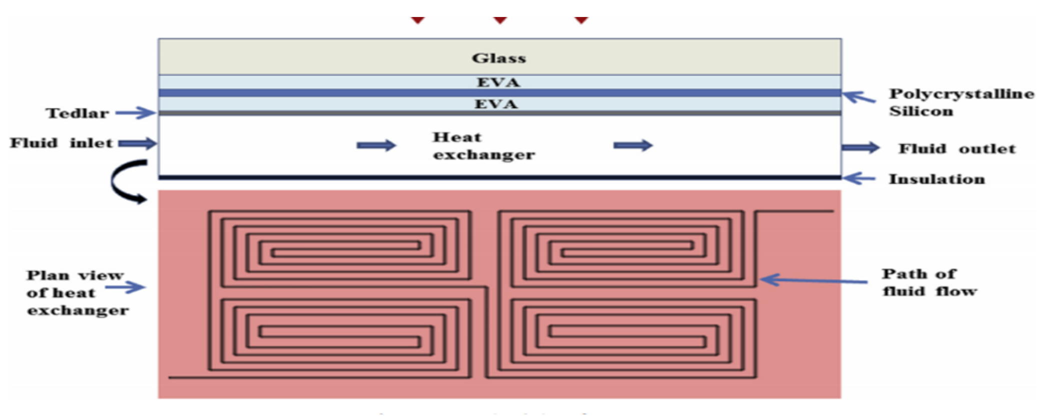

Figure 2-13 PV/T with separation flow[1].

Joo Hee et al (2019) [27]**.** They investigated the influence of the working fluids such as water and (CuO/water, Al_2O_3/water) nano-fluids on the efficiency of the PVT system with various flow rates of working fluid. The flow rate, which affects the performance of the PVT system, showed the highest efficiency at 3 L/min, compared with 1, 2, and 4 L/min. additionally. The results indicated that the PVT system employing CuO/water as a nanofluid has increased by 21.30% and 0.07% in thermal and electrical efficiencies, respectively, compared to the system based on water fluid flow with no significant increase in electrical efficiency. The PVT system using Al_2O_3/water as a nano-fluid enhanced the thermal efficiency by 15.14%, but there was no variation with electrical efficiency in both water and Al_2O3/water-based systems.

Salaheldin Alous et al(2019)[28]**.** They checked the effect of using multi-walled carbon nanotubes (MWCNT) and graphene nano platelets with water as a working fluid with a concentration of 0.5wt% on the effectiveness of PVT systems. Outdoor experiments were tested with volume flow rate of 0.5 L/min for the mentioned nanofluids and distilled water as a based fluid. From energetic and exergetic viewpoints, the results of the study have been analyzed and indicated in terms of photovoltaic energetic conversion where the MWCNT-water nanofluid offered the best effectiveness compared to graphene Nano platelets-water nanofluid and distilled water. The highest thermal energetic efficiency was detected by the graphene nano platelets-water nanofluid. Moreover, adding thermal collector with photovoltaic module (PV) improved the overall energetic efficiency by 53.4% for distilled water, 57.2% for MWCNT-water, and 63.1% for graphene-water. Attributed to exergetic efficiency, the excess in overall exergetic efficiency was 11.2%, 12.1%, and 20.6% for PVT module cooled by distilled water, MWCNT-water nanofluid, and graphene Nano platelets-water nanofluid respectively**.**

2.4 PV/T With Phase Change Material (PCM)

The integration of a phase change material (PCM) as thermal storage material with PV panels contributes to the reduction of the temperature of PV and extracts more heat from its back side. This can improve the PV efficiency. This combination with a PV panel was able to effectively reduce the heat loss to ambient. When the sun set or solar radiation is less dense and unavailable, the heat stored into the PCM can be transferred to the working fluid. This can lengthen the preparation time for the required building [12].

Xiaojiao Yang et al (2017**)** [12]**.** They studied the employment of PCM layer to improve the performance of the PV/T system by experimentally testing and comparing the PV/T-PCM and PV/T systems overall energy efficiencies. Under a controlled indoor environment with a radiation of 800 W/m^2 and water flow rate of 0.15 m^3/h, the initially energy-saving efficiency for the PV/T-PCM system was improved by 14%. These results show that the combination of a PCM into a PV/T system can visibly enhance the energy effectiveness of the system.

Sajan Preet et al (2017)[29]**.** They made a comparison between three various type of PV system; convectional PV panel, water employ photovoltaic thermal system (PV/T) with double absorber plate and water employ photovoltaic /thermal system with (PCM). In water employ PV/T system, double absorber using one absorber plate is attached to PV panel and second absorber plate is attached to copper pipes with the same shape of profile as that of piping configuration as seen in Figure 2-14. Paraffin wax RT-30 is employed as phase change material in water based PV/T PCM. The experiment was performed at three different mass flow rates, 0.013 kg/sec, 0.023 kg/sec, and 0.031 kg/sec, and its influence on electrical and thermal efficiency has been analyzed. The result indicated that the photovoltaic/thermal technology has influenced the solution to extend higher electrical and thermal effective systems.

Figure2- 14 PV/T with PCM and copper pipes [30].

M.S. Hossain et al (2017**)**[30]**.** They created and improved a photovoltaic/thermal (PV/T) with phase change materials (PCM) system, and recorded its energy, exergy and economic performance. Lauric acid as PCM put in leak proof aluminum foil jacket is maintained around the flow channel permitting an extended period of thermal storage. The PV/T-PCM system has been tested at different volume flow rates (0.5-4) liter per minutes (LPM) to obtain the best effectiveness of the system. Highest thermal efficiency of PV/T-PCM system achieved at 2 LPM was found to be 87.72%. Highest electrical efficiency of PV and

PV/T-PCM systems has been detected 9.88% and 11.08% at (4LPM) respectively. The highest improvement of exergy efficiency of PV and PV/T-PCM system has been recorded 7.09% and 12.19% (0.5LPM) respectively, to check the feasibility of its commercialization an economic analysis of the proposed system has also been presented with a view.

Jiaxn zhao et al (2018**)**[31]**.** They integrated the PV system with various PCM thickness simulated and referenced with the attribute PV system. The result showed the main important parameter in cooling the PV temperature the latent heat capacity and the natural convective performance of PCM. The PCM's natural convective heat transfer rate was 4 to 5 times higher than the conductive heat transfer rate. The simulation result indicated that the temperature of PV can be less by up to 24.9°C when adding PCM and thence the electricity output was able to be raised by 11.02%.

Al-musaw et al (2019)[32]**.** They studied the influence of pure water, SiO2/water nanofluid as coolants and (PCM) on the performance of a photovoltaic thermal (PV/T) system numerically investigated as seen in 2-15. The simulations are applied on two PV/T system with PCM (PV/T-PCM system) and without (PV/T system), being studied and compared under difference Parameters such as, PV surface temperature, thermal, and electrical efficiencies of the systems. Moreover, the results of nanofluid as a coolant fluid are compared with those that employ a pure water. From the results the average decreased in PV cell temperature reached to 16 ℃ in the water-based PV/T-PCM compared to that of the PV/T system. These results lead to a raise in the thermal efficiency by 25% and 8% in the electrical efficiency. However, employing SiO_2 nanofluid in the PVT/PCM system as a coolant fluid raised the thermal efficiency by 3.51% and 10.40% (with 1 and 3 mass% mass fraction), respectively, compared to the PV/T-PCM water based as a coolant fluid. The result of this study indicated that the thermal efficiency of the PV/T-PCM system increased when using phase-change material with higher melting temperature.

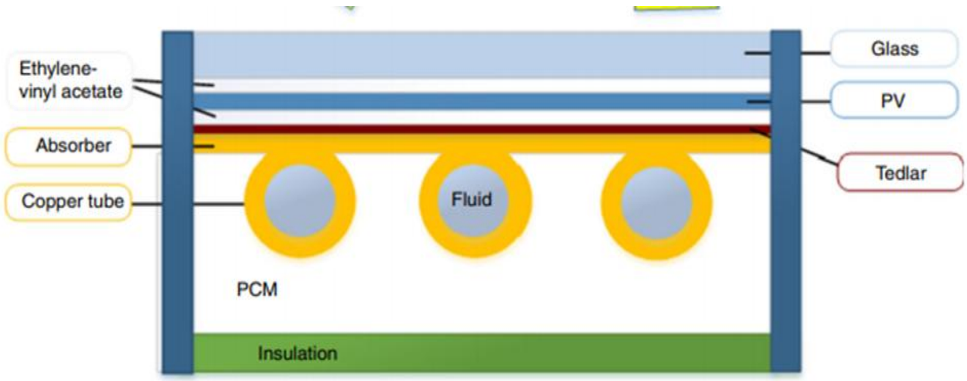

Figure 2-15 Cross section view of PV/T with PCM [33]

Taher Maatallah et al (2019**)**[33]**.** They analyzed experimentally the exergo-economic of photovoltaic thermal (PV/T) water based system with serpentine flow type and PCM as shown in 2-16. They compared the overall efficiency of PVT water-based-PCM and PV water-based panels with attribute PV, with different outdoor environmental conditions, it has been recorded that the combination a PCM with PV/T improved the thermal and overall efficiency by 26.87% and 40.59% respectively. Also, they compared that with an increase in electrical efficiency by 17.33% compared with attribute PV panel. It has been detected that the payback time for the PVT-PCM water-based system is about 6 years on the overall exergy analyses, which is 11.26% shorter compared to attribute PV panels. Also, the PV/T-PCM water-based system has long-term lifecycle transformation efficiency evaluated with attribute PV panel by about 27%.

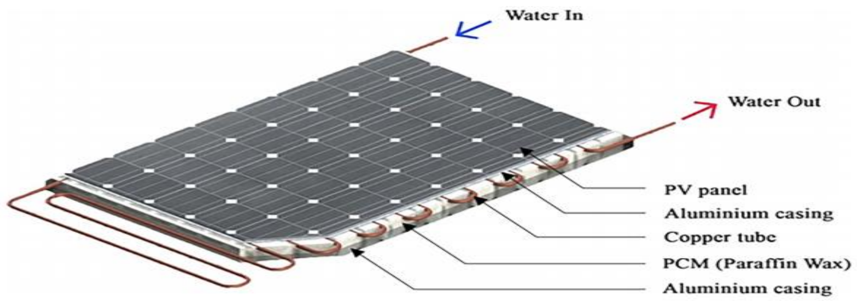

Figure 2-16 PCM paraffin wax with PV/T and serpentine flow [34].

Canan Kandilli (2019**)**[34]**.** He experimentally tested a natural zeolite used as a thermal energy storage material combine with PV/T. The essential target of the studded is to introduce natural zeolite as a heat storage material for PV/T systems, cumbered with two other type such as, paraffin and stearic acid. The PV/T systems combination with phase change materials and natural zeolite have been structured as illustrated in 2-17. The experiment's average overall energy efficiency values for PV/T were 33% for paraffin, 37% for stearic acid, 40% for zeolite, and 32% for attribute PV/T systems. Also, 10, 8, and 9 years the payback period was detected for the PV/T system with paraffin, zeolite, stearic acid, and attribute PVT, respectively.

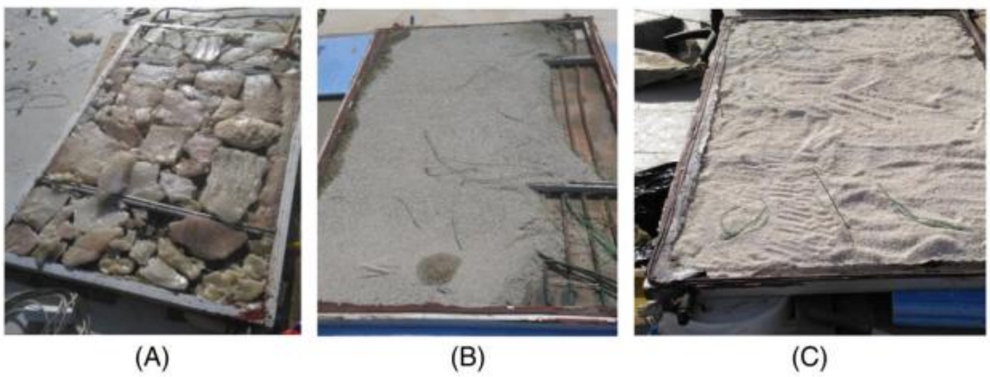

Figure 2-17PV/T with (A), paraffin, (B) natural zeolite, and (C) stearic acid [35].

Ali Hassan et al(2020**)[7].** They tested experimentally three various systems consisting of PV/PCM, PVT/PCM system and PVT/PCM system integrated with (graphene/water) nanofluid circulated through pipes inside (RT-35HC) PCM and compared all these systems with conventional PV as indicated in 2-18.Different volume concentrations of graphene nanoparticles were tested (0.05%, 0.1%, 0.15%).

The flow rates were (20, 30, 40) LPM. A better enhancement is recorded with 40LPM flow rate, and 0.1vol% nanoparticle concentration. The examined data showed that the maximum decreased in PV temperature was 23.9°C, 16.1°C and 11.9°C in nanofluid-used PVT/PCM system, water-used PV/T-PCM system and PV-PCM system respectively. The higher improvement in electrical efficiency was 23.9%, 22.7% and 9.1% respectively, as compared to traditional PV. It has been found that hybrid PV/T-PCM system with nanofluid based as compared to water-based hybrid PV/T-PCM system recorded 17.5% higher thermal efficiency. The overall efficiency was improved by 12%. The results showed that integrated nanofluid and PCM with hybrid PV/T system ensure the better performance than using PCM alone.

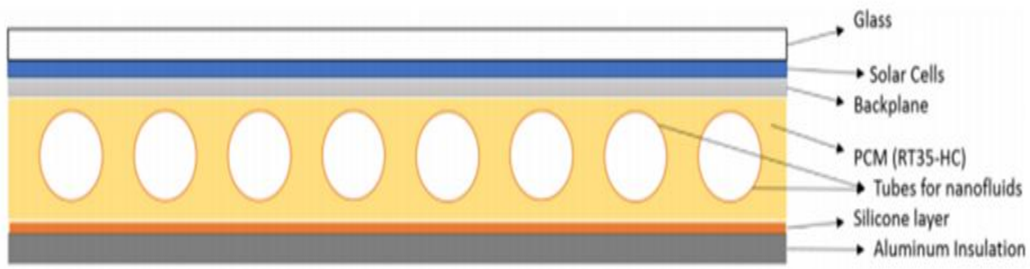

Figure 2-18 PV/T system with PCM and nanofluid [7].

Hongtao Xu et al (2020**)**[35]**.** They presented a comprehensive study of a solar photovoltaic/thermal system combined with phase change material PV/T-PCM system. A fatty acid was used as the PCM with temperature melting point of 37 °C. A solar collector filled with PCM, which contained rectangular metal fins to improve heat transfer, was used to coolant the PV. Circulation a water to improve the overall solar energy exploitation efficiency in the PV/T-PCM system. The results showed that the combine a PCM with solar collector could significantly reduce the temperature alteration of the PV panel and enhance the photoelectric efficiency.

2.5 PV/T Combine With (Air and Water) System

It is the combination of a dual-fluid heat exchanger with a PV/T. This system is not only able to generate electricity but it also can simultaneously produce hot air and hot water by having two types of thermal collector mode in one system. The temperature of PV panel will be decreased and cell efficiency has been with higher enhancement. Depending on the energy needs and applications, the employ of both fluids also generate a higher range of thermal applications. The improvement system by integrating both type of heat transporter mode is to show the best performance of PV/T technology and to get higher efficiencies. The integration of two systems is also to cover the determinants and weaknesses of separate PV/T water and air thermal collector systems. In terms of cost, the integration as one-unit system displays reduction structure cost and shows less payback time period.

Jie Ji et al (2014)[11]. They proposed and constructed a new structure of tri-functional photovoltaic/thermal solar collector as seen in 2-19.The collector is able to produce electricity and hot air or water with each other. The employer can select the working way readily according to their requirement. They experimentally investigated the performance of collector under various conditions. The results indicated that the daily thermal efficiency in the PV/T air-heating module has achieved 46.0% with and electrical efficiency of 10.2% when the air mass flow rate was 0.042 kg/s. The maximum increase in air temperature achieved was 20 ℃ during the day when the increase air mass flow rate both daily thermal and electrical efficiencies increased. In PV/T water-heating module, the electrical efficiencies ranged from 9.6% to 11.8% in comparison with the performance of various types of solar collectors. The tri-functional PV/T collector is proved to be energy-efficient in various working modes and can be used for different applications.

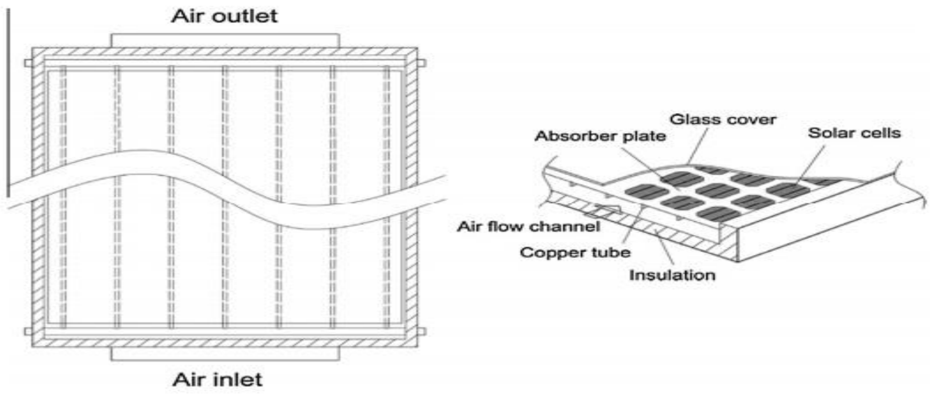

Figure2- 19 Schematic of triple function PV/T system [12].

Mohd Nazari et al (2014**)**[36]**.** They presented and improved a structure of a photovoltaic /thermal (PV/T) solar collector integrating with PV panel with a serpentine-shaped copper tube as the water heating collector and a single pass air channel as the air heating collector as shown in 2-20. This module of collector can produce both hot air and water in addition to generating electricity. The total efficiency is increasing per unit area compared to the attribute PV/T solar collector. The employ of both fluids (bi-fluid) also creates a higher range of thermal applications. The simulations detected that when using single fluid air or water, the overall thermal and electrical efficiency of the solar collector is considered as satisfactory and when operated together the overall performance is higher.

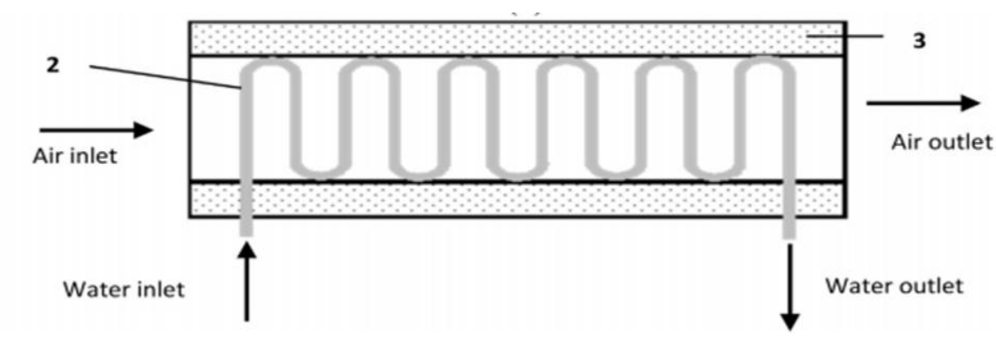

Figure 2-20 bi-fluid PV/T solar collector[37].

M.Y. Othman et al (2015**)**[37]**.** They presented and investigated experimentally a PV/T Combine system fabricated from two heating system; double pass flat plat air collector and copper water tube thermal collector in terms of electrical and thermal efficiency as illustrate in 2-21. The experimental testing result of the collector detected that the outlet temperature is 24.40C with air and water flow rate is ranged from 0.02 kg/s to 0.05 kg/s when radiation level of 800 W/m^2. The average output electrical power of 145 W and electrical efficiency of the collector is 17%. The PV/T Combine system overall thermal efficiency was 70%, when the experiment was carried for a period of 120 minutes.

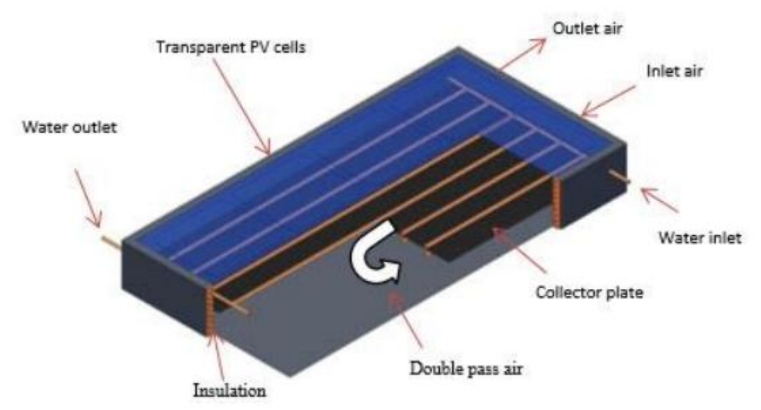

Figure 2-21 PV/T combination flat plate collector water and air heating system [38].

M.Y. Othman et al (2016**) [39].** They experimentally evaluated a transparent photovoltaic (PV) modules connected in parallel so as to generate electricity with double pass flat plat air duct and water tube attached on top and bottom of the collector plate as shown in 2-22. The analyses of the system are calculated based on Hottele Whilliere Bliss equation, with controlled indoor environment at radiation level of 800 W/m^2, and mass flow rate of 0.05 kg/s and 0.02 kg/s for air and water the outlet temperature specified reading of 27.4 ℃. The electrical efficiency accomplished was 17% with average electrical power produced of 145 W and thermal efficiency achieved was 76%.

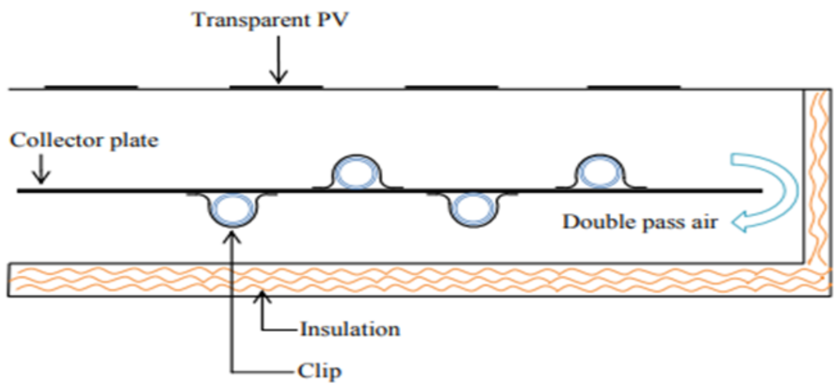

Figure 2-22 PV/T combine with double pass air duct and water[39]

Kamaruzzaman Sopian (2016**)[40].** He theoretically and mathematically improved structure of PV/T solar collector with CPC combined with double pass air channel and a square stainless steel water tube as seen in Figure 2-23. Systems have been proposed and progressed to study the performance of the combined module. The steady-state one-dimensional energy balance equations governed the analysis. The highest thermal, electrical and overall efficiencies generated were 53.3%, 13.26% and 88.19%, respectively at the optimum water mass flow rate value of 0.02 kg/s and 0.07 kg/s air mass flow rate. From the results of analysis, the dual pass and dual fluids arrangement in this study were seen as favorable in order to improvement solar energy employment.

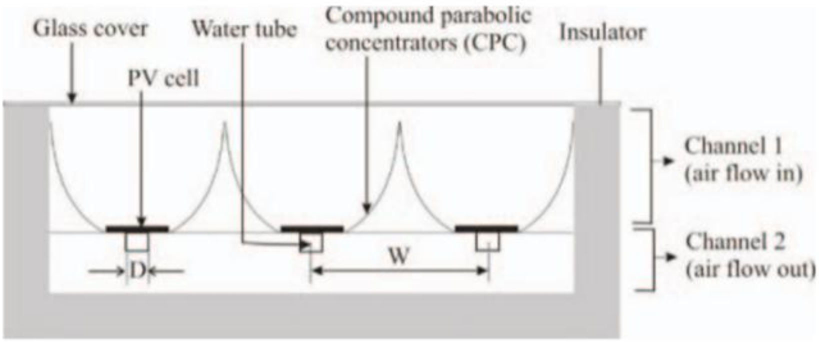

Figure 2-23 PV/T combine with CPC and double pass air flow [40].

M. Imtiaz Hussain et al (2019**)[41].** A mathematically modeling and a CFD simulation have been performed for dual-fluid photovoltaic/thermal (PV/T) system by using MATLAB® and ANSYS FLUENT® software, that employs both nanofluid and air, to clarify the best nanofluid type for the PV/T collector. They evaluated the difference of metal oxide nanoparticles such as (CuO, Al2O3, and SiO2) with various concentrations which were sparse in the base fluid (water). The results indicated that the CuO nanofluid with 0.75% concentration as compared to the other two nanofluids has the highest thermal conductivity and the optimum thermal stability, the total overall efficiency was found to be 90.3% and 79.8% for CuO nanofluid with air and water with air respectively see Figure 2-24.

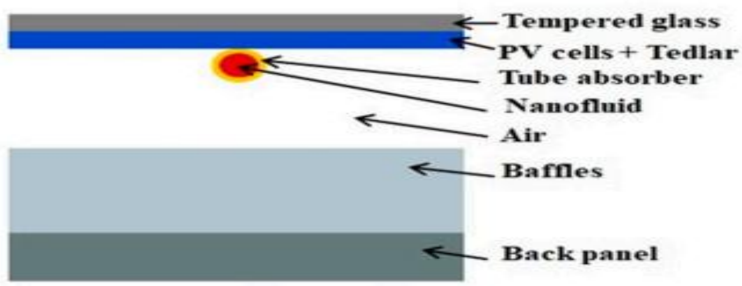

Figure 2-24 cross-section view for dual fluid PV/T collector considering a single pipe [41]

S.S.S. Baljit(2019**)[42].** He proposed a photovoltaic thermal (PV/T) with dual-fluid solar collector integrated with two types of concentrators, FL and CPC as illustrated in 2-25. He analyzed the performance of the collector with both air and water as the working fluids. The results display that integrating two fluids improves the thermal and electrical efficiencies. The total thermal and electrical efficiencies gained are 67.% and 13.02%, respectively, at water and air mass flow rates of 0.0164 kg/s and 0.0103 kg/s, respectively, and a solar intensity of 650 W/m^2, and 12.40% to 13.10% various in the electrical efficiency of the dual-fluid modes and 11.00% to 12.60% for that of the single-fluid modes and 25% higher in thermal efficiency of the dual-fluid than that of single-fluid modes.

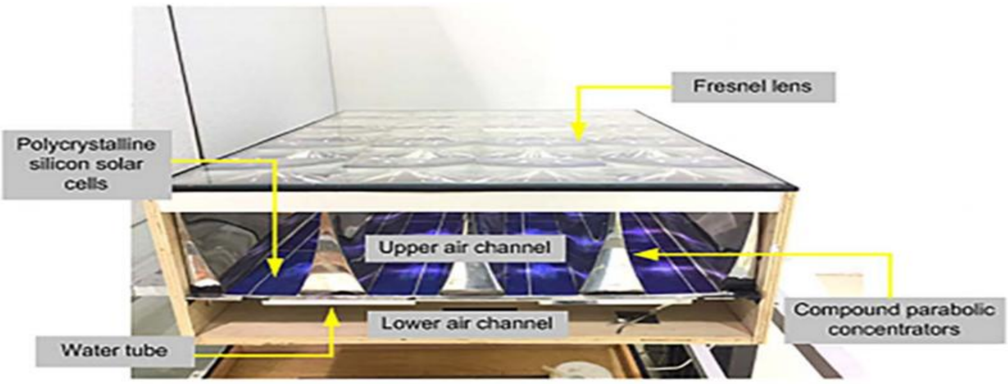

Figure 2-25PV/T combine (air and water) with CPC and FL [42].

Muhammad and Jun(2020) [42]**.** They investigated the performance of PV/T with dual-fluid (water/air) as shown in 2-26, by energy, exergy and economic analyses of a system, compared with a conventional PV module and single-fluid PV/T systems. Experimentally they evaluated the daily and yearly performance of all of the mentioned above. The results indicated that the dual-fluid PV/T systems have significantly higher energy and exergy efficiencies than those of single-fluid PV/T systems, by 20% and 11%, respectively, and the cost of energy is reduced by 80%, 60%, and 45% respectively, with the dual-fluid PV/T system and water and air type PV/T systems according to local domestic electricity price.

Figure 2-26 Double fluid with PV/T [43].

2.6 Summary of Literature Review

The main limitation in the employ of photoelectric PV panels to generate electrical energy is the drop in efficiency as it temperature rises. The reason for the low efficiency in high temperature is due to the semiconductor material from which the photoelectric panels are made, because of the importance of PV panels researchers have tended to find various ways to cool them. Integrated air thermal collector, water thermal collector and combine (air and water) thermal collector with a PV panels to exchange heat contribute to cool it and lower the reduction in it is efficiency and employed extracted heat energy in thermal application as illustrates in Table 2-1.

Table 2-1 illustrate a summary of the references studied PV/T system

References	Module type	Study type	Enhancement		
			Electrical efficiency	Thermal efficiency	Overall efficiency
[14],2013	PV/T air double pass with slice	experimental			29 – 37%
[15],2013	PV/T with V-groove stainless steel wool honeycomb	experimental	7.04%, 6.88% 7.13%	71%with V-groove 86%,with stainless steel wool and 87%with honeycomb	
[16],2014	PV/T with, single -pass double -duct, single -duct double- pass and single -duct single- pass	experimental			
[17],2017	PV/T double pass PV/T with porous media	experimental			Increase 3%
[18],2019	PV/T air collector with a ∇corrugated absorber	experimental			
[19],2019	PV/T with air duct up and down PV	experimental			
[20],2020	PV/T air with aluminum honeycomb SAC	experimental			64%.
[21],2020	PV/T double pass air	experimental	12.65 %	56.73%	85 %

[22] , 2017	PV/T water	Numerical and experimental			NUM 84.4% and EX 80%
[23],2019	PV/T water and ethylene glycol (EG)	Experimental			
[24] ,2020	PV/Twater with (web,direct, spiral)types channels	Experimental			18.5%, 28.0% and 35.0%,
[25],2020	PV/T water with sheet-tube absorber	experimental			
[6] ,2016	PV/T with (SiO2,TiO2 and SiC) nanofluids and rectangular channel absorber	experimental		13.52%	81.73%
[26],2017	PV/T water and (Al2O3,TiO2 and ZnO) nanofluid	experimental			12.34%, 15.93%, 18.27% and 15.45%, exergy
[27],2018	PV/T with water and (CuO, SiO2, and ZnO) Nanofluid	experimental	Improved by 12.70%	Improved by 5.76%	
[1],2018	PV/T with Water/MWCNT nanofluid	Experimental and numerical		Enhance by 4 and 3.67% num and ex	89.2 and 87.65%, num and ex
[28] ,2019	PV/T with CuO /water nanofluid PV/T with Al2O3 /water	Experimental	Increased by 0.07%	increased by21.30% and 15.14%	

	nanofluid				
[28] ,2019	PV/T with MWCNT) and graphene nanoplatelets	Experimental		57.2% for MWCNT-water, and 63.1% for graphene-water	
[13],2017	PV/T- PCM	experimentally			
[29], 2017	PV/T-PCM	experimentally			
[31], 2018	PV/T-PCM	experimentally	9.88% and 11.08%	87.72%	
[32],2018	PV/T PCM and SiO2 nanofluid	numerically	raised by 25%	raised by 8%	
[33], 2019	PV/T-PCM	experimentally	raised by 11.02%.		
[34],2019	PV/T PCM	experimentally	17.33%	26.87%	40.59%
[35] ,2019	PV/T with paraffin, stearic acid, zeolite, and attribute PV/T	experimentally			33% 37% 40% 32%
[7] ,2020	PV/PCM with (graphene/water) nanofluid	experimentally	improved by 9.1% 22.7% 23.9%		
[36],2020	PV/T-PCM	experimentally			

[12],2014	PV/T air and water	experimentally	10.2%	46.0%	
[37],2014	PV/T single pass air and water	mathematically		76%	
[38],2015	PV/T double-pass air channel and water	experimentally	17%	70%	
[39], 2016	PV/T double-pass air channel and water	experimentally	17%	76%	
[40],2017	PV/T with CPC double pass air channel and water	theoretically and mathematically	13.26%	53.3%	88.19%
[41],2019	PV/T with CuO-nanofluid and single pass double duct air	mathematically			90.3% with CuO-nano fluid and air 79.8%with water and air
[42],2019	PV/T combine air and water with FL and CPC	experimentally	13.02%	67%	
[43],2020	PV/T(water/ air) dual-fluid	experimentally			

2.6 Scope of Present Work

After reviewing previous studies the current study includes.

- The use of an air thermal collector of type double pass single duct with steel wool as a porous medium.

- The use of an water thermal collector made from copper plate with copper pipe surrounded by paraffin wax as phase change material (PCM).

- Investigate the using an MWCNT-nanofluid instead of water with air as cooling fluid on the electrical and thermal performance of the system.

- Exergy and Performance analysis of combined double pass PV/T with PCM, porous media for tow mode of fluid flow air plus water and air plus MWCNT-nanofluid as an cooling fluid

Chapter Three

METHODOLOGY

3.1 OVERVIEW

This chapter deals with the methodology followed to achieve the goals specified in the first chapter. A 3D simulation by using comsol multiphasic program has been produced to detection the optimum design for water thermal collector ,pipes diameter and number, a Copper pipes of various inner diameters , were tested with different pipes number to reduction the temperature of PV panels and increase its efficiency and extracting the largest amount of heat from the bottom surface of the PV panel. This chapter illustrates the different theoretical and numerical methods of the research.

3.2Numerical Water thermal collector Model

3.2.1 Physical Model

Copper pipes with different diameters have been tested for PV/T water collector, where the study is done for the various thermal collector copper pipes diameter with a different arrangement of the number of pipes under the solar PV panel as illustrated in Table 3-1 below. Water was circulated inside the thermal collector pipes as a cooling fluid.

In the analysis and simulation, the following considerations were made:

1- CFD simulation was made 3D.
2- Study state solution.
3- Water pipes were fully insulated from outside.
4- Incompressible flow.
5- Fully developed and laminar flow.
6- Heat flux was constant.
7- Heat transfer with fluid.
8- Inlet water temperature and ambient temperature are equal.
9- Constant properties.

3.2.2 Governing Equations and Boundary Condition

Numerical analyses have been presented using steady-state conditions, that was performed using commercially attainable Comsol program. The Continuity, momentum and energy equations which was governed by PDE has been solved for the laminar, stationary and incompressible flow. Heat transfer in fluid was coupled and the effect of velocity and pressure are almost implicit for pressure governing equation algorithm. The commanding equations (continuity, momentum, and energy) below should be set to solution numerical simulation of the (PVT) system. CFD simulation under investigation was commanded by the 3D, steady state computational field for the continuity, energy and incompressible Navier Stokes equations. In the Cartesian tensor system, these equations could be illustrated as[44].

Continuity equation:

$$\frac{\partial u}{\partial x} + \frac{\partial v}{\partial y} + \frac{\partial w}{\partial z} = 0 \qquad (3\text{-}1)$$

Momentum equation[46]:

$$\rho\left(u\frac{\partial u}{\partial x} + v\frac{\partial u}{\partial y} + w\frac{\partial u}{\partial z} \right) = \rho g_x - \frac{\partial P}{\partial x} + \mu\left(\frac{\partial^2 u}{\partial x^2} + v\frac{\partial^2 u}{\partial y^2} + w\frac{\partial^2 u}{\partial z^2} \right) \text{ in x direction} \qquad (3\text{-}2)$$

$$\rho\left(u\frac{\partial v}{\partial x} + v\frac{\partial v}{\partial y} + w\frac{\partial v}{\partial z} \right) = \rho g_y - \frac{\partial P}{\partial y} + \mu\left(\frac{\partial^2 v}{\partial x^2} + v\frac{\partial^2 v}{\partial y^2} + w\frac{\partial^2 v}{\partial z^2} \right) \text{ in y-direction} \qquad (3\text{-}3)$$

$$\rho\left(u\frac{\partial w}{\partial x} + v\frac{\partial w}{\partial y} + w\frac{\partial w}{\partial z} \right) = \rho g_z - \frac{\partial P}{\partial x} + \mu\left(\frac{\partial^2 w}{\partial x^2} + v\frac{\partial^2 w}{\partial y^2} + w\frac{\partial^2 w}{\partial z^2} \right) \text{in z-direction} \qquad (3\text{-}4)$$

Energy equation [40]:

$$u\,\frac{\partial T}{\partial x} + v\,\frac{\partial T}{\partial y} + w\,\frac{\partial T}{\partial z} = \alpha\left[u\,\frac{\partial^2 T}{\partial x^2} + v\,\frac{\partial^2 T}{\partial y^2} + w\,\frac{\partial^2 T}{\partial z^2}\right] \qquad (3\text{-}5)$$

where u,v,w = velocity field (m/s)

3.2.3 CFD Analysis

A computational fluid dynamic (CFD) analysis is employed to study and calculate the compound fluid flow, temperature distribution and heat transfer in (PV/T) water system, CFD simulator program was performed by using Comsol Multiphysics software program. It is done by solving various equations and the algorithms for fluids passing through the study area, which involved the initial and boundary conditions on the needed area of study. Compared to other experimental studies, CFD theories give the flexibility for analysis various construction systems at the same time and at a lower price. In the present study, the CFD simulation analysis has been conducted to verify the effect of heat absorber design on the performance of

(PV/T) system, revolved distilled water as cooling fluids in (PV/T) system to improve the electrical and thermal performance.

Table 3-1 Different suggestions for water thermal collector design

NO.	**Pipes number**	**Thermal distribution**		
		Din=8mm	**Din=10mm**	**Din=12mm**
1	**8**	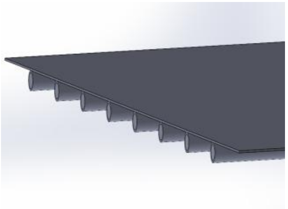	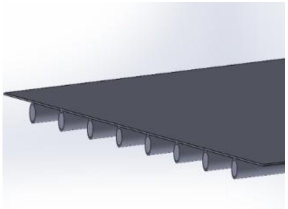	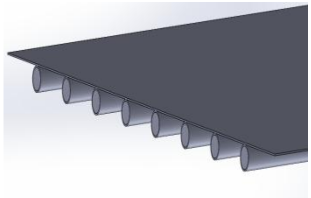
2	**10**	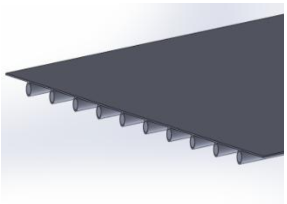	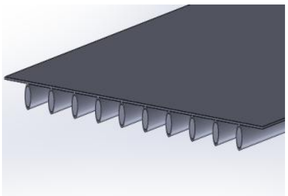	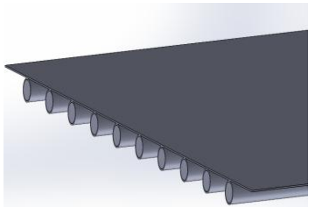
3	**12**	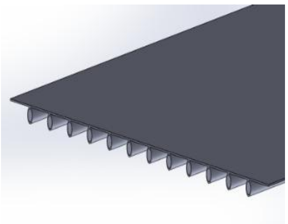	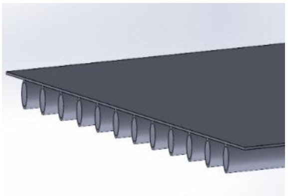	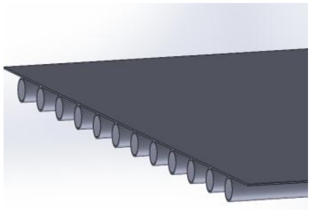
4	**14**	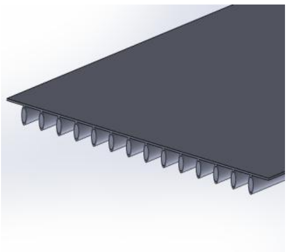	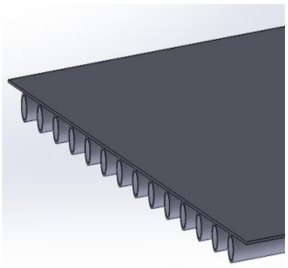	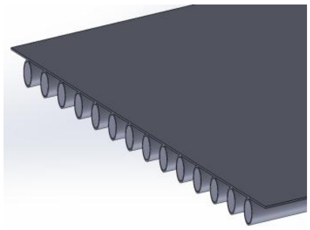

5	**16**	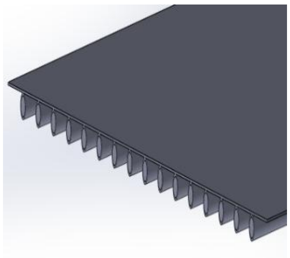	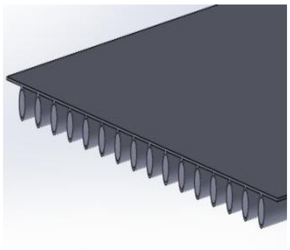	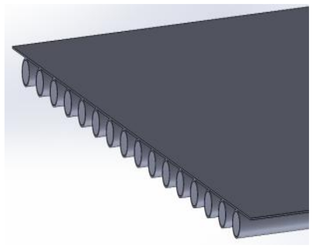

3.2.4 Meshing and Solution Model

The mesh generation on of the most important factors affect the accuracy of the results in any analysis and simulation process. The convergent solutions of the partial differential equations depend on generating convenient mesh. In this simulation, fine mesh faces were used depending on the geometrical shape of collector and operating condition as shown clearly in Figure 3-1.

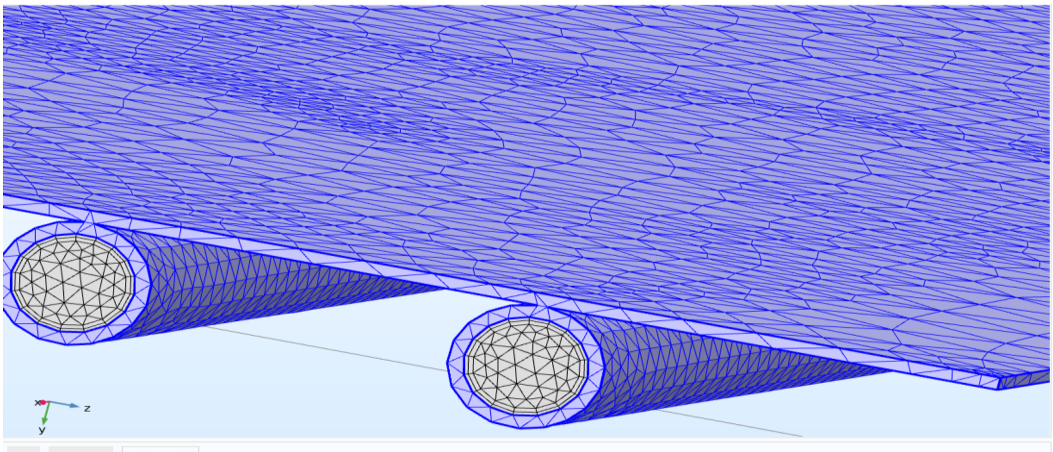

Figure3-1Mesh Generation

Various tests were carried out to generate the grid with different size elements to achieve the best results in order to reach the stability of the temperature with the appropriate number of elements depending on the temperature of the outlet water as shown in Figure 3-2.

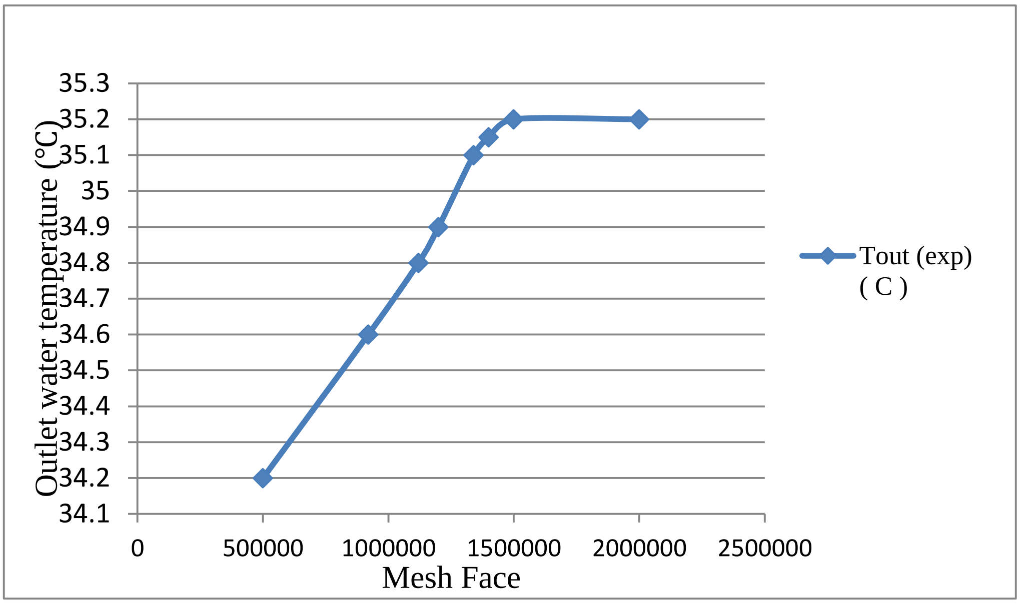

Figure3-2 Average outlet water temperature versus with mesh face for mesh generation test

3.2.5 Numerical Verification

In each numerical analysis operations, verification is a very substantial step. In this study, to validate the numerical model, a comparison was conducted between the numerical analysis and a previous study that used the results produced by Ahmad Fudholi [47]to legitimize the CFD analysis. This demands the analysis of the gained results of the CFD validation for average outlet water temperatures (T_{out}) for PV/T and thermal efficiency (η_{th}), 4.9% was the error percentage between the CFD validation and the results for previous study. The average outlet water temperature for the PV panel is illustrated in Figure 3-3, where the outlet water temperatures are reduced as the mass flow rate rises.

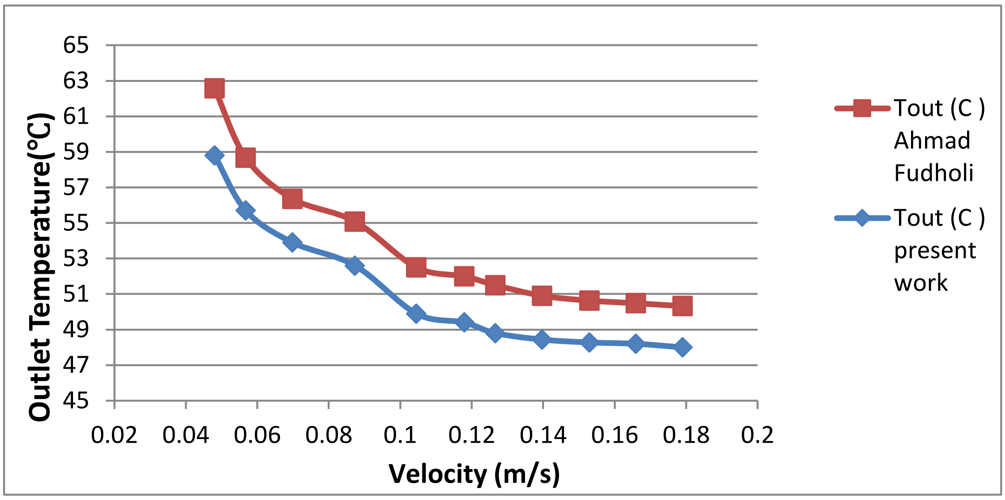

Figure3-3 Outlet water temperatures according to different mass flow rates for the CFD analysis results compared with [48]

Figure 3-4 illustrates the PV/T water thermal efficiency with various mass flow rate, when the mass flow rate increases, the thermal efficiency is raised .

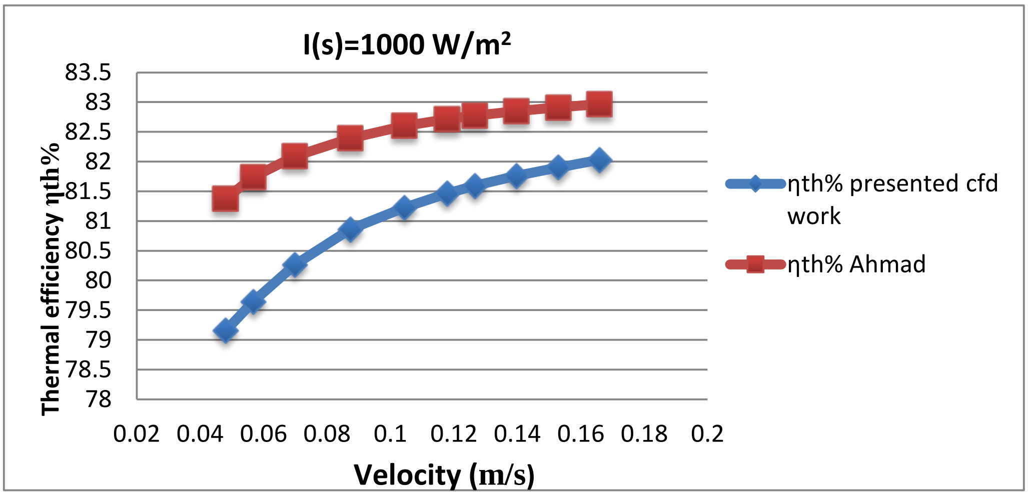

Figure3-4 Thermal efficiency with different mass flow rates for the CFD analysis results compared with [48].

3.3 Electrical Analysis for Photovoltaic PV Panel.

The maximum power flows from a maximum power point for PV Panel can be expressed as[48].

$$P_{max}=I_{max}\times V_{max} \tag{3-6}$$

Electrical efficiency (ηelc) of (PV) panel represents the maximum power of the PV panel to the solar irradiance absorbed by the solar cells. It can be calculated as [48].

$$\eta_{elc}=\frac{Pmax}{AC\times G} \quad (3\text{-}7)$$

The ratio of the maximum power to the open circuit voltage and short-circuit current is the fill factor (FF) which can be calculated as [51].

$$FF=\frac{Pmax}{Isc\times Voc} = \frac{Imax\times Vmax}{Isc\times Voc} \quad (3\text{-}8)$$

One of the most significant parameters influencing on the performance and efficiency of PV panel is packing factor (PF), the (PF) is pointing to the ratio of the single cell area multiplied by the number of cells to the area of the PV module (Am) as illustrated in the equation (3.4). Often, it has a value lower than one [51].

$$PF=\frac{Ac\times Nc}{Am} \quad (3\text{-}9)$$

The module efficiency (ηm) from the mathematical result can be calculated from cell efficiency (ηc) multiplied by packing factor (PF).

$$\eta_{m}= \eta_{elc}\times PF \quad (3\text{-}10)$$

The electrical efficiency for the PV panel that depended on temperature can be calculated from [51].

$$\eta_{elc}=\eta_{ret}\ [1-B_{ref}\,(T_{s}-T_{ref})] \quad (3\text{-}11)$$

where η_{ret}, T_{ref} are the electrical efficiency and temperature for PV panels at STC, TS PV cell base temperature, and β_{ref} temperature coefficient equals to (0.0045 °C-1) at PV cell reference temperature.

3.4 Thermal Analysis for (PV/T) combine System.

When the two fluids utilized with each other, the thermal power acquired by the dual-fluid solar collector is various compared to a traditional flat plate collector. In the presented PV/T combine system, the net thermal acquired is calculated as a combine of thermal energy participation by the air portion and the water portion.

The heat transferred from the solar radiation, fallen on the PV panels to the air and water heat exchanger attached beneath to the base surface of PV panels, is acquired by the computation of the ratio of convection which is exchanged from the basis of the PV module to the water and air which is flowed under the PV panels. Moreover, the ratio of convection is exchanged from the water and air passing to the surrounding air or versa. Depending on the energy needs and applications, the employing of two types of fluids (air and water) also generates a higher range of thermal applications. The improvement system by integrating both types of heat transporter mode is to display the best performance for PV/T technology and to get higher efficiencies [39].

The useful energy Qu ordinarily derived by Hottel-Whillier- Bliss equation [37].

$Q_u = \dot{m}\, C_p(T_o - T_i)$ (3-12)

where ṁ, C_P mass flow rate and specific heat for fluids flow and $T_{o,}$ T_i outlet and inlet temperature.

Equation (3-12) can be used to complete the calculation of the thermal efficiency ηth, which can be expressed by dividing the total useful thermal energy gained from both heat exchanger fluids air and water to the total incident solar radiation and area of the collector as in [40].

$\eta_{th} = \frac{Qu(air)+Qu(water)}{AC\times G}$ (3-13)

Equation (3-14) illustrates the relation between absorber solar radiation and thermal losses as in [51]

$Qu = A_C \times F_R\, [S - U_L\, (Ti - Ta)]$ (3-14)

S can be determined from equation (3.15)

$S = \alpha\, \tau_{pv}\, G$

The factor of heat removal efficiency F_R can be calculated from [51]

$F_R = \frac{\dot{m}\times Cp}{AC\times UL}[1-\exp[\frac{AC\times UL\times F'}{\dot{m}\times Cp}]$ (3-16)

F' is fins Corrected efficiency and it determined from [26]

$$F' = \frac{\frac{1}{UL}}{w[\frac{1}{UL(D+(W-D)f)}+\frac{1}{cb}+\frac{1}{\pi\, Di\, hfi}]} \quad (3.17)$$

f factor of fin efficiency it can be calculated from [26]

$$f = \frac{\tanh[M\,(\frac{(w-D)}{2})]}{M(\frac{(w-D)}{2})} \quad (3.18)$$

M can be calculated from [28]

$$M = \sqrt{\frac{UL}{(Kabs\times labs)+(Kpv\times lpv)}} \quad (3.19)$$

U_L equal to tub heat loss Ut can be calculated from[26]

$$U_t = \frac{1}{\frac{Ng}{\frac{c}{Tp}(\frac{Tp-Ta}{Ng+f})^{0.33}+\frac{1}{hw}}} + \frac{\sigma(Tp^2-Ta^2)(Tp-Ta)}{\frac{1}{\varepsilon p+0.05Ng(1-\varepsilon p)+\frac{2Ng+f-1}{\varepsilon g}-Ng}} \quad (3.20)$$

$f = (1-0.4hw+0.0005hw^2)(1+0.091Ng)$ (3.21)

$c = 365.9(1-0.0088\beta+0.0001298\beta^{2})$ (3.22)

From this equation it is conceivable to find the valuable heat gain of the solar collector by rearranging the equation(3.9) as in [48]

$$\eta_{th} = F_R(\tau\alpha) - F_R U_L \left(\frac{Ti - Ta}{G}\right) \tag{3.23}$$

3.5 Thermodynamic Analysis

To compute the inclusive performance and the path of energy transfer through a mechanical system, a thermodynamic analysis is used. Energy, entropy and exergy represent to the thermodynamics divaricate concepts. The exergy of a system is the higher probable useful work through a process that turns the system into thermal equilibrium state. That is, exergy is the ultimate ability of energy to produce a useful work as the system turn to the equilibrium, however irreversibility raises the entropy at the detriment of exergy [49]. Dependence on a thermodynamic approach from the first and second laws viewpoint. So, for obtaining an efficient method to analysis PV/T combine system energy and exergy analyses are produced which is referred to the first and second laws[50].

3.5.1 Energy Analysis

The energy balance for PV/T combine system as illustrated in Figure 3-8, by assumption that the system united control volume and steady state condition can be analyzed as[50][42]:

$$\sum \dot{E}_{in} = \sum \dot{E}_{out} + \sum \dot{E}_{loss} \tag{3.24}$$

$$\dot{E}_{sun} + \dot{E}_{mass,in} = \dot{E}_{elc} + \dot{E}_{mass,out} + \dot{E}_{losses} \tag{3.25}$$

$$\dot{E}_{losses} = \dot{E}_{sun} - \dot{E}_{elc} - \dot{E}_{th} \tag{3.26}$$

$$\dot{E}_{th} = \dot{E}_{mass,out} - \dot{E}_{mass,in} \tag{3.27}$$

$$\dot{E}_{th} = \dot{m}_a C_{Pa}(T_{o,a} - T_{i,a}) + \dot{m}_w C_{Pw}(T_{o,w} - T_{i,w}) \tag{3.28}$$

$$\eta_{th} = \frac{\dot{E}th}{Ac \times G} \tag{3.29}$$

The overall efficiency, η_{ov} for a (PV/T) combine system is equal to the ratio of the total gained of the combine-fluid PV/T system thermal power, to the sun power during a selected time period combined with electrical efficiency of the PV/T combine system [53]. The total overall efficiency is calculated as follows:

$$\eta_{ov} = \eta_{th,tot} + \eta_{elc} / \eta_{pp} \tag{3.30}$$

where η_{pp} is the efficiency of the power plant have value varies from 0.20 to 0.40 related to the quality of coal used [51],[41]. In this study, the value of η_{pp} tacked is 0.38 as in [52],[53].

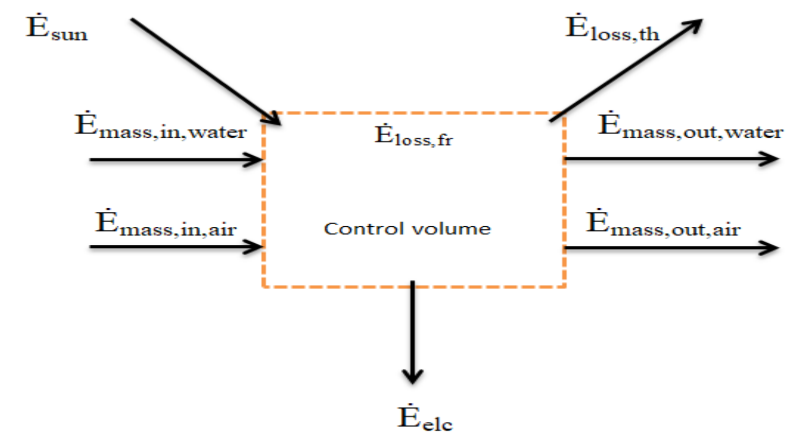

Figure3-5Energy analysis for PV/T combine system

3.5.2 Exergy analysis

Exergy represents the various between the overall energy of the system and the energy losses (unavailable energy), only when the environment and whole processes of the system are reversible. Exergy is preserved. As an exergy analysis is presented on a system, exergy is demolished whenever an irreversible process occurs, like PV/T systems. Thermodynamic imperfections can be quantified as exergy devastation, which are lost work or lost potential for generation of work. Analysing exergy demolished by each component in a process can identify what portion should be focused on to enhance system efficiency. Exergy analysis can be stated if a design of an energy system is efficient and by how its efficiency could be improved by reducing the Incompetent in the system [52]. The exergy analysis in the same way as energy analysis. Figure 3.9 illustrates the exergy pass diagram of a PV/T combine system, assuming the PV panel and the thermal collectors as a single control volume. Considering a steady state condition, the exergy analysis could be computed as follows in [53][25].

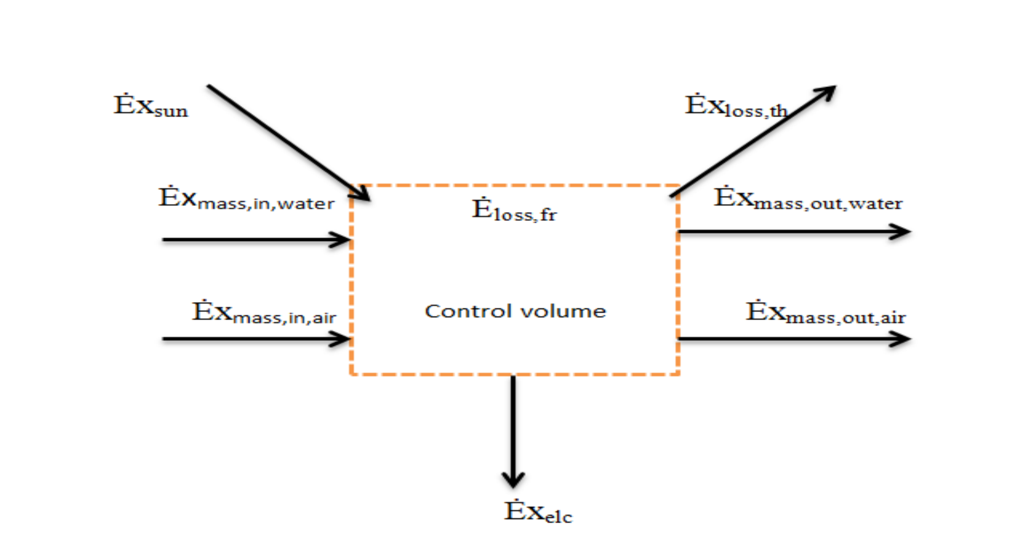

Figure3- 6Exergy analysis for PV/T combine system

$$\sum \dot{E}x_{in} = \sum \dot{E}x_{out} + \sum \dot{E}x_{loss} \quad (3.31)$$

$$\dot{E}x_{sun} + \dot{E}x_{mass,in} = \dot{E}x_{elc} + \dot{E}x_{mass,out} + \dot{E}x_{losses} \quad (3.32)$$

$$\dot{E}x_{losses} = \dot{E}x_{sun} - \dot{E}x_{elc} - \dot{E}x_{th} \quad (3.33)$$

$$\dot{E}x_{sun} = G \times AC\,[1 + \frac{1}{3}(\frac{Ta}{Ts})^4 - \frac{4}{3}(\frac{Ta}{Ts})] \quad (3.34)$$

where, T_a and T_s are the temperature of the ambient and the sun (as a black body T sun ≅ 5800 K), respectively. The exergy of the mass flow rate can be defined as in[54].

$$\dot{E}x_{th} = \dot{E}x_{mass,out} - \dot{E}x_{mass,in} \quad (3.35)$$

$$\dot{E}x_{th} = \dot{m}_w(\psi_{out} - \psi_{in}) + \dot{m}_{air}(\psi_{out} - \psi_{in}) \quad (3.36)$$

where

$$\psi_{out} = (h_{out} - h_{amb}) - T_{amb}(S_{out} - S_{amb}) \quad (3.37)$$

$$\psi_{in} = (h_{in} - h_{amb}) - T_{amb}(S_{in} - S_{amb}) \quad (3.38)$$

In the above equation, the changes in entropy, S and enthalpy, h for fluid flow can be defined as[45],[55]:

$$\Delta h = h_{w,out} - h_{w,in} = C_{P,w}(T_{w,o} - T_{w,in}) \quad (3.39)$$

$$\Delta h = h_{a,out} - h_{a,in} = C_{p,a}(T_{w,o} - T_{w,in}) \quad (3.40)$$

$$\Delta S = S_{out} - S_{in} = Cp \ln(\frac{Tout}{Tin}) \quad (3.41)$$

For water

$$\Delta S = Cp_{,w} \ln(\frac{T_{w,o}}{T_{w,in}}) \quad (3.42)$$

For air

$$\Delta S = Cp_a \ln\left(\frac{T\,a,o}{Ta,in}\right) \tag{3.43}$$

By substituting Eqs. (3.36) to (3.43) into Eq. (3.35), we have:

$$\dot{E}x_{th} = \dot{m}_w\, Cp_w[T_{\,w,o} - T_{w,in} - T_{amb} \ln\left(\frac{T\,w,o}{Tw,in}\right)] + \dot{m}_a\, Cp_a[\,T_{\,a,o} - T_{a,in} - T_{amb} \ln\left(\frac{T\,a,o}{Ta,in}\right)]$$

(3.44)

The exergy of the PV unit can be calculated as in [58]:

$$\dot{E}x_{elc} = \eta elc \times G \times AC\,[1 + \frac{1}{3}\left(\frac{Ta}{Ts}\right)^4 - \frac{4}{3}\left(\frac{Ta}{Ts}\right)] \tag{3-45}$$

The electrical and thermal exergy efficiencies of systems are equal to the ratio of the output electrical and thermal exergy, respectively, to the sun exergy during a selected time period similar to the energy analysis. So, the overall exergy efficiency for PV/T combine system can be calculated as in [58]:

$$\eta_{ov} = \frac{\dot{E}x\ th + \dot{E}xelc}{\dot{E}x\ sun} \tag{3-46}$$

Chapter Four

Experimental Study

4.1 Introduction

This chapter presents description of the experimental work that was done through this study, where all of the system components used for experimental work have been built and inaugurated in the Technical College of Najaf, Al-Furat Al-Awsat Technical University, Iraq. Geographically, the devices location is installed outdoor characterization of a photovoltaic thermal PV/T combine collector system under ambient weather conditions.

4.2 Photovoltaic Thermal (PV/T) Combine System

PV/T combine cooling system which used both air and water as cooling fluid consists of the required and appropriate components to lower the temperature of the PV panel. The first main part in the system is the PV panel to be installed and cooled at system startup. The second main part is the fluid flow collector, which contended sheet and copper pipes attached to the beneath side of PV panels. These are all surrounded by PCM filled content as shown in Figure 4-1. The third part is the water pump used to employ the cooling liquid into the thermal collector pipes of the system contains. The fourth part includes two air ducts; one above the PV panels and the other to the back side of PCM content. The fifth part is air fan used to employ the cooling air into the air ducts. In addition to the water tank and heat exchanger, the complete system was installed on a steel structure that was able be motioned at select height and select angle. The photograph of the experimental setup is shown in Figure 4-2. The schematic diagram of the complete experimental setup is shown in Figure 4-3.

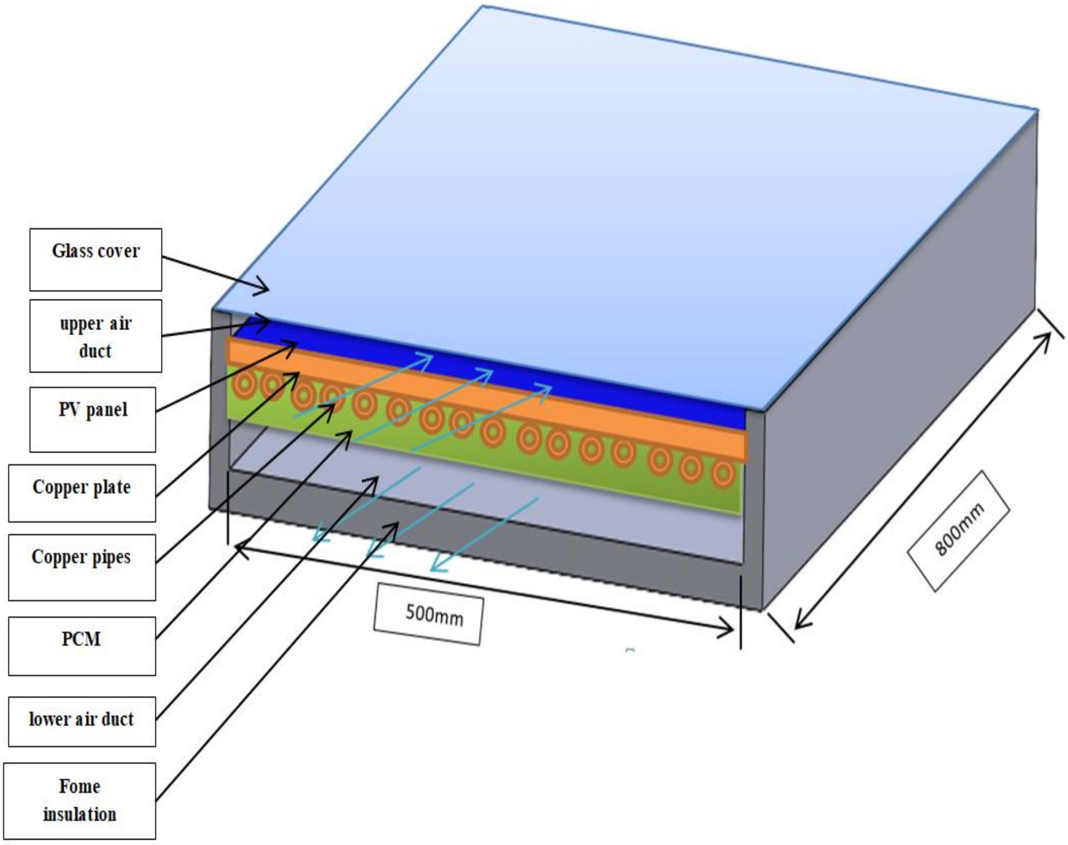

Figure4-1Section view for PV/T combine system double duct single pass

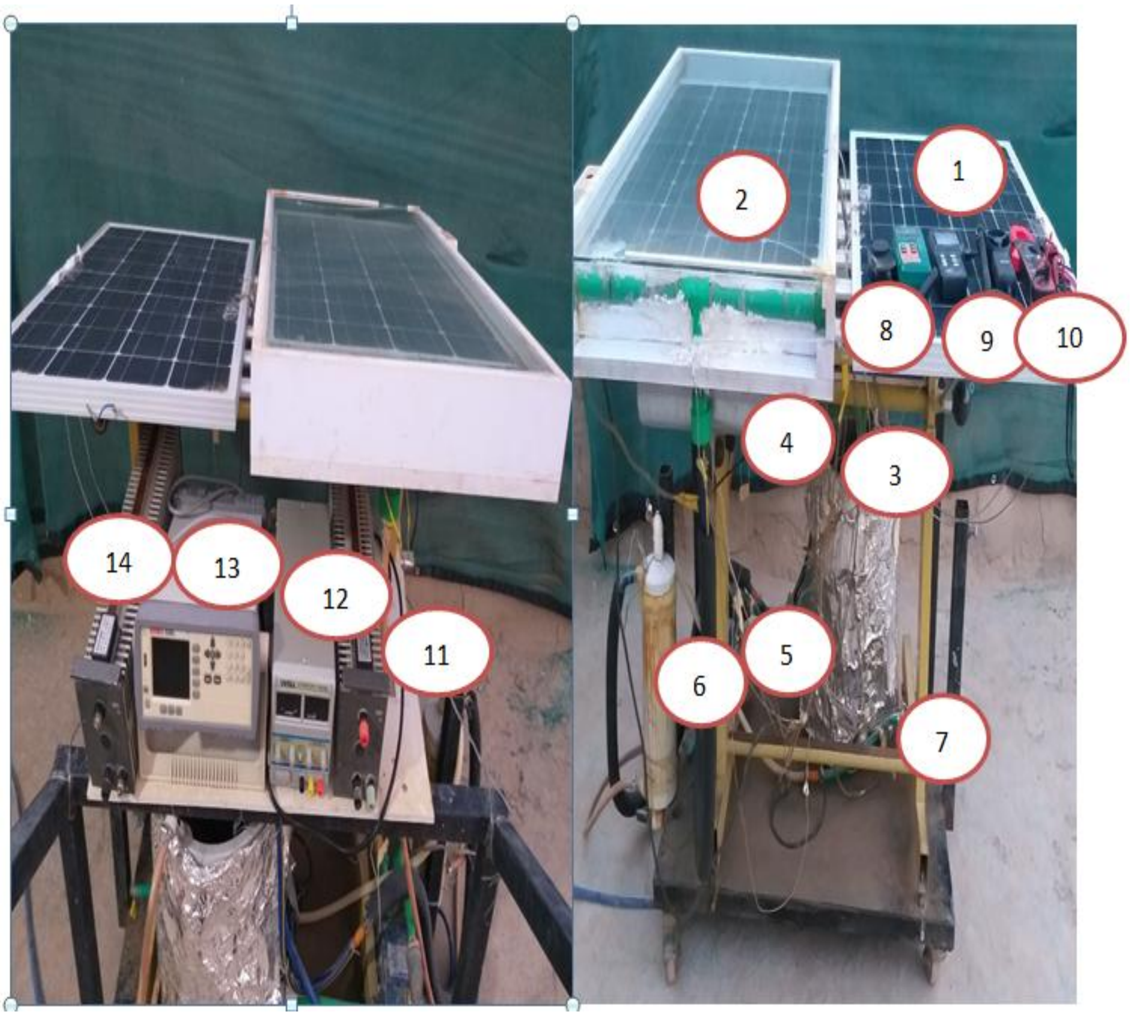

Experimental Rig Setup

1- PV panel	2- PV/T combine system	3-Storage Tank
4- Air Fan	5-Water Pump	6-Heat exchange
7- Adjustable structure	8-Pyranometer	9-Anemometer
10-Clap meter	11- and 14- variable resistance	
12-DC power supply	13-Date logger	

Figure 4-2Photograph of the experimental rig setup of the PV/T combine system with its all parts

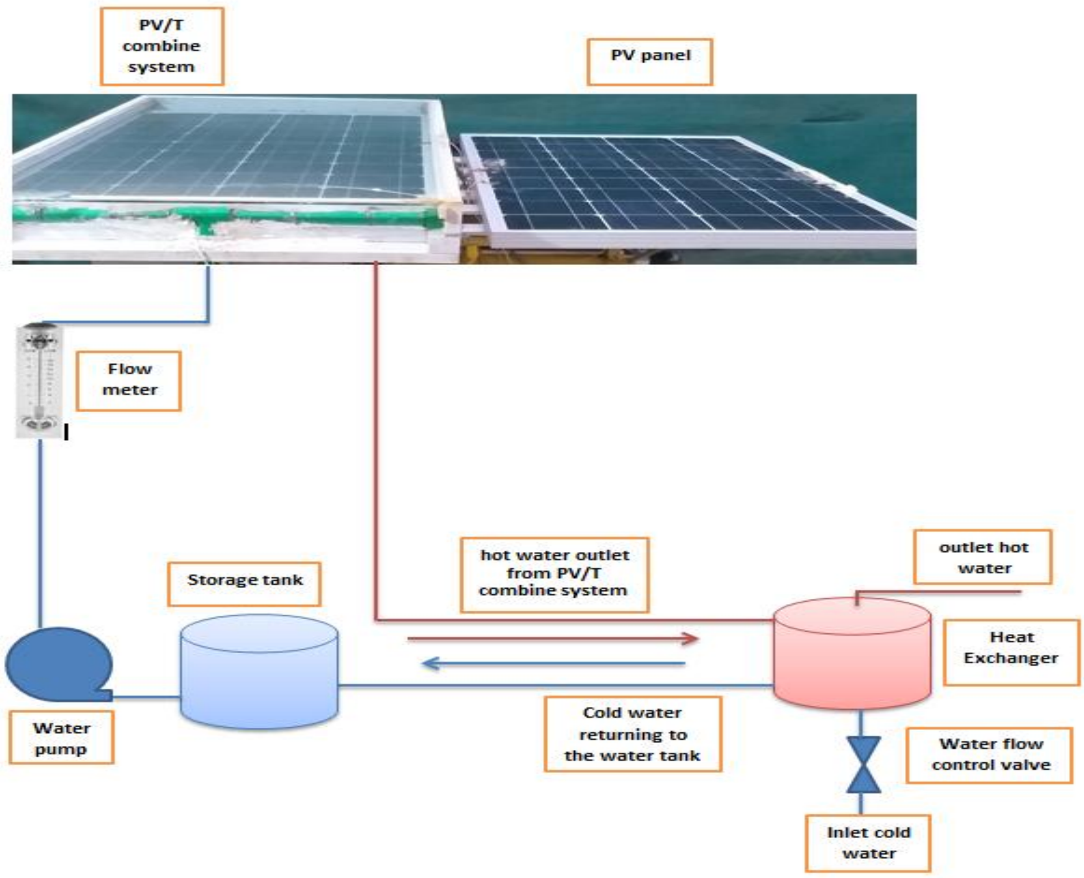

Figure 4-3Schematic diagram of the PV/T combine system

4.2.1 Photovoltaic(PV) panels.

The PV panel is the essential part of the system. The photovoltaic module (Monocrystalline) is mostly the formation of three main layers (Glass, EVA, Tedler). The devices were installed with the photovoltaic system outdoors under ambient weather test conditions, Figure 4-4, and the specifications provided in the Table 4-2.

Figure 4-4PV panel Mono crystalline type

Table 4-1 Photovoltaic PV specifications

Details	**Specifications**
Solar cell type	Mono crystalline silicon
Cell dimension (mm)	62.5*125
Module dimension (mm)	800*500
Number of cells	36
Maximum power	60W
Maximum power voltage(Vmp)	17.9V
Maximum power Current(Imp)	3.35A
Open circuit voltage (Voc)	20.8V
Short circuit current (Isc)	3.68A
Electrical efficiency(η_c)	15%
Standard Test Conditions	AM 1.5 1000W/m^2 , 25℃

4.2.2 Sheet and Tube Water Thermal Collector

The water flow thermal collector is one of the main essential parts of the PV/T combine system, attached to the back base of the PV panel as shown in Figure 4-5. The dimensions of the copper plate carefully selection are the same as the dimensions of the photovoltaic panel with 800mm length, 500mm width and 1mm thickness. The diameter and number of a copper pipes of the water flow thermal collector have been carefully selection according to the simulation result, where the best temperature distribution for PV panel.

Figure 4-5Sheet and tube water thermal collector

4.2.3 Phase Change Material (PCM) Container

Paraffin wax was used as phase change material (PCM) with specific properties as in and as illustrated in Appendix A1. It fills the content behind the PV panel and surrounds the copper tubes and the plate as illustrated in Figure 4-6. It contributes to maintaining the temperature of PV, as it draws heat from the bottom side of the PV plate and pipes and maintains heat when the sun rays are not available or after sunset.

Figure 4-6PCM container

4.2.4 Air Duct

Double pass single duct air thermal collector type was made from foam insulation material with one inlet and one outlet, where the air flow in the upper duct which was located between the class cover with 3mm thickness and upper surface of PV panel than to the lower duct which was located under the lower side of the PCM contender and foam insulation material. A plate from stainless steel was used as an absorber plate and the duct was filled with steel wool (porous media) as shown in Figure 4-7.

Figure4-7Double pass single duct with steel wool as (porous media)

4.2.5 Water Pump

The pump is also one of the main significant parts of the PV / T combine system. It is employed to circulate water into thermal collector copper pipes. The pump is a DC variable-speed pump type which consumes a maximum power of about 8W of power. It is powered by a variable DC power supply. The amount of the entering water is controlled by changing the amount of power supplied to the water pump. As a result, a flow meter may be used to measure it; therefore, varied water flow rates may be obtained. The pump characteristics and type are shown in Figure 4-8 and Table 4-3 respectively.

Figure 4-8Water Pump

Table 4-2 Pump Characteristics

Parameter	characteristics
Max-Power	8 W
Voltage	12 V
Max-Head	5 m
Max-Flow Rate	10(L/min)

4.2.6 Air Fan

The fifth essential part of the system is air fan. It works to draw air from outside to the upper duct at the top of the PV panel, passing through the lower duct. A DC variable-speed air fan was used with (12 V, 30 W, and 2800 r.p.m rated speed) as shown in Figure 4-9. It is powered by a variable power supply. The amount of the passing air was controlled by changing the fan speed by changing the amount of power supplied. So, it must be measured by air speed meter. The fan has been mounted at the lower duct.

Figure4-9DC variable-speed air fan

4.3 Measuring Devices

To list the results that will be carried out through the work system, a collection of measuring devices has been used to suit the working conditions. Calibration was performed for each device. Also, in the following paragraphs, the functions and specifications of each device are elucidated in specifics.

4.3.1 Pyranometer (Solar Power Meter)

One of the devices affecting the efficiency and performance of the PV panels is used to measure the intensity of solar radiation falling on the plate. This device has a regulation key employed to calibrate the device by testing the device in the dark, where it must be reading (0) W / m^2. For the experiment, the intensity of solar radiation is variable with time and environment weather conditions. The pyrometer device contains a sensor and LCD screen as shown in Figure 4-10. The device range and specs as shown below, in Table 4-2, and shown in Appendix (B):

Figure 4-10Solar power meter(Pyrometer) device

Table 4-3 Characteristics of Pyrometer Device.

Characteristics	Details
Maximum reading	(2000W/m^2)
Accuracy	typically, within±10W/m^2.
Angular accuracy	cosine corrected <5% for angle <60^0
Sampling time	0.25 second
Operating Temperature	0^0 C-50^0 C, moreover, Humidity: below 80% RH

4.3.2 Data Logger Device

It is a device employed to gauge the temperatures. It contains many channels as shown in Figure 4-11. It is essential to measure the PV panel surface temperature, inlet and outlet water temperature, inlet and outlet air temperature, PCM temperature. The device that was used is of the type Anpat (AT4532) with (32) channels, which is compatible with Type -K and Type- T thermocouples with (0.2 % ±1℃) to read accuracy.

Figure4-11Anpat (AT-4532x)Data logger thermometer device.

4.3.3 Anemometer

Anemometer device was employed to measure the wind speed and temperature of ambient air as well as fan speed. This measurement was taken every (15) minute. The device kind is AR-836 with two parts; the first part is a fan and a temperature sensor to calculate the temperature of air flow rate and speed. The second part includes the screen to display digital values for reading and control keys for operating and selecting unit of measurement as shown in Figure 4-12.

Figure 4-12Anemometer (AR-836) device

4.3.4 Flow-Meter

The flow meter was employed to measure the rate of water passing into the copper pipes thermal collector. Through this device, the flow velocity of the water can be known. The type of flow meter is AM-4206M as shown in the Figure 4-13. The flow-meter was calibrated by a known volume container with a stop watch.

Figure 4-13AM-4206M Flow meter device

4.3.5 Clamp meter

It is a (UNI-T) UT 203 type clamp meter device as shown in Figure 4-14. It is employed to measure the voltage and current produced by the photovoltaic PV panel at the altering load from zero ohm to the highest possible value of the resistance to calculate the maximum electrical power for the photoelectric panel performance in the case of cooling and without cooling for PV module and PV/T combine system together. For voltage monitoring in an open circuit state, the PV panel load is connected in parallel. For current measurement in a close circuit, the PV panel load is connected in the series position.

Figure 4-14(CT-9830) Clamp Meter Device

4.3.6 Power Supply

An electric power equipped device was employed to supply the requisite power to the pump and fan to control the electrical consumption as shown in the Figure 4-15. The device has two analog monitors to show the voltage and current and to know the value of power that the pump and fan needed. The pump speed can also be adjusted via the power supply device. It also has the ability to install alternating current electricity to power additional gadgets.

Figure 4-15Power Supply D.C. Device

4.3.7 Variable Resistance Load

To get the maximum electrical power for solar PV panels, the variable resistance is used that can be obtained without voltage drop, by plotting the relation between voltage and the current at the different load of resistance beginning with zero ohms. Figure 4-16 illustrates the type of different resistance used for conventional PV panel and PV/T combine system.

Figure 2-16Variable Resistance Load.

4.3.8 Thermocouples Sensor

Temperature thermocouples were put in various locations at the system to measure temperature. The thermocouples of K-type were with different lengths as shown. They were connected to the digital data logger device. The thermocouples used to measure a temperature range, as well as the accuracy ratio of the readings. All thermocouples, that were used, were calibrated in order to obtain the best temperature readings by comparing its reading with that of a mercury thermometer reading as specified in the Appendix B. To ensure the thermocouples thermal conductivity, a heat sink squeezer and an aluminum conductive heat bar were used, as shown in Figure 4-17, Figure 4-18 and Figure 4-19 respectively. They were carefully fixed at various locations as follows.

1. Six thermocouples installed on PV panel, four of them were put at equal distances on the upper surface to measure the surface temperature at various times and the other two were installed on the base surface to measure the PV panel back side.
2. Four thermocouples were distributed at various locations for PV/T combine system; two of them were at the PV base surface and the remaining two were installed at mid-depth for phase change materials (PCM) to compute temperature.
3. Two thermocouples were installed on the upper surface of PV panel for PV/T combine system to measure surface temperature.

4. Two thermocouples were put at inlet and outlet water flow bath to measure the temperature of water before inter and after leaving the PV/T combine system water collector.
5. Two thermocouples were put at inlet and outlet air flow duct to measure the temperature of air before inter and after leaving the PV/T combine system air duct.
6. One thermocouple was used to measure the ambient temperature.

Figure 4-17K-type Thermocouples

Figure 4-18heat sink squeezer

Figure 4-19

Aluminum conductive heat bar

4.4 Preparation of Nanofluids

A fluid that contains nanoparticles that are attached to it is called a nanofluid. There are two steps used to prepare the nanofluids; the first are the making of nanoparticles as a minute particles (powder- form), by physical or chemical ways, such as ablation of laser, milling, processing of sol-gel, etc. The second step is that commenting it in a liquid as a base fluid[56]. The two-step way is used for preparation. Also, the nanoparticles can be created on large range distilled water using as a base fluid to suspended MWCNT nanoparticles with 1% concentrations as shown in Figure 4-20a. To prepare the nanofluids by using two-step method, the MWCNT nanoparticles were prepared as a powder form by the manufacturer.

Gum Arabic, as shown in Figure 4-20b, has been added during the MWCNT-nanofluid preparation process, working as surfactant which surfaces active agents that assist to lower the surface tension of a liquid and the interfacial tension of a two-phase system. The MWCNT nanoparticles suspended the process in distilled water made by TELSONIC ULTRASONICS CT-12 with 12 liters volume container device as shown in Figure 4-20c. 60 minutes of ultra-sonication was shown to be the most stable time for the MWCNT-nanofluid samples as in .

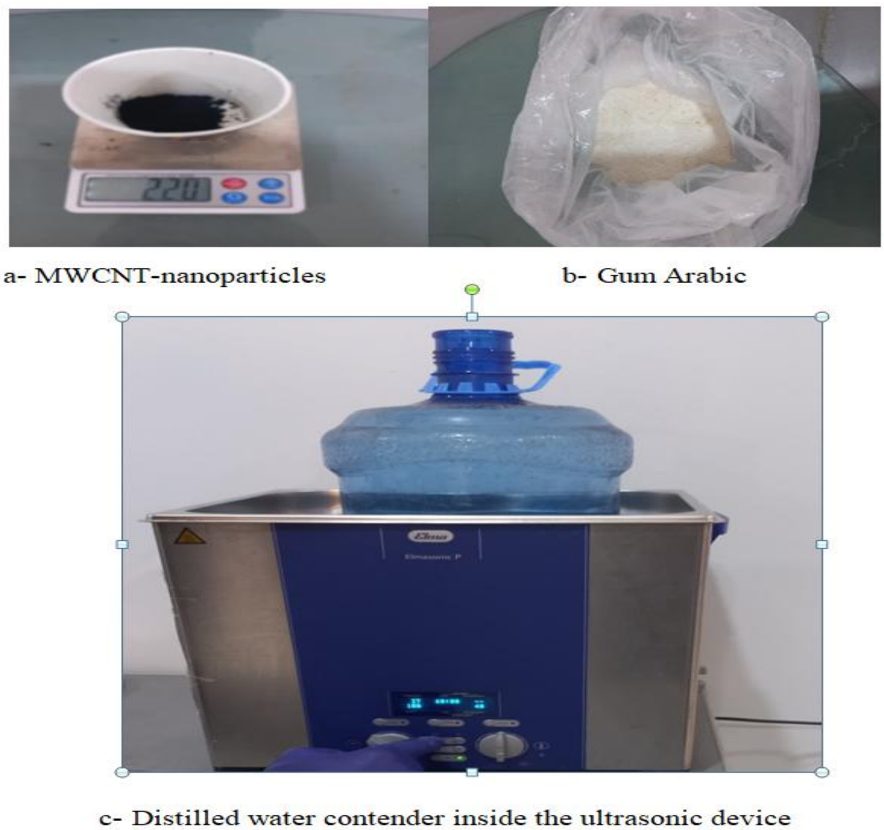

Figure4-20MWCNT-nanofluid preparation step

4.5 MWCNT-Nanoparticles Thermo-physical properties

For all kinds of nanoparticles, density, thermal conductivity and viscosity represent the main thermo-physical properties on which the properties of the nanofluid product depend on. Table 4-1 indicates the properties of the MWCNT–nanoparticles used in this experiment specified by the manufacturer (Guangzhou Hongwu Material Technology Co., Ltd.) which were used to prepare the nanofluids.

Table 4-4 Characteristics of the MWCNT-nanoparticles

Details	**Characteristics**
Nanoparticles type	MWCNT

Appearance	Black powder
Purity	99%
Thermal conductivity K_{np} (W/m.k)	3000
Density $\boldsymbol{\rho}_{np}$ (kg/m^3)	2100
Specific heat Cp_{np} (J/kg.k)	796
Size (nm)	D: 30-60 nm , L: 5-20 um

4.6 MWCNT-nanofluids Thermo-Physical Properties

Distilled water is chosen as the base fluid with characteristics that are affected by temperature, which were determined by using the water's average temperature. The thermal conductivity, density, specific heat, and viscosity of the base fluid can be calculated as in [2],[57] . It is worth noting that the temperature unit used in these equations is Kelvin.

$$k_{bf} = 0.6067(-1.26523+3.704(\frac{T}{298.15})-1.43955(\frac{T}{298.15})^2) \quad (4\text{-}1)$$

$$\rho_{bf} =(-0.00448).T^2+ 999.9 \quad (4\text{-}2)$$

$$C_{p,bf} =(-0.0000463).T^3+(0.0552).T^2-(20.86).T+6719.637 \quad (4\text{-}3)$$

$$\mu_{bf} = (0.00002414.(10^{(\frac{247.8}{T-140})}) \quad (4\text{-}4)$$

after calculated the thermo-Physical Properties of a base fluid (distilled water) from the above equations, These properties will be entered into the equations for calculating the properties of nanofluids as in [2],[60].

$$\rho_{nf} = \Phi.\rho_n + (1- \Phi).\ \rho_{bf} \quad (4\text{-}5)$$

Φ is nanofluid volume fraction that can be fined from

$$\Phi= \frac{\frac{mn}{\rho n}}{\frac{mn}{\rho n}+\frac{mbf}{\rho bf}} \quad (4\text{-}6)$$

$$C_{p,nf} = \frac{\Phi.(\rho n\ Cp,n)+(1- \Phi).(\rho bf\ CP,bf)}{\rho nf} \quad (4\text{-}7)$$

4.7Experiment Procedure

1- The measurement devices must be placed and secured in place after all of the PV/T combined system elements have been assembled. The measurement devices that were utilized can be explained as follows

a- Solar radiation measuring: The solar radiation meter is positioned at the same tilt angle of the bounty collector . Direct incident radiation is measured every 15 minutes. The work starts from 7 am to 8 pm.

b- Wind speed and ambient temperature measuring: An anemometer probe is placed near the PV/T combined system to measure wind speed every 15 minutes. The ambient temperature is also measured by placing an anemometer probe in the shade every 15 minutes.

c- Both the air fan and the water pump are turned on 15 minutes before taking the readings to reach the steady state

2- The measuring devices work from the time the experiment began from 7:00 in the morning until 8:00 in the evening.

3- Readings are recorded either manually (such as recording data of solar radiation, ambient temperature, and wind speed) every 15 minutes or automatic recording (temperatures) from data logger device (such as inlet ,outlet water and air temperatures (Tb) for PV,PCM .

4- Experiments were conducted on the surface Technical Engineering college of Najaf/Iraq. The work was carried out from June 2021 to July 2021. Using water and air as cooling fluid was carried out in June, and experiments using MWCNT-nanofluids and air as cooling fluid were carried out in July 2021.

CHAPTER FIVE

Results and Discussion

5.1 Introduction

The governing equations for the suggested photovoltaic thermal PV / T combine system for the electrical and thermal performance were specified. These equations were solved by using the COMSOL simulation program to determine the best design module. The theoretical and practical results were gathered as follows:

1- The numerical analysis of the PV / T water system were conducted for selecting the best design by using COMSOL Metaphysics program.

2- The outcomes of the experiment of the PV / T combine system were acquired from the experimental readings and the readings gather from the equipment and devices used in the tests work. These results will be presented and discussed later in this chapter.

5.2 Numerical Analysis

Achieving the preferable design by using COMSOL simulation program to improve the performance and efficiency of the PV solar panels. Depending on the temperature distribution on the surface of the PV panels and the temperature of the water coming out of the copper pipes after the heat exchange process that occurs between the bottom surface of the panels and the water passing through the copper pipes, the best design of the water heat exchanger has been determined.

Figures and Table 5-1 and Table 5-2 illustrate the simulation results of the modeling structure for the suggested water thermal collector. The simulation results showed that the best diameter of copper pipes was with (8 mm for the inner diameter and with 10 mm for the outer diameter) and the best number of copper pipes that can be used in the thermal water collector are 16 distributed under the PV solar panel as shown in Figure5-3.

5.2.1 Modeling Water Thermal Collector Based on the Diameter and Number of Water-Passing Pipes

The Comsol CFD program simulation result illustrated the optimum water collector design with 8mm inner copper pipes diameter and 16 pipes, distributed under the base of PV panel as shown in Table 5-1. This design was determined because it had the lowest temperature distribution and the highest temperature of the outlet water, among the other different designs that were of different diameters and different distribution of the number of pipes as shown in Figure 5-1 and Figure 5-2.

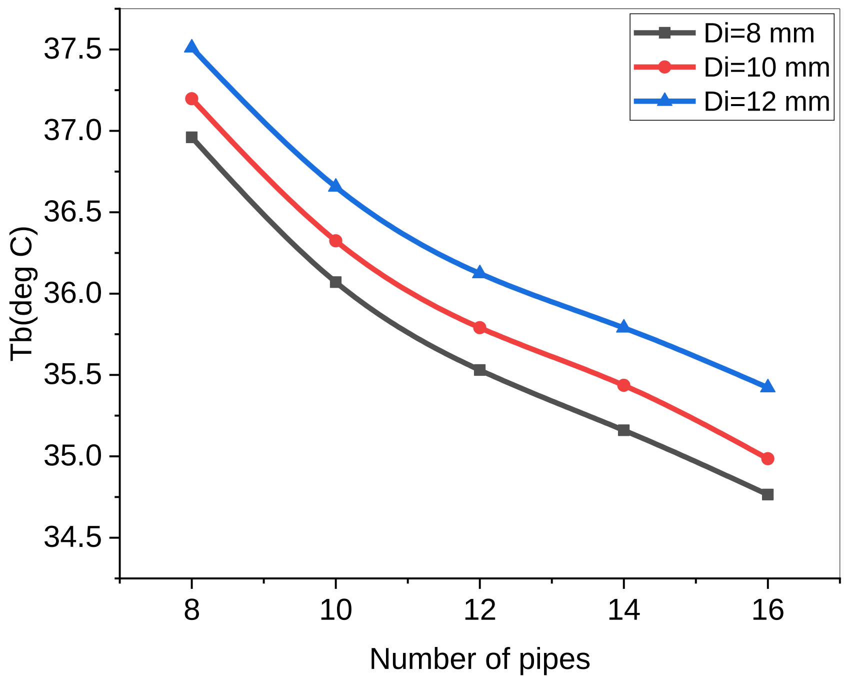

Figure5-1 Change in base temperature (Tb) with different pipes diameter and number of pipe

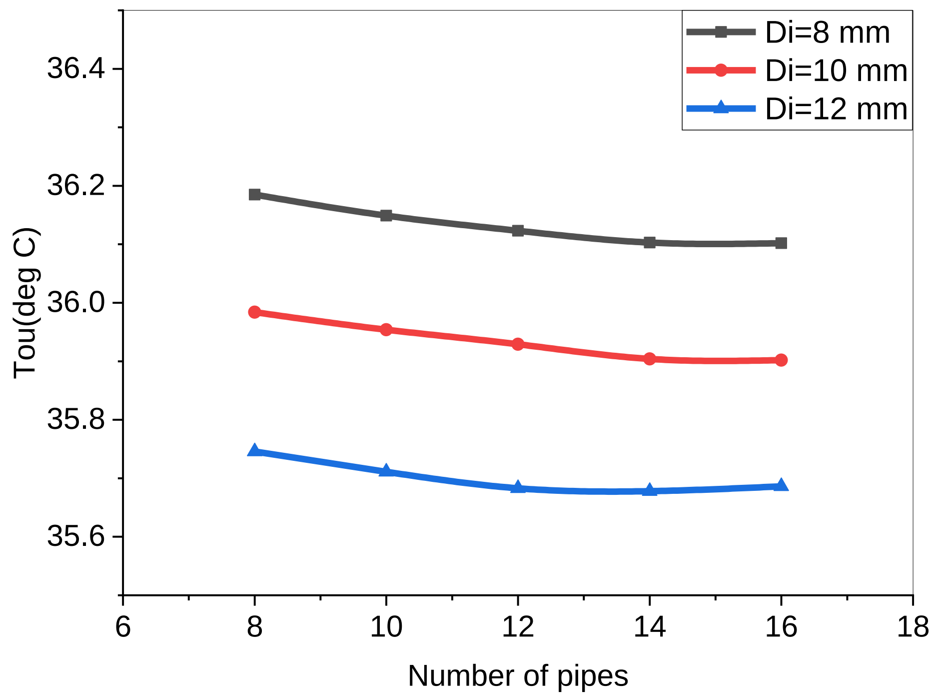

Figure5 -2Change in outlet water temperature (Tout) with different pipes diameter and number of pipe

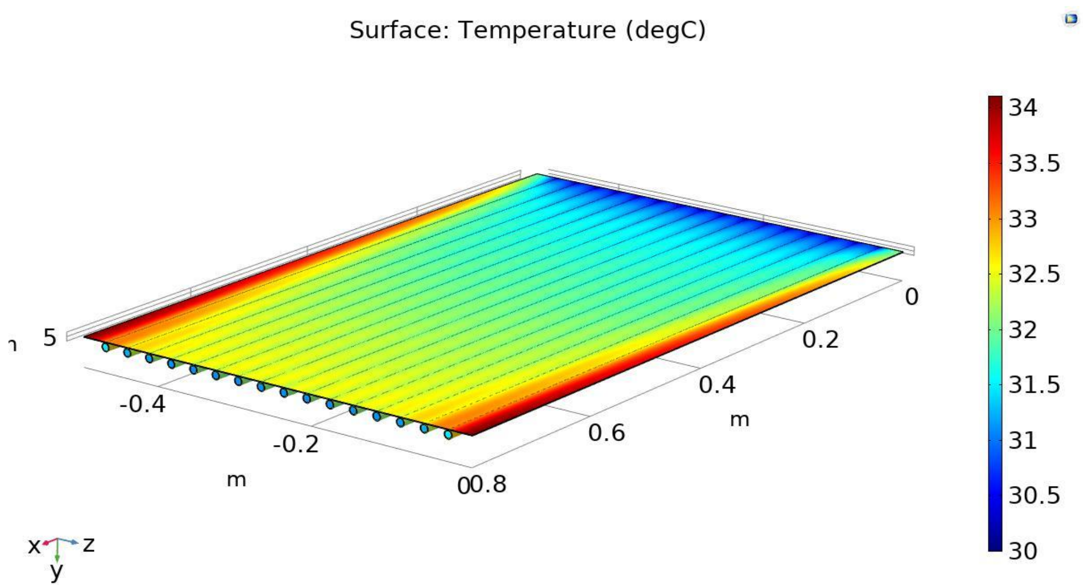

Figure5-3 Temperature distribution for the optimum design

Table 5-1Thermal distribution gained from the simulation results for different collector design

NO.	Pipes number	Thermal distribution								
		Din=8mm			Din=10mm			Din=12mm		
		Tb (℃)	Tin (℃)	Tout (℃)	Tb (℃)	Tin (℃)	Tout (℃)	Tb (℃)	Tin (℃)	Tout (℃)
		36.86	30	36.18	36.97	30	35.98	37.51	30	35.74
1	8	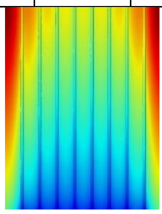			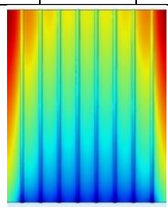			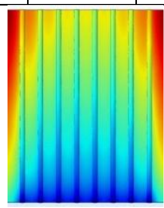		
2	10	35.9	30	36.14	36.04	30	35.95	36.49	30	35.71
		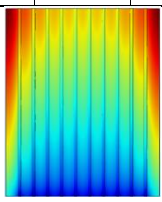			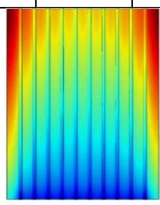			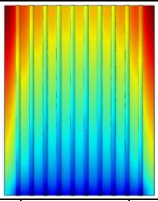		
3	12	35.37	30	36.12	35.49	30	35.92	35.91	30	35.68
		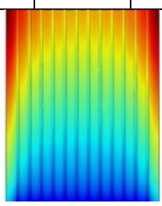			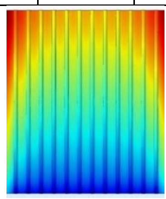			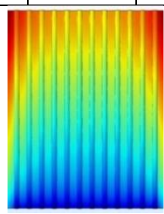		
4	14	35	30	36.10	35.10	30	35.9	35.46	30	35.67
		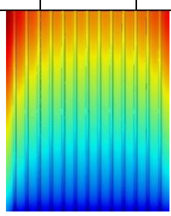			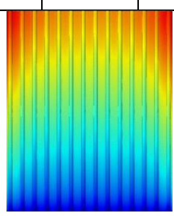			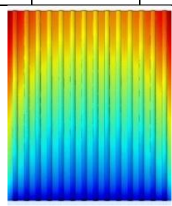		
5	16	34.7	30	36.10	34.85	30	35.9	35.18	30	35.68

		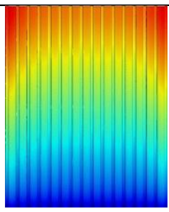	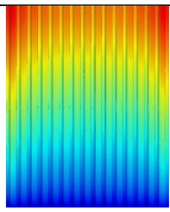	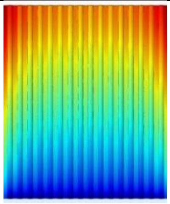

5.2.2 Modeling the Optimum Water Thermal Collector Based on Variation in the Flow Rate.

Figure 5-4 and Figure 5-5 illustrate the reduction that occurs in both base temperature (Tb) and outlet water temperature (Tout) as volume flow rate increased from (1-5) L/min at 1000W/m^2 solar radiation and as shown in the Table 5-2.

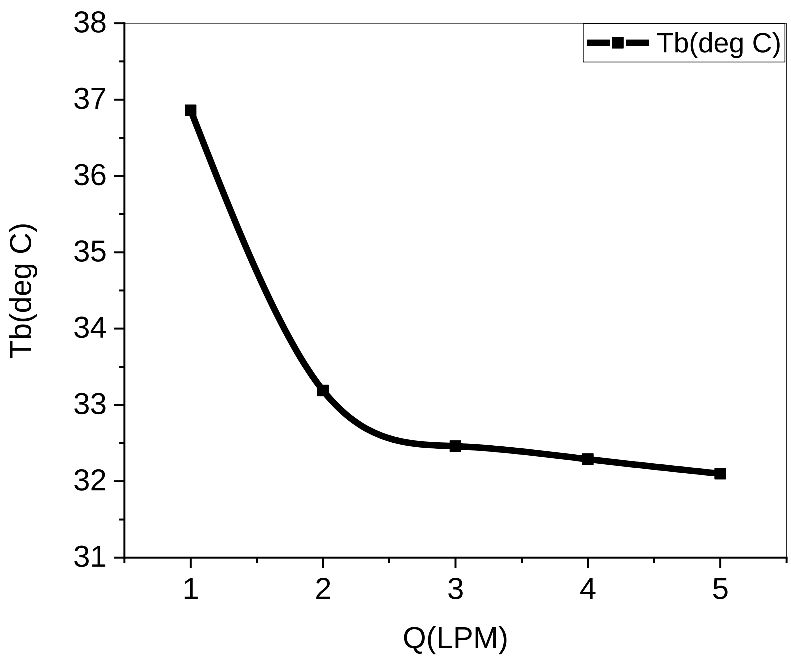

Figure5-4 Variation in base temperature(Tb) with different volume flow rate

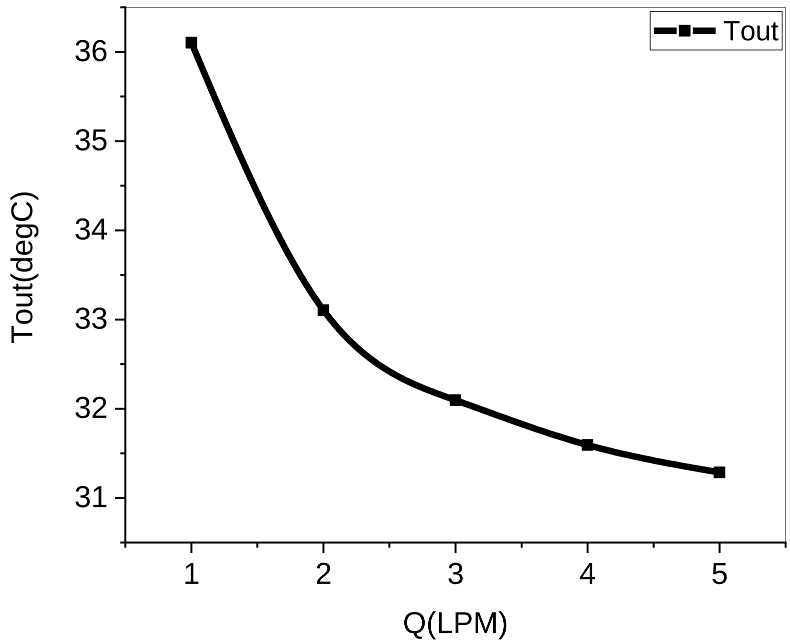

Figure5-5 Variation in outlet water temperature (Tout) with different volume

Table 5- 2Thermal distribution for optimum design gained from the simulation results by changing the flow rate

No.	Thermal Distribution	Din (mm)	Number of pipes	m ($\frac{L}{min}$)	Tb (°c)	Tin (°c)	Tout (°c)
1	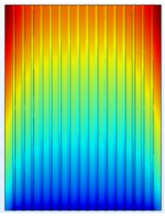	8	16	1	36.86	30	36.18
2	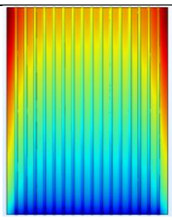	8	16	2	33.189	30	33.105
3	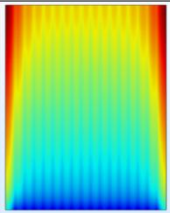	8	16	3	32.593	30	32.096

4	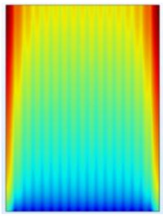	**8**	**16**	**4**	**32.289**	**30**	**31.594**
5	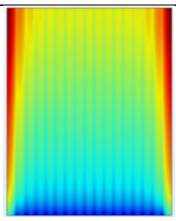	**8**	**16**	**5**	**32.1**	**30**	**31.286**

5.3 Experimental Analysis

The actual objective of this section is to test the effective and practical performance and efficiency of the PV/T combine double base single air duct system with phase change materials (PCM), porous media by integrated air and water in addition to Multi-walled carbon nanotube (MWCNT) nanofluid as a heat removable medium. The experimental work has been built and inaugurated in the Technical College of Najaf, Al-Furat Al-Awsat Technical University, Iraq. Geographically, the devices location is installed outdoor; via characterization of a photovoltaic thermal PV/T combine collector system under ambient weather conditions for the selected day of June and July from 7am to 8pm. The readings were taken and recorded every 15 minutes. A comparison was made for PV/T combine system under two modes of fluids; flow air plus water and air plus MWCNT-nanofluid with conventional PV and without any cooling system under different mass flow rate for air, water and MWCNT-nanofluid. The results of the practical tests were obtained under the influence of various parameters that have an actual effect on the performance of the PV/T combine system, such as mass flow rate for air, water, ambient temperature, solar irradiance, wind speed. In order to know the possibility of combining photovoltaic panels PV and thermal collectors, these parameters have been carefully analyzed because these parameters have the ability to show whether the combine thermal collector of air and water can enhance the electrical performance of the photovoltaic panels PV.

5.3.1 Photovoltaic (PV) Module (without thermal collector)

Rising in cell temperature leads to an increase in self-concentration and the value of reverse saturation current rises as illustrated in Figure 5-6. However, it reduces the amount of the circuit voltage, as illustrate in Figure 5-7. It causes a decrease in the maximum amount of energy generated by the cell, as shown in Figure 5-8, because the current and voltage represent the main parameters that the electrical power generated by the cell depends on [58].

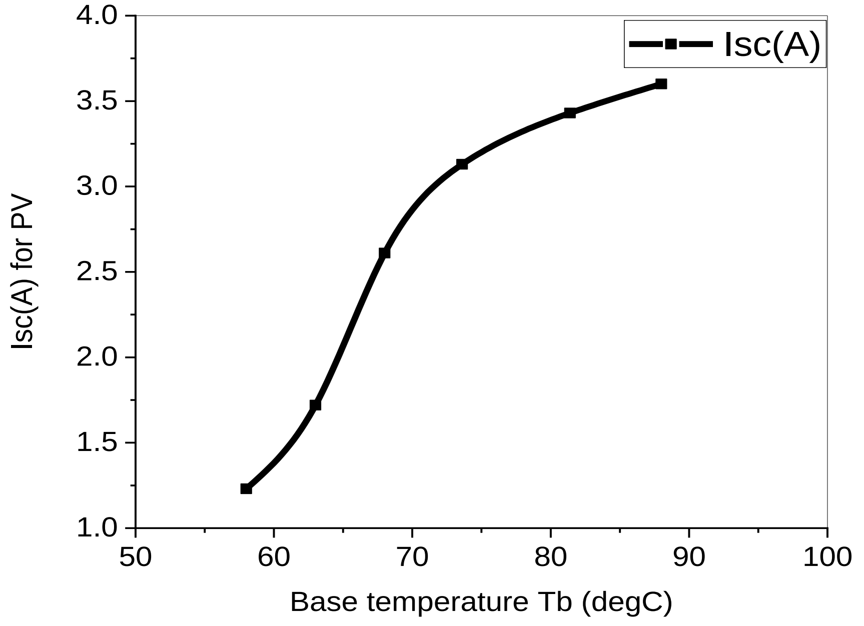

Figure5-6Variation in short circuit current (Isc) with the base temperature (Tb)

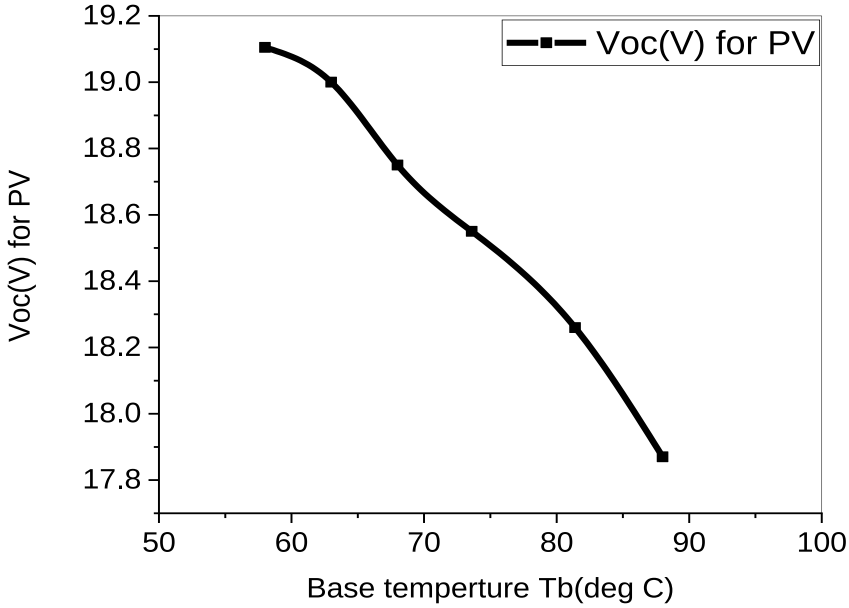

Figure5-7 Variation in open circuit voltage (Voc) with the base

Moreover, the variation in maximum power (Pmax) has been specified clearly as in Figure 5-8 and Table 5-3 which indicate an increase in power from 16.04 W to 52.447 W, when the solar radiation is increased from 300W/m^2 to 1200 W/m^2.

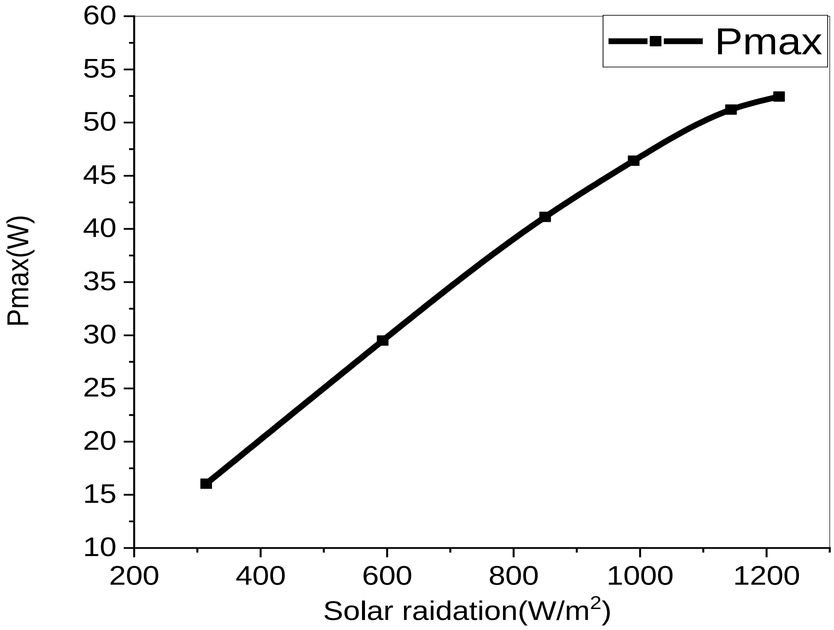

Figure5-8 Variation in maximum power (Pmax)for PV module

The electrical efficiency for PV module is decreased from 12.77 % to 10.74% when the solar radiation is raised from 300 W/m^2 to1200 W/m^2.

Table 5- 3Specifications of PV module with various solar radiation

Property	**case**				
	solar radiation(W/m^2)				
	300	**500**	**700**	**900**	**1200**
Ambient temperature Ta (℃)	38.7	39.9	42	44.3	49.7
Surface temperature Ts (℃)	58	63.76	73.876	81.23	84.543
Base temperature Tb (℃)	59.6	64.67	75.634	83.456	88.23
Electrical efficiency η_{elc}(%)	12.77	12.435	12.097	11.193	10.74
Maximum power [Pmax(pv)](W)	16.04	29.49	41.13	51.219	52.447
Open circuit voltage Voc(V)	19.05	19	18.75	18.55	17.87
Short circuit current Isc(A)	1.23	1.72	2.61	3.13	3.6

Compared to the characteristics of PV module at Standard Test Conditions STC, the PV module indicated much reduction in efficiency. The PV module generated Voc = 20.8 V, Isc = 3.68 A with (STC), and the electrical efficiency reached to15% by the manufacturer, as mentioned in Table 4-1 in chapter four. Accordingly, the power and efficiency amounts with experimental work conditions indicated reductions compared to the ones produced by the manufacturer because that the electrical efficiency of PV module has been reduced as its temperature raises. During working the base, temperature (Tb)of the PV module raised to 88 ℃ and this will drive to a reduction in energy and efficiency.

5.3.2 Photovoltage Thermal PV/T Combine System with Water and Air as a Cooling Fluid

The test for PV/T combine system experimentally was performed under ambient weather conditions from the intensity of solar radiation, the ambient temperature and wind speed. During the tests, PV module was used near to PV/T combine system to ensure that it was exposed to the same ambient weather conditions and the data is received from them at the same time. This test was conducted to find out the effect of fluids (water, air) mass flow rate as a coolant on the electrical and thermal performance of the PV/T combine system and to determine the best mass flow rate, under selected water mass flow at (0.0166,0.033 , 0.05,0.066, 0.0833) kg/s and air mass flow at (0.0244,0.0317 ,0.0504) kg/s. The temperatures (Ambient, Inlet water, Outlet water, PV module (back and front) and PV/T collector (back and front) were read and recorded to find the power and efficiency for PV module and PV/T combine system. The readings produced by the PV/T combine system were analyzed and compared to the conventional PV module.

5.3.2 .1 Influence of Water Mass Flow rate Change

In this test, the performance of PV/T combine system was investigated under different water mass flow rate (0.0166,0.033,0.05,0.066) kg/s with constant air mass flow rate at 0.0244kg/s.

a. Base Temperature (Tb) .

As operational temperatures rise, the conversion efficiency of PV cells from solar energy to electricity drops[5]. The increased in solar radiation leads to an increase in the temperature of the base surface (Tb) of the PV panels for PV/T combine system as illustrated in Figure 5-9 and specified in Table5-4. Also, it shows the reduction that occurs in (Tb) as water mass flow rate increased reaching to 0.05 kg/s water mass flow rate. After this, the basic temperature (Tb) does not fluctuate significantly. At lower solar radiation 300 W/m^2, the base temperature (Tb) reached to (43.8,42.4,41.2, 40.934) ℃ at water mass flow rate (0.0166 , 0.033,0.05 ,0.066) kg/s. At higher solar radiation at 1200 W/m^{2,} the base temperature reached to (57.9 ,55.8 ,53.5 53.235) ℃ at water mass flow rate (0.0166 ,0.033 ,0.05 ,0.066) kg/s. It also illustrates the increase in the mass of water flow contributes significantly to lowering the base temperature (Tb) with constant air mass flow at 0.0244kg/s. The greatest reduction in base temperature was obtained at 0.05kg/s water mass flow rate under different solar radiation.

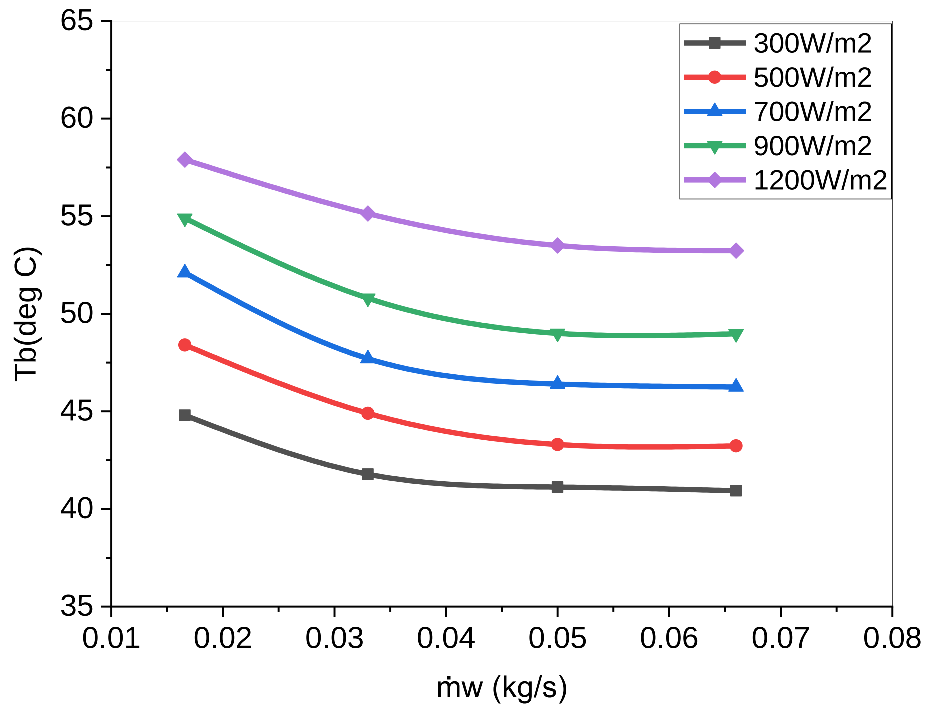

Figure5-9 Variation in base temperature(Tb) under different solar radiation and water mass flow

a. Open Circuit Voltage (Voc)

In PV, module linear dropped in open circuit voltage (Voc) at an increasing temperature rates [59]. This change can be seen visibly as in Figure 5-10 and illustrated as in the Table 5-4. It also shows the rising that occurred in (Voc), when mass of water flow increased under different solar radiation, at lower solar radiation 300W/m^2 the (Voc) value, reached to (19.34, 19.37, 19.7) V at (0.0166 ,0.033,0.05) kg/s and when the solar radiation was increased to1200 W/m^2, the (Voc) decreased and reached to (18.44, 18.83, 19.31) V as shown in Figure 5-10. The highest values were obtained in (Voc) at 0.05kg/s under different the solar radiation because it has the lowest surface temperature (Tb).

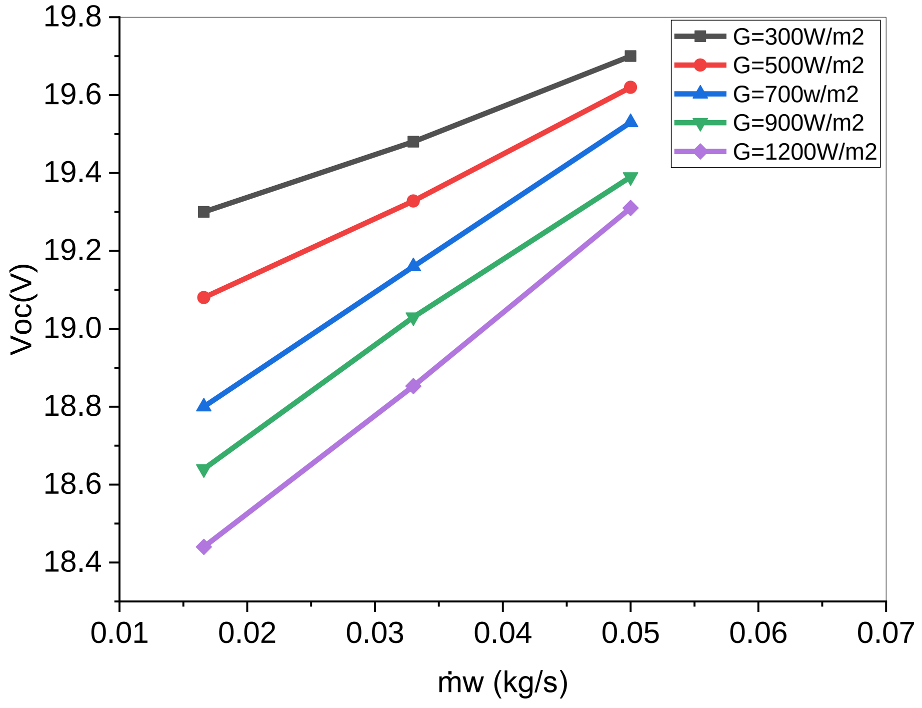

Figure5-10 Variation in open circuit voltage(Voc) under different solar radiation and water mass flow rate

b. Short Circuit Current (Isc)

As for the results of the oscillation of the temperature for PV module, the Isc raised proportionally with the increase in solar radiation from 300W/m^2 to 1200 W/m^2 .This is because of the raise in the production of electron-hole pairs by thermal energy [60]. As shown in Figure 5-11 and as illustrated in the Table 5-4, when the mass of water flow rate increased, the (Isc) decreased under all solar radiation rates, where the (Isc) values were (1.14, 0.95, 0.79) A at (0.0166, 0.033, 0.05) kg/s with lower solar radiation and when the solar radiation increased to 1200W/m^2 the (Isc) values reached to (3.88, 3.6, 3.27) A as shown in Figure 5-11, the highest reduction in the current was obtained at 0.05kg/s.

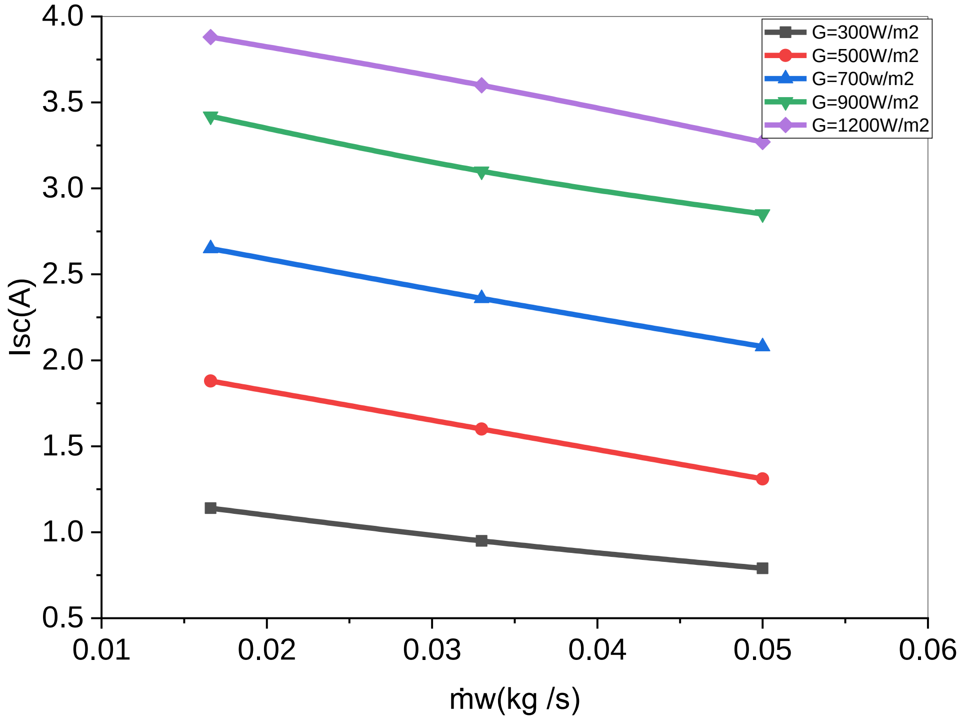

Figure5-11 Variation in short circuit current (Isc) under different solar radiation and water mass flow rate

Table 5- 4 Characteristics of PV/T Combine System with Water and air for different Solar Radiation and at ṁw = 0.05kg/s

Property	**Case**				
	Solar Radiation (W/m^2)				
	300	**500**	**700**	**900**	**1200**
Ambient temperature T_a (°C)	35.9	38.6	40.5	44.1	44.6
Inlet water temperature T_{in} (°C)	33.4	37.1	37.8	38.1	38.2
outlet water temperature T_{out} (°C)	33.7	37.8	39.7	40	40.2
$\Delta T = [T_{out} - T_{in}]$ (°C)	0.3	0.7	1.7	1.9	2
Inlet air temperature T_{in} (°C)	37.2	40.9	42.5	46.5	48.4
outlet air temperature Tout (°C)	40.3	44	45.4	49.1	50.7
ΔT =[Tout- Tin] (°C)	3.5	3.1	2.9	2.6	2.3
Surface temperature T_s (°C)	37.2	40.4	42.2	43.6	44.9
Base temperature T_b (°C)	42.2	43	49	52.6	53.5

Reduction in surface temperature (°C) $\Delta Ts = [T_{s\,(PV)} - T_{s\,(PV/T)}]$	22.1	23.9	33.1	45.1	50.4
Reduction in base temperature (°C) $\Delta T_b = [T_{b\,(PV)} - T_{b\,(PV/T)}]$	15.8	20	21.6	28.8	34.5
Electrical efficiency η_e (%)	13.839	13.785	13.38	13.137	13.076
Percentage increase in electrical efficiency (%) $[\eta_{(PV/T)} - \eta_{(PV)}] / \eta_{(PV)}$	8.349	10.856	12.052	17.367	21.667
Enhance electrical efficiency (%) $\eta_{enhance)} = \eta_{(PV/T)} - \eta_{(PV)}$	1.0665	1.35	1.458	1.944	2.328
Maximum Power $P_{max\,(PV/T)}$ (W)	17.381	32.69	46.088	60.114	63.812
Water pump power consumption $P_{(pump)}$ (W)	3.5	3.5	3.5	3.5	3.5
Air fan power consumption P(fan) (W)	2.5	2.5	2.5	2.5	2.5
Enhance Power (W) $P_{(enhance)} = [P_{max(PV/T)} - P_{max(PV)} - P_{(pump)} - P(fan)]$	-4.66	-2.797	-1.042	2.895	5.364
Open circuit voltage V_{oc} (V)	19.7	19.62	19.53	19.39	19.31
Short circuit current I_{sc} (A)	0.79	1.31	2.08	2.51	3.27

5.3.2.2 Influence of Air Mass Flow Rate Change

The effect of changing the mass of the air passing was tested by changing the fan speed on the electrical and thermal performance of the PV/T combine system with constant water mass flow, after the best performance was obtained in the previous test when the mass of water was 0.05 kg/s in terms of electrical efficiency and base temperature (Tb), open circuit voltage (Voc), short circuit current (Isc). This test was conducted under different air masses flow at (0.0244,0.0317,0.0504) kg/s.

a. Base Temperature (Tb)

As shown in Figure 5-12, the increase in the amount of incident solar radiation from 300W/m^2 to 1200W/m^2 leads to a raised in base temperature (Tb) from 41.2°C to 53.5°C when the air mass was 0.0244 kg/s. It also shows the lower solar radiation

300W/m^2 (Tb) values which reached to (41.2, 43.8, 44.2) ℃ at (0.0244, 0.03167, 0.0504) kg/s mass of air passing, and at higher solar radiation 1200W/m^2 (Tb) values which reached to (53.5 , 56,57.9) ℃ with (0. 0244 ,0.03167,0.0504) kg/s mass of air passing. The reason for this rise in (Tb) is due to the decrease in the time required for heat exchange with an increase in the amount of air mass passing.

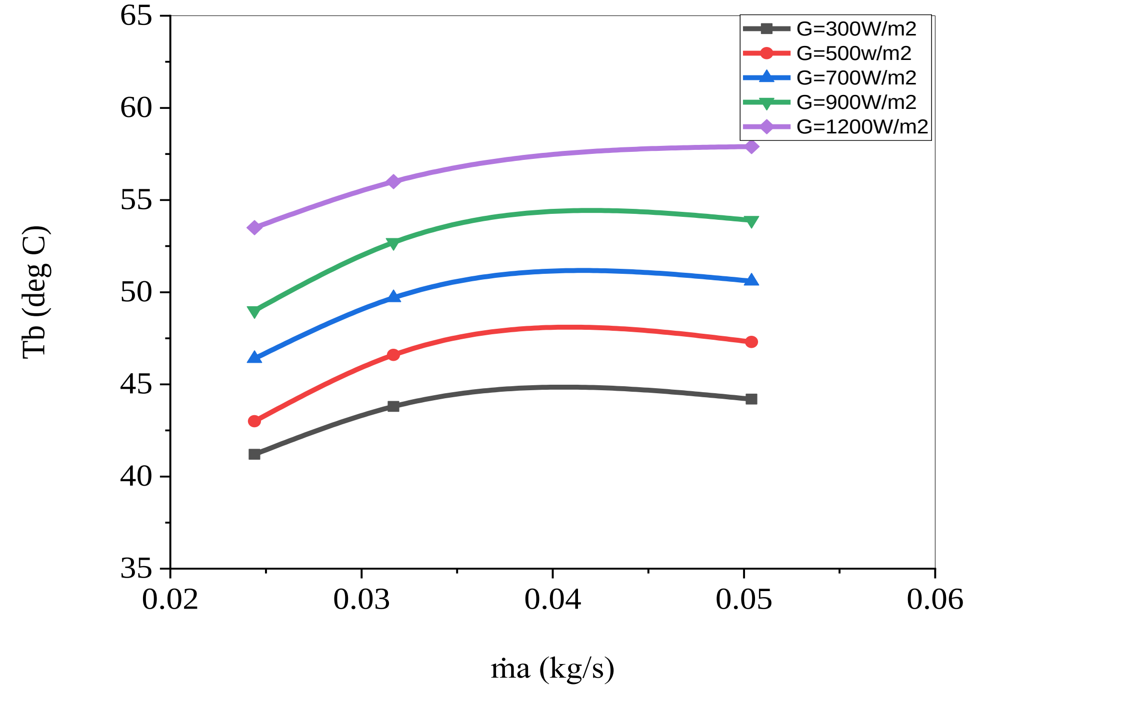

Figure5-12 Variation in base temperature(Tb) under different air masses flow and solar radiation

b. Open Circuit Voltage (Voc)

Figure 5-13 illustrates a linear drop in open circuit voltage (Voc) when the solar radiation increase as a result of the high temperature of the PV panel, where at lower solar radiation 300 W/m^2, the (Voc) reached to (19.8,19.622,19.26) V at (0.0244 ,0.03167,0.0504) kg/s and (19.31 ,18.9 ,18.12) V at 1200W/m^2 at the same air mass flow rate, under different solar radiation. The highest voltage values were obtained at 0.0244 kg/s air mass flow as shown Figure5-13 and specified in Table5-5.

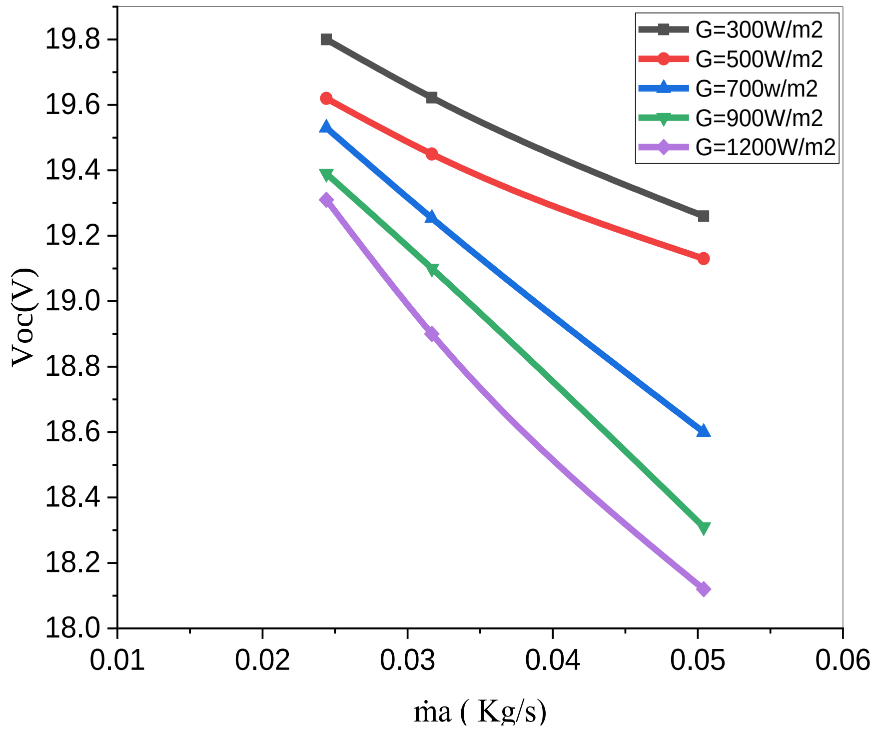

Figure5 -13Variation in (Voc) under different air masses flow and solar radiation

c. Short Circuit Current (Isc)

Figure 5-14 shows the linear increase in short circuit current (Isc) with the increase in the amount of solar radiation. It shows, at lower solar radiation 300 W/m^2, the (Isc) value which reached to (0.79,1.08,1.81) A and to (3.27,3.38,3.872) A at 1200W/m^2 solar radiation under the same air mass flow rate at (0.0244, 0.03167, 0.0504) kg/s as specified in Table 5-5.

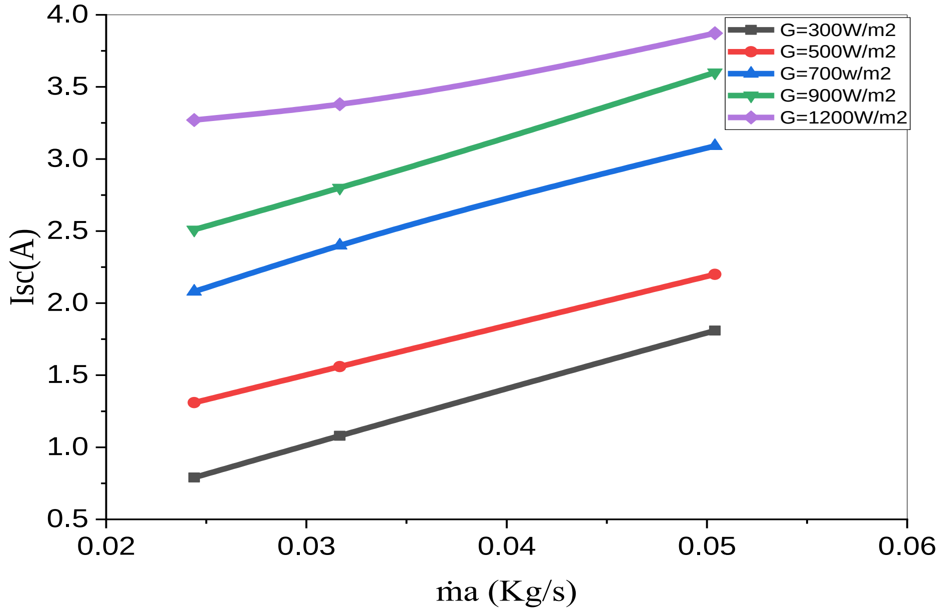

Figure5-14Variation in (Isc) under different air masses flow and solar radiation

Table 5- 5Characteristics of PV/T combine system at ṁw = 0.05kg/s and 1200 W/m2 solar radiation

Property	**Case**		
	Air mass flow (kg/s)		
	0.0244	**0.03167**	**0.0504**
Ambient temperature T_a (°C)	44.6	48.7	47.6
Inlet water temperature T_{in} (°C)	38.2	39.9	39.1
outlet water temperature T_{out} (°C)	40.2	41.6	41.6
$\Delta T = [T_{out} - T_{in}]$ (°C)	2	2.1	2.5
Inlet Air temperature Tin (°C)	48.4	54.9	52.6
outlet Air temperature Tout (°C)	50.7	57	54.2
$\Delta T = [T_{out} - T_{in}]$ (°C)	2.3	2.1	2.1
Surface temperature T_s (°C)	38.9	47.3	53.3
Base temperature T_b (°C)	53.5	56	58.9
Reduction in surface temperature $\Delta Ts = [T_{s\,(PV)} - T_{s\,(PV/T)}]$ (°C)	50.4	36.5	31.8

Reduction in base temperature $\Delta T_b = [T_{b\,(PV)} - T_{b\,(PV/T)}]$(°C)	34.5	27.8	25
Electrical efficiency η_e(%)	13.076	12.907	12.711
Percentage increase in electrical efficiency (%) $[\eta_{(PV/T)} - \eta_{(PV)}] / \eta_{(PV)}$	21.667	17.011	15.307
Enhance electrical efficiency $\eta_{enhance)} = \eta_{(PV/T)} - \eta_{(PV)}$	2.3287	1.876	1.687
Maximum Power $P_{max\,(PV/T)}$ (W)	63.812	62.988	62.033
Water pump power consumption $P_{(pump)}$ (W)	3.5	3.5	3.5
Air fan power consumption P(fan) (W)	2.5	5	8.45
Enhance Power (W) $P_{(enhance)} = [P_{max(PV/T)} - P_{max(PV)} - P_{(pump)} - P_{(fan)}]$	5.364	1.657	-2.715
Open circuit voltage V_{oc} (V)	19.31	18.9	18.12
Short circuit current I_{sc} (A)	3.27	3.38	3.872

5.3.3 Performance and Efficiency of the PV/T Combine System with Water and Air as a Cooling Fluid

The performance and effectiveness of the PV/T combine system are determined based on electrical, thermal and overall efficiency, under different outdoor environment conditions, solar radiation and ambient temperature. Different water and air masses flow rates were applied (0.0166,0.033 , 0.05, 0.066, 0.0833) kg/s for water and (0.0244,0.03167 ,0.0504) kg/s for air.

5.3.3.1 Influence of Water Mass Flow Rate

Water was circulated inside the copper pipes that are distributed on the bottom surface of PV panels for PV/T combine system extracts heat and thus contributes to lowering the temperature of the PV/T combine system in addition to the air passing through the upper and lower duct. This contributes to increasing both electrical and thermal efficiencies and improving system performance.

a. Electrical Efficiency

The highest amount of electrical efficiency reaching to 13.839% when a solar radiation was 300 W/m^2 as shown in Figure 5-15. When solar radiation reached to 1200 W/m^2 the electrical efficiency was raised from 12.678 % to 13 % as shown in Figure 5-15 and specified in Table 5-6.

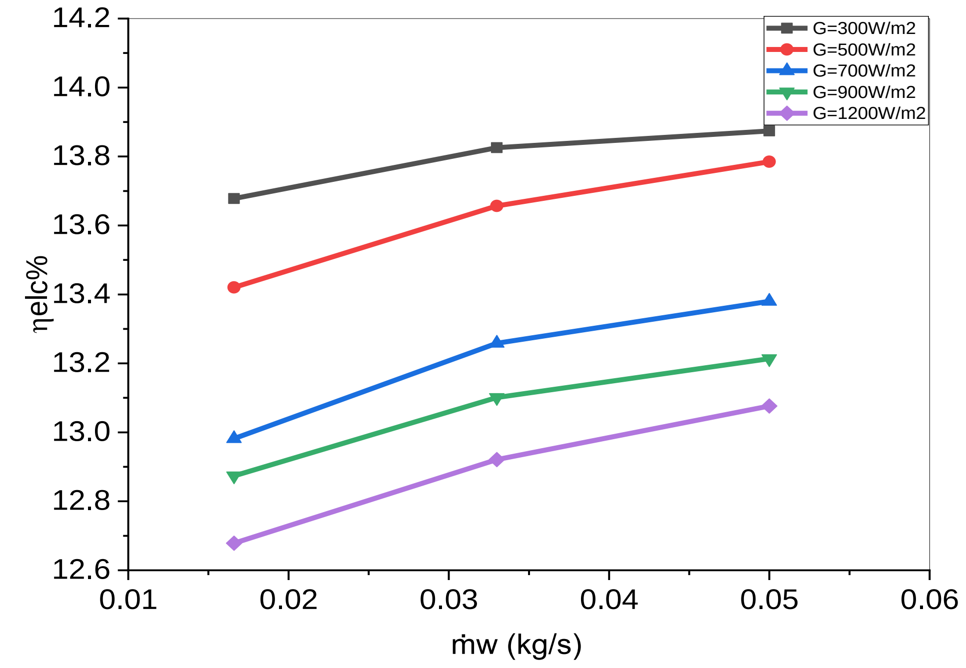

Figure5-15 Change in electrical efficiency (ηelc)with different water mass flow and various solar irradiance

Table 5- 6 Change in electrical efficiency with base temperature under different solar

ṁw (kg/s)	300 (w/m^2)		500 (w/m^2)		700 (w/m^2)		900(w/m^2)		1200(w/m^2)	
	Tb (ºC)	η_{el} (%)	Tb (ºC)	η_{el} (%)	Tb (ºC)	η_{el} (%)	Tb (ºC)	η_{el} (%)	Tb (ºC)	η_{el} (%)
0.0166	43.8	13.68	48.4	13.42	52.1	12.98	54.9	12.87	57.9	12.67
0.033	42.4	13.82	44.9	13.65	47.7	13.25	50.8	13.1	55.8	12.92
0.05	41.2	13.8	43	13.78	46.4	13.38	49	13.2	53.5	13

C.Thermal and Overall Efficiency

PV/T combine system feasibility may possibly be determined by overall efficiency expression (η_{ov}), overall efficiency represents the combining of the total thermal efficiency of the system ($\eta_{th,tot}$) which includes both the thermal gain resulting from the process of circulating water inside the thermal water collector ($\eta_{th,w}$) and circulating air in the upper and the lower duct of the thermal air collector ($\eta_{th,a}$) with the electrical gain of the system (η_{elc}). This test was carried out by rotating different masses of water flow (0.0166, 0.033, 0.05, 0.066, 0.0833) kg/s with a constant air mass 0.0244 kg/s.

Figure 5-16 and Figure 5-17 show the variation that occurs in both total thermal efficiency ($\eta_{th,tot}$) and overall efficiency(ηov) expression with increased in water mass flow rate under different solar radiation ,at lower solar radiation 300W/m^2 the ($\eta_{th,tot}$) value reached to (18.633, 24.519, 28.738, 29.986, 29.787)% and (η_{ov}) reached to (45.567, 54.923, 66.179, 67.789, 66.947) % under (0.0166, 0.033, 0.05, 0.066, 0.0833) kg/s water mass flow rate as explained in Table 5-7.

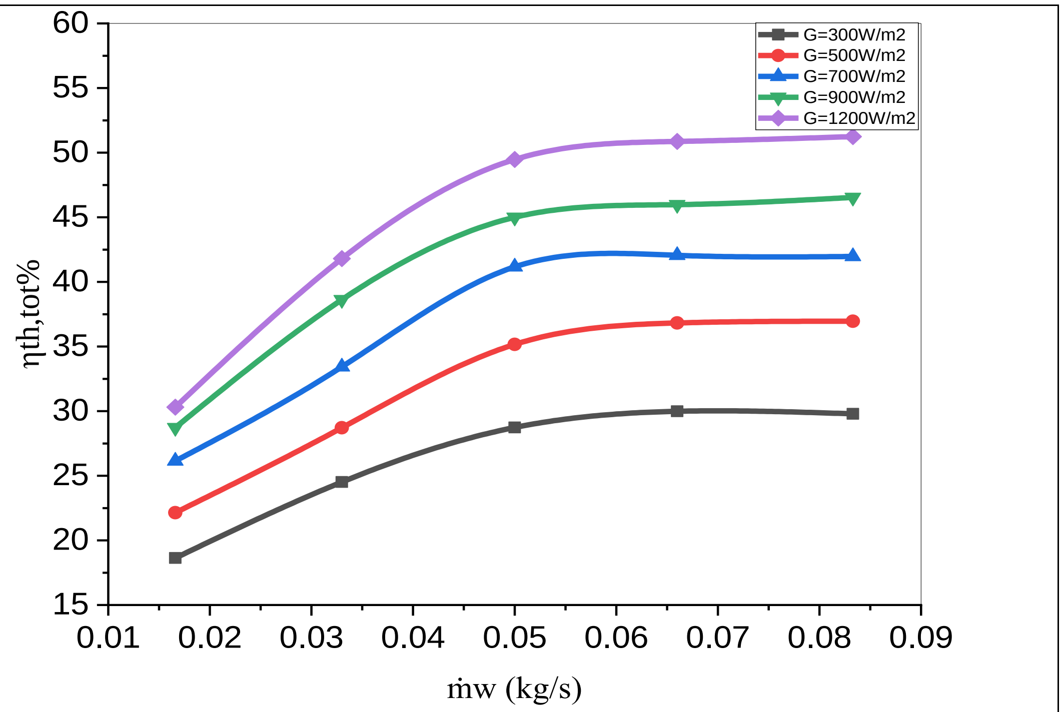

Figure5-16 Variation in total thermal efficiency with different solar radiation and water mass flow rate

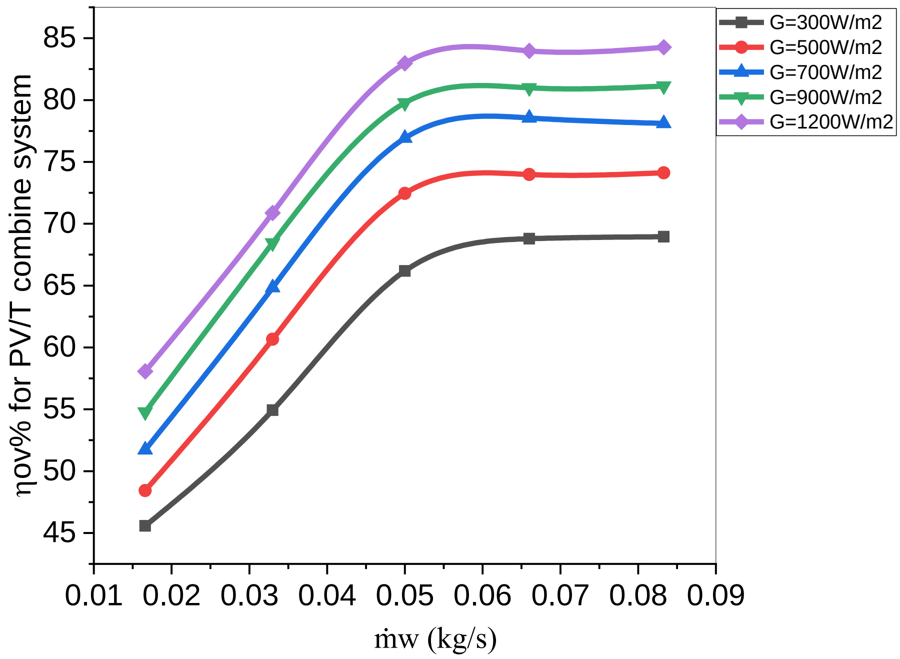

Figure5-17Variation in overall efficiency with different solar radiation and water mass flow rate

When the solar irradiance raised to 1200W/m^2, the increase has reached to (30.3, 41.8, 49.475, 50.866, 51.23) % in ($\eta_{th,\ tot}$) and to (58.06, 70.87, 82.966, 83.97, 83.26) % in (ηov) under (0.0166, 0.033, 0.05, 0.066, 0.0833) kg/s water mass flow rate. We conclude from the above two figures that the change that occurs in both total thermal efficiency and overall efficiency after 0.05kg/s is little or almost noticeable.

Table 5- 7 Performance of PV/T combine system for different solar radiation at ṁw = 0.05kg/s

Property	**Case**				
	Solar Radiation (W/m^2)				
	300	**500**	**700**	**900**	**1200**
Electrical efficiency η_{elc} (%)	13.839	13.785	13.38	13.213	13.076
Total thermal efficiency $\eta_{th,tot}$ (%)	28.738	35.162	41.16	44.996	49.475
Overall efficiency η_{ov}(%)	66.17	72.45	76.81	79.76	82.96

5.3.3.2 Influence of Air Mass Flow Rate

The best mass flow for water at 0.05kg/s was determined from the previous test at which the highest change was obtained in both electrical and thermal performance of the PV/T combine system. However, this test includes the analysis of the performance of the PV/T combine system by circulating different masses of air at (0.0244, 0.0317, 0.0504) kg/s and constant water mass flow at 0.05kg/s.

a. Electrical Efficiency

Figure 5-18 illustrates when solar radiation increased from 300W/m^2 to1200 W/m^2 this leads to a decrease in electrical efficiency from 13.78% to 12.435% when the air mass flow was 0.0244kg/s. when air mass flow rate rising from 0.0244 kg/s to 0.0317 kg/s at 1200 W/m^2. This corresponds to reduction in electrical efficiency from 13.07% to 12.811% as shown in Figure 5-18 and as illustrated in Table 5-8.

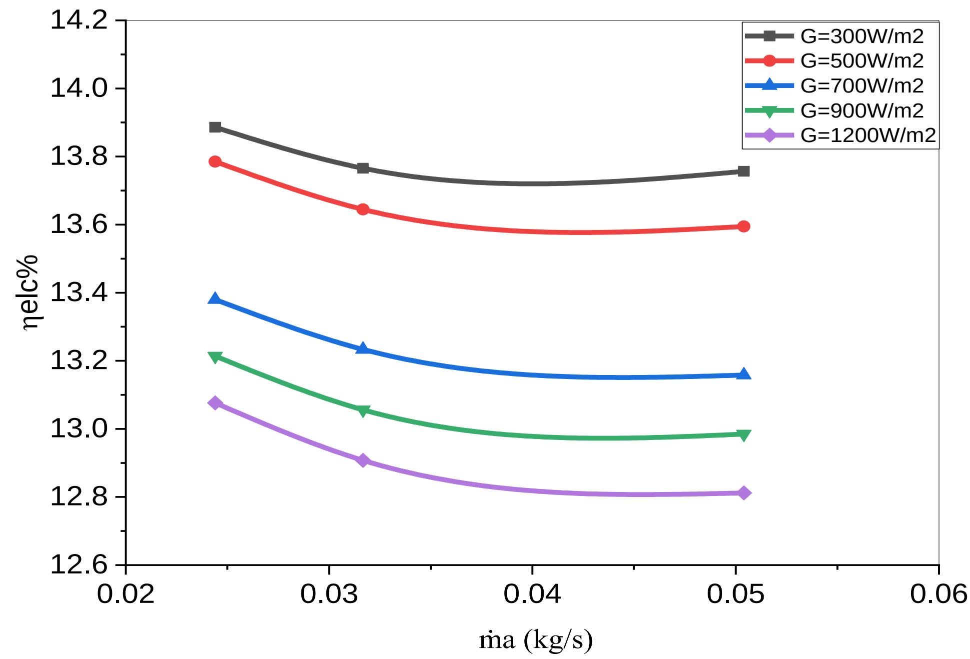

Figure5-18Variation in electrical efficiency with air mass flow rate increase

Table 5- 8 Performance of PV/T combine system for different solar radiation and at ṁw = 0.05kg/s

ṁ (kg/s)	300 (w/m^2)		500 (w/m^2)		700 (w/m^2)		900(w/m^2)		1200(w/m^2)	
	Tb (ºC)	η_{el} (%)	Tb (ºC)	η_{el} (%)	Tb (ºC)	η_{el} (%)	Tb (ºC)	η_{el} (%)	Tb (ºC)	η_{el} (%)
0.0244	41.2	13.88	43	13.78	46.4	13.38	49	13.21	53.5	13.07

0.0317	43.8	13.76	46.6	13.64	49.7	13.23	52.7	13.056	56	12.9
0.0504	44.2	13.75	47.3	13.59	50.6	13.15	53.9	12.984	57.9	12.81

b.Thermal and Overall Efficiency

Figure 5-19 and Figure 5-20 illustrate the reduction that occurs in both total thermal efficiency (ηth, tot) and overall efficiency (ηov) with an increase in air mass flow rate under different solar radiation, where at lower solar radiation 300w/m^2, the (ηth, tot) values reached to (28.738, 22.957,17.62) % and those of (ηov) reached to (66.179, 60.66, 56.249) % under (0.0244 , 0.0317,0.0504) kg/s air mass flow rate as explained in Table 5-9.

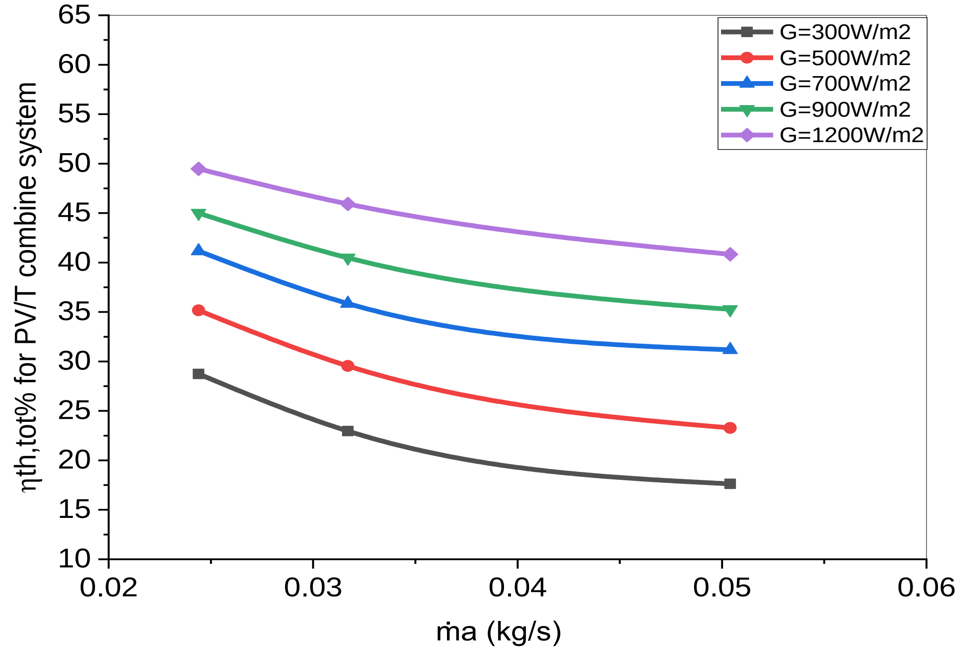

Figure5-19Total thermal efficiency under different solar radiation and air mass flow rate

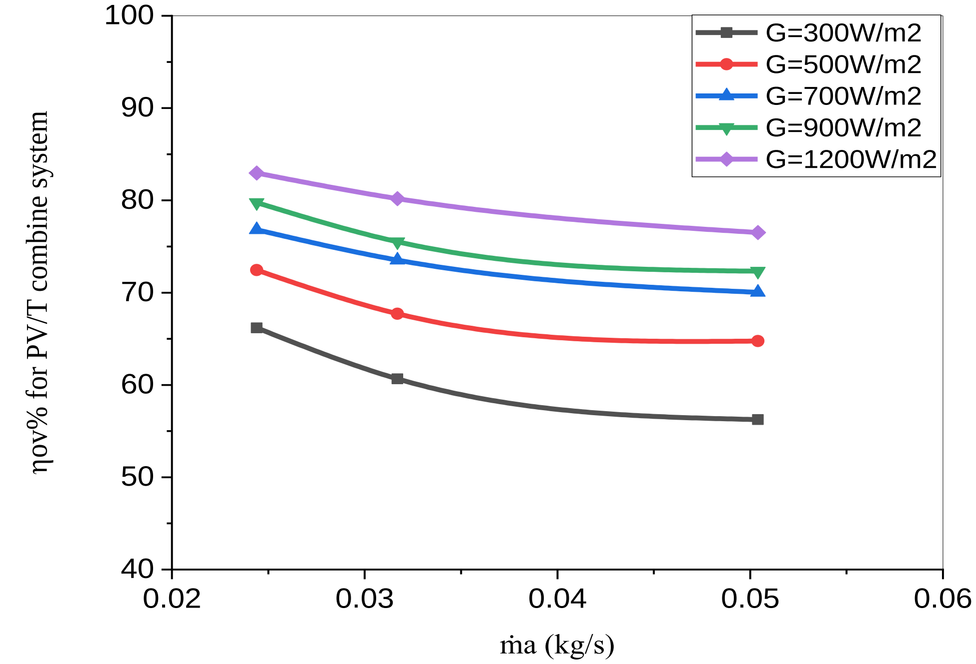

Figure5-20 Overall efficiency under different solar radiation and air mass flow rate

When the solar irradiance raises to 1200W/m^2, the decrease has reached to (49.475,45.92,40.83) % in (ηth, tot) as shown in Figure 5-19 and explained in Table 5-9, and to (82.966, 80.187, 76.516) % in (ηov) under (0.0244 , 0.0317,0.0504) kg/s air mass flow rate as shown in Figure 5-20 and explained in Table 5-9.

Table 5-9 Performance of PV/T combine system at 1200W/m2 solar radiation and constant water mass flow $\dot{m}w$ = 0.05kg/s, with different air mass flow

Property	**Case**		
	Air mass flow (kg/s)		
	0.0244	**0.0317**	**0.0504**
Electrical efficiency η_{elc} (%)	13.076	12.907	12.811
Total thermal efficiency $\eta_{th,tot}$ (%)	49.475	45.92	40.83
Overall efficiency η_{ov}(%)	82.96	80.18	76.516

5.3.4 PhotoVoltage Thermal PV/T Combine System with Air and MWCNT- nanofluid as a Cooling Fluid

PV/T combine system performance test was done by using MWCNT-nanofluid with 1% volumetric concentration with air instead of water as cooling fluid. The test was conducted under the same conditions as the PV/T system performance test when water and air were used as cooling and at the same outdoor tested conditions and with the same amount of mass passed for both water and air.

5.3.4.1 Influence of MWCNT- nanofluid Mass Flow Rate Change

Testing the effect of changing the mass of MWCNT- nanofluid on the electrical and thermal performance for PV/T combine system under (0.0166, 0.033, 0.05, 0.066, 0.083) kg/s MWCNT- nanofluid mass flow rate with constant air mass flow at 0.0244kg/s. the MWCNT-water offers significant thermal and electrical energy benefits, making solar systems more efficient and compact [61].

a. Base Temperature (Tb)

Figure 5-21 show the decreased in base temperature (Tb) for PV/T combine system with an increased in the mass of the MWCNT-nanofluid under different solar radiation as with water, where at lower solar radiation 300W/m^2 the (Tb) reached to (41, 40.6, 39) ℃ with (0.0166, 0.033, 0.05) kg/s MWCNT-nanofluid mass flow rate.

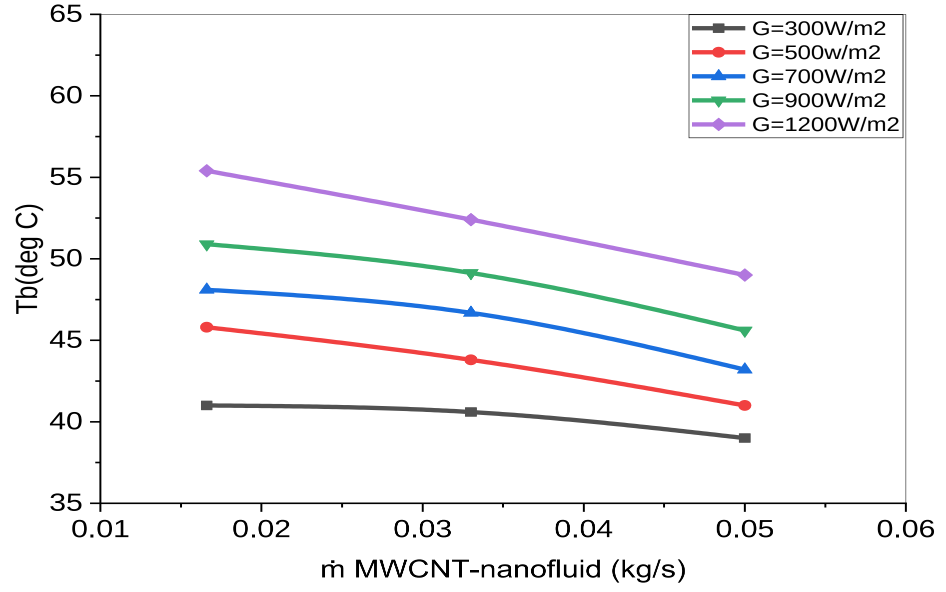

Figure5-21 Various in base temperature (Tb) with MWCNT-nanofluid mass flow rate

When the solar radiation increased to 1200W/m^{2,} the (Tb) increased and reached to (55.4, 52.4, 49.3) ℃ with (0.0166, 0.033, 0.05) kg/s MWCNT-nanofluid mass flow rate as shown in Figure 5-21 and explained in Table 5-10. Figure 5-21 also illustrates the decline that occurs in (Tb) for PV/T combine system with water and air cooling fluid than (Tb) for PV/T combine system with ṁ MWCNT-nanofluid and air cooling fluid was because MWCNT-nanofluid improves heat transfer due to its higher thermal conductivity.

b. Open Circuit Voltage (Voc)

Figure 5-22 illustrates the increase in (V_{OC}) as MWCNT-nanofluid mass flow increased under different solar radiation as explained in Table 5-10. It also shows that the highest values for (Voc) were obtained at lower solar radiation 300w/m^2, where it reached to (19.38, 19.4, 19.8) V at (0.0166, 0.033 , 0.05) kg/s. The highest voltage value was obtained 19.8V at 0.05kg/s.

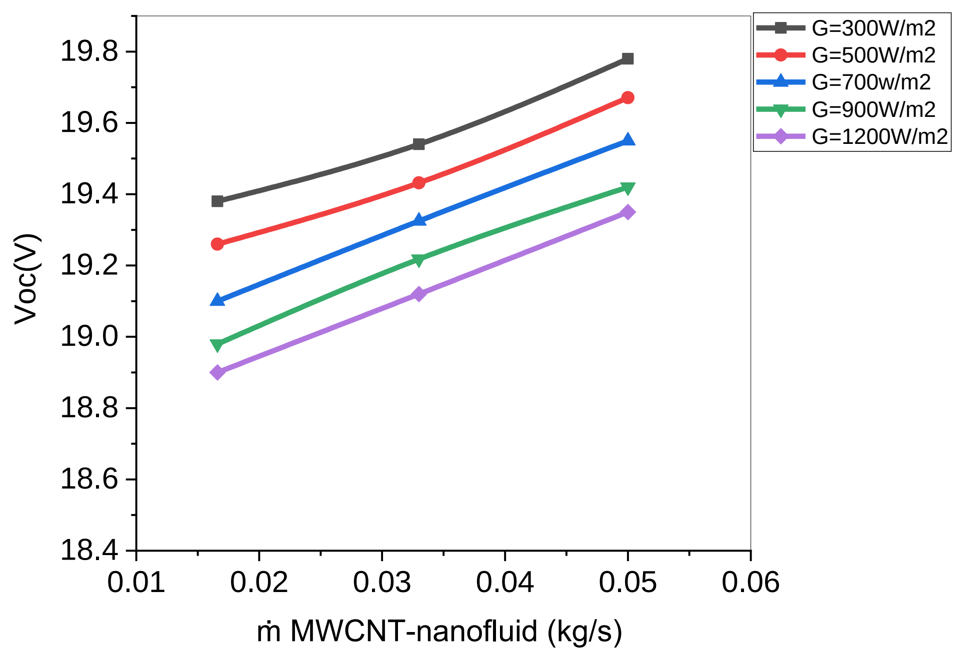

Figure5-22 Variation in (Voc) with various mwcnt-nanofluid mass flow rate

When the solar radiation increased to 1200W/m^2, the (Voc) decreased and reached to (18.9, 19.12, 19.35) V under (0.0166, 0.033, 0.05) MWCNT-nanofluid mass flow rate as shown in Figure 5-22 and as illustrated in Table 5-10.

b. Short Circuit Current (Isc)

Figure 5-23 shows that the reduction in (Isc) as MWCNT-nanofluid mass flow rate increased, the lower reduction was achieved at 0.05kg/s mwcnt-nanofluid mass flow. At lower solar radiation 300w/m^2, the (Isc) reached to (0.81, 0.68 ,0.51) A at (0.0166, 0.033, 0.05) kg/s as shown in Figure 5-23 and simplified in Table 5-10.

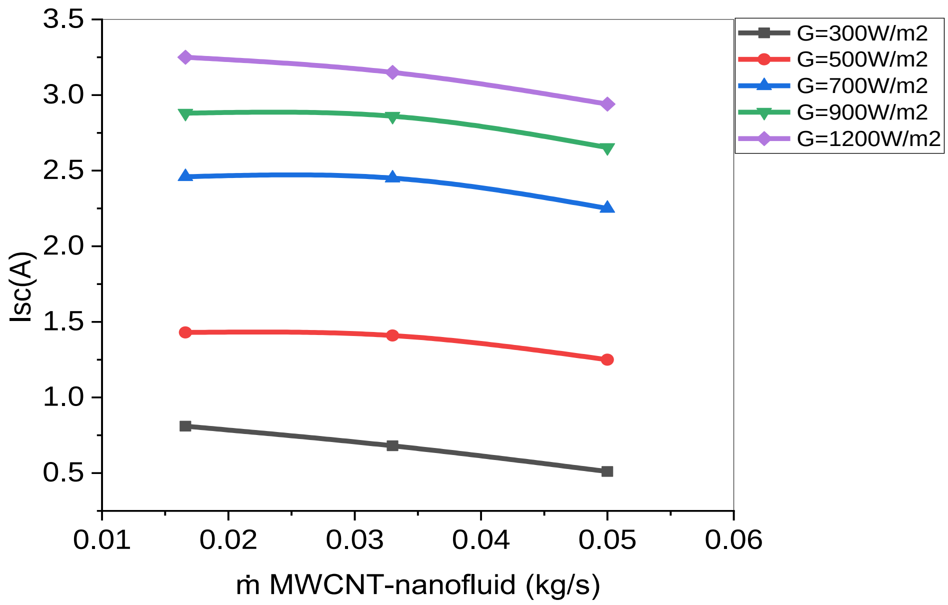

Figure5-23 Variation in (Isc) with various MWCNT-nanofluid mass flow rate

At higher solar radiation 1200W/m^2, the values of (Isc) reached to (3.25, 3.15, 2.94) A at (0.0166, 0.033, 0.05) kg/s as shown in Figure 5-23 and simplified in Table 5-10. The lowest amount of (Isc) was obtained when using the mwcnt-nanofluid and air as a cooling fluid with PV/T combine system than using water and air. The reason for this is due to the increase in the thermal conductivity of the MWCNT-nanofluid, which leads to an increase in the heat extracted and thus reducing the formation of the electron-hole pair.

Table 5- 10 Characteristics of the PV/T combine system with mwcnt-nanofluid and air under different solar radiation at ṁmwcnt = 0.05kg/s

Property	**Case**				
	Solar Radiation (W/m^2)				
	300	**500**	**700**	**900**	**1200**
Ambient temperature T_a (°C)	36.2	38.2	42.9	43.7	45.6
Inlet water temperature T_{in} (°C)	34.7	35.2	37.3	37.5	39.5
outlet water temperature T_{out} (°C)	35.2	36.4	39.4	39.9	42.1
$\Delta T = [T_{out} - T_{in}]$ (°C)	0.5	1.2	2.1	2.4	2.6
Inlet air temperature T_{in} (°C)	37.2	40.2	43.7	44.5	46.1
Outlet air temperature Tout (°C)	39.8	42.5	45.6	45.8	46.7

ΔT =[Tout- Tin] (℃)	2.6	2.3	1.9	1.3	0.6
Surface temperature T_s (°C)	36.2	37.35	37.6	38.5	40.9
Base temperature T_b (°C)	39	41	42.2	47.2	49.3
Reduction in surface temperature (°C) $\Delta Ts =[T_{s\,(PV)} - T_{s\,(PV/T)}]$	21.03	28.95	36.8	46.06	47.3
Reduction in base temperature (°C) $\Delta T_b =[T_{b\,(PV)} - T_{b\,(PV/T)}]$	17	24	30.8	34.8	37.7
Electrical efficiency η_e (%)	14.055	13.92	13.839	13.501	13.359
Percentage increase in electrical efficiency (%) $[\eta_{(PV/T)} - \eta_{(PV)}] / \eta_{(PV)}$	8.89	13.17	19.146	21.06	23.529
Enhance electrical efficiency (%) $\eta_{\,enhance)} = \eta_{(PV/T)} - \eta_{(PV)}$	1.1475	1.62	2.187	2.349	2.544
Maximum Power $P_{max\,(PV/T)}$ (w)	20.801	33.408	46.056	61.188	65.195
Water pump power consumption $P_{(pump)}$ (w)	3.5	3.5	3.5	3.5	3.5
Air fan power consumption P(fan) (w)	2.5	2.5	2.5	2.5	2.5
Enhance Power (w) $P_{(enhance)}=[P_{max(PV/T)} - P_{max(PV)} - P_{(pump)} - P(fan)]$	-4.301	-2.112	0.9189	4.645	6.4183
Open circuit voltage V_{oc} (V)	19.7	19.62	19.53	19.39	19.31
Short circuit current I_{sc} (A)	0.79	1.31	2.08	2.51	3.27

5.3.4.2 Influence of Air Mass Flow Rate Change

In this test, the effect of the air mass flow rate change is to be recognized on the PV/T combine system performance with holding the mass of MWCNT -nanofluid at 0.05kg/s as in using water and air as cooling fluid with PV/T combine system.

a. Base Temperature (Tb)

Figure 5-24 shows the increase that occurs in base temperature (Tb) as mass of air flow increase under different solar radiation and as specified in Table 5-11. It also shows that the lower (Tb) was received at 300W/m^2 and reached to (39, 41.5 ,42) ℃

at (0.0244, 0.03167, 0.0504) kg/s air mass flow rate as shown in Figure 5-23 and specified in Table 5-11. When the solar radiation increase to 1200W/m^2, the (Tb) increased and reached to (49.3, 53.9, 54.4) ℃ at (0.0244, 0.03167, 0.0504) kg/s air mass flow rate as shown in Figure 5-24 and specified in Table 5-11. It also shows the reduction that occurs in (Tb) by using MWCNT-nanofluid as cooling fluid compared to using water for the same masses of air passing at different solar radiation.

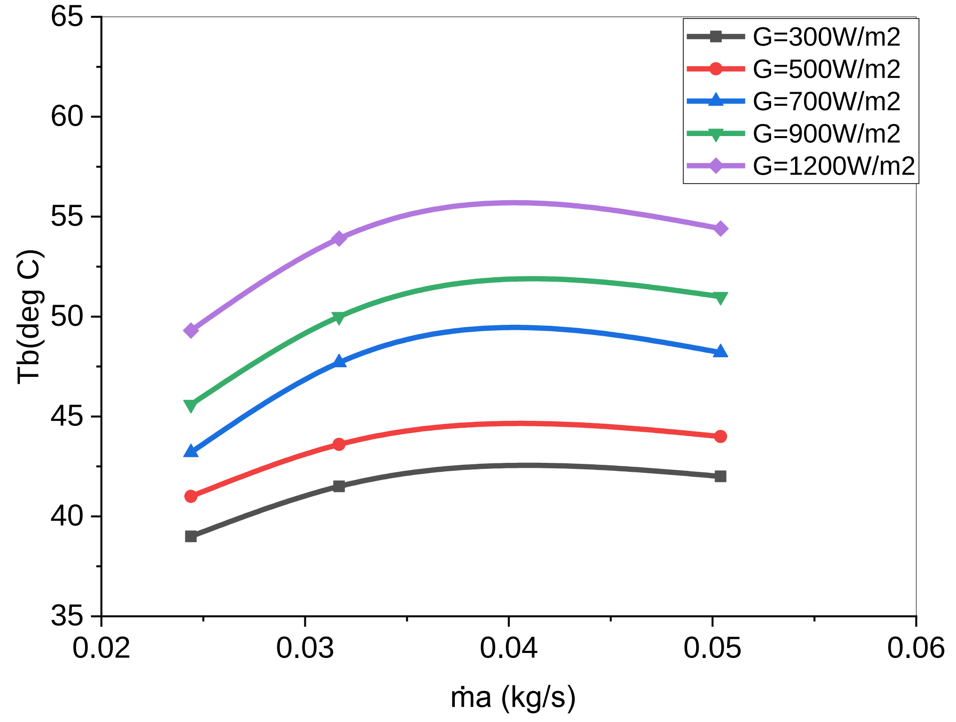

Figure5-24 Variation in (Tb) with different air mass flow rate and solar radiation

b. Open Circuit Voltage (Voc)

Figure 5-25 illustrates the reduction that occurs in open circuit voltage (Voc) as mass of air passing increased. It also shows that the higher amount of (Voc) was received at 300W/m^2 and reached to (19.9, 19.75, 19.43) V at (0.0244, 0.03167, 0.0504) kg/s air mass flow rate as illustrated in Figure 5-25 and specified in Table 5-11. At higher solar radiation 1200W/m^2, the (Voc) decreased and reached to (19.48, 19.32 ,18.95) Vat (0.0244, 0.03167, 0.0504) kg/s air mass flow rate as illustrated in Figure 5-25 and specified in Table 5-11.

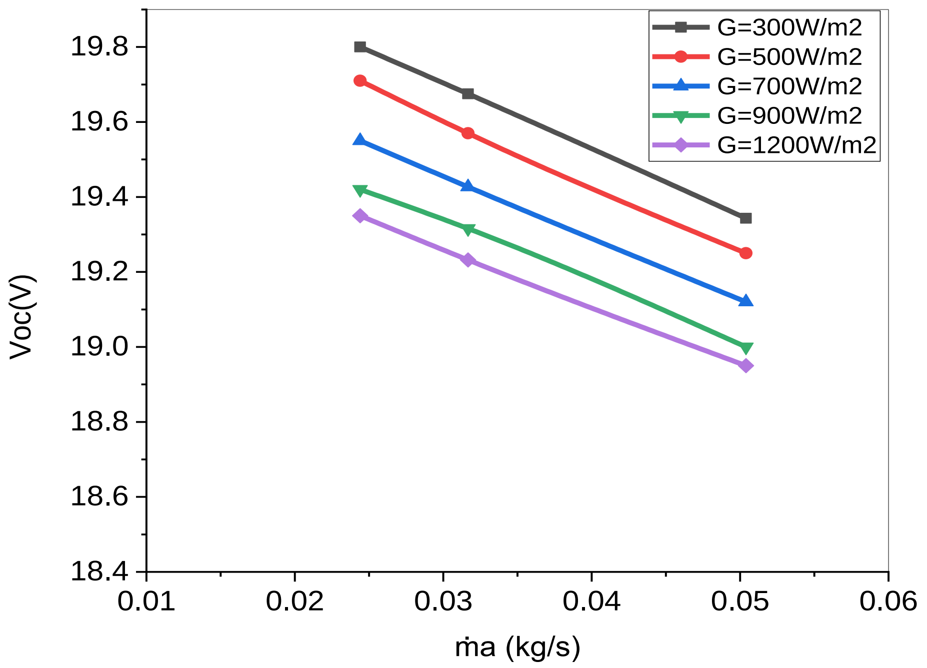

Figure5-25 Variation in (Voc) with air mass flow rate

c.Short Circuit Current (Isc)

Figure 5-26 illustrates the rising that occurs in short circuit current (Isc) as the mass of air pass increases. It shows the lowest value for (Isc) which was received at 300 W/m^2 and reached to (0.61, 0.95, 1.59) A at (0.0244, 0.03167, 0.0504) kg/s as illustrated in Table 5-11. When the solar radiation was raised and arrived to 1200W/$m^{2,}$ the (Isc) increased and reached to (3, 3.23, 3.64) A at (0.0244 ,0.03167 ,0.0504) kg/s as shown in Figure 5-26 and illustrated in Table 5-11.

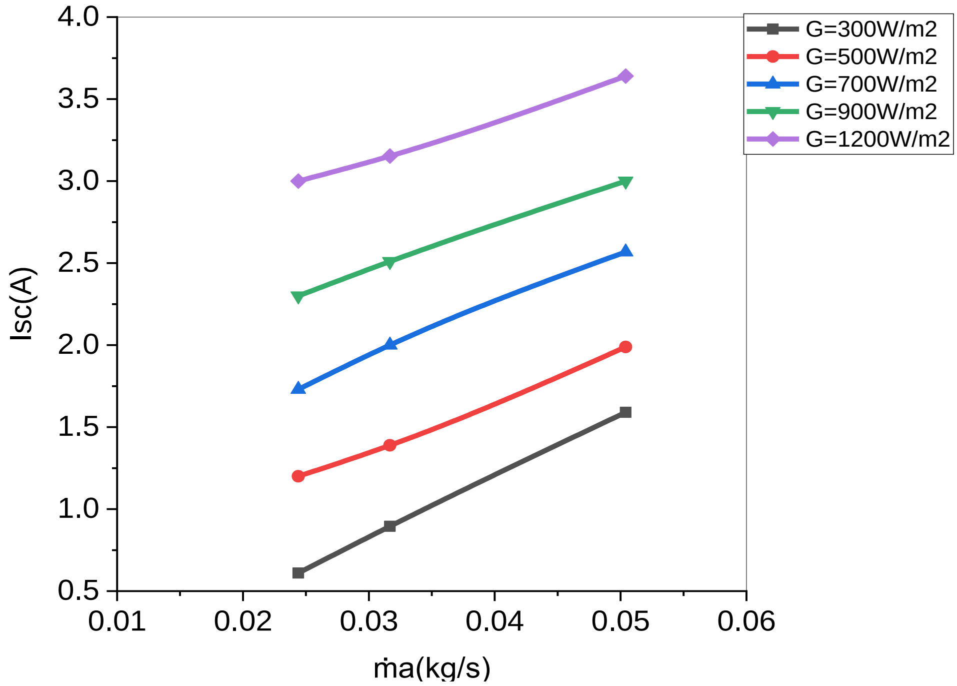

Figure5-26 Variation in (Isc) with air mass flow rate

Table 5- 11Characteristics of the PV/T combine system with mwcnt-nanofluid and air under 1200W/m2 solar radiation at ṁmwcnt = 0.05kg/s

Property	**Case**		
	Air mass flow (kg/s)		
	0.0244	**0.03167**	**0.0504**
Ambient temperature T_a (°C)	44.6	48.7	47.6
Inlet water temperature T_{in} (°C)	38.2	39.9	39.1
outlet water temperature T_{out} (°C)	40.2	41.6	41.6
$\Delta T = [T_{out} - T_{in}]$ (°C)	2	2.2	2.5
Inlet Air temperature Tin (°C)	54.9	54.9	55.5
Outlet Air temperature Tout (°C)	50.7	57	57.1
$\Delta T = [T_{out} - T_{in}]$ (°C)	2.3	2.1	1.6
Surface temperature T_s (°C)	38.9	47.3	53.3
Base temperature T_b (°C)	53.5	56	58.9

Reduction in surface temperature $\Delta T_s = [T_{s\,(PV)} - T_{s\,(PV/T)}]$ (°C)	50.4	38.9	31.3
Reduction in base temperature $\Delta T_b = [T_{b\,(PV)} - T_{b\,(PV/T)}]$(°C)	37.7	27.8	25
Electrical efficiency η_e(%)	13.359	12.907	12.711
Percentage increase in electrical efficiency (%) $[\eta_{(PV/T)} - \eta_{(PV)}] / \eta_{(PV)}$	23.529	17.011	12.192
Enhance electrical efficiency $\eta_{enhance)} = \eta_{(PV/T)} - \eta_{(PV)}$	2.544	1.876	1.687
Maximum Power $P_{max\,(PV/T)}$ (W)	65.195	62.988	62.033
Water pump power consumption $P_{(pump)}$ (W)	3.5	3.5	3.5
Air fan power consumption P(fan) (W)	2.5	5	8.45
Enhance Power (W) $P_{(enhance)} = [P_{max(PV/T)} - P_{max(PV)} - P_{(pump)} - P_{(fan)}]$	6.4183	1.657	-2.715
Open circuit voltage V_{oc} (V)	19.31	18.9	18.12
Short circuit current I_{sc} (A)	3.27	3.38	3.872

5.3.5 Performance and Efficiency of the PV/T Combine System with MWCNT-nanofluid and Air as a Cooling Fluid

The thermal and electrical characteristics for PV/T combine system were investigated by using MWCNT-nanofluid and air with PV/T combine system instead of water and air as cooling fluid at the same tested conditions and the same masses flow for both air and water.

5.3.5.1 Influence of MWCNT-nanofluid Mass Flow Rate Change

In this test, the electrical efficiency, total thermal efficiency, and overall efficiency are calculated for the PV/T combine system with different mass flow rates (0.0166, 0.033, 0.05) kg/s for MWCNT-nanofluid and constant air mass flow at 0.0244kg/s.

a. Electrical Efficiency

Figure 5-27 illustrates the raised in electrical efficiency with MWCNT-nanofluid mass flow rate was increased , At 300 W/m^2 solar radiation indicated the raised in electrical efficiency from 13.92% to 14.055% with MWCNT-nanofluid mass flow rate was increased from0.011 to 0.05kg/s .where at 1200W/m^2 the electrical efficiency increased from 12.948% to 13.35% as shown in Figure 5-27 and explained in Table 5-12.

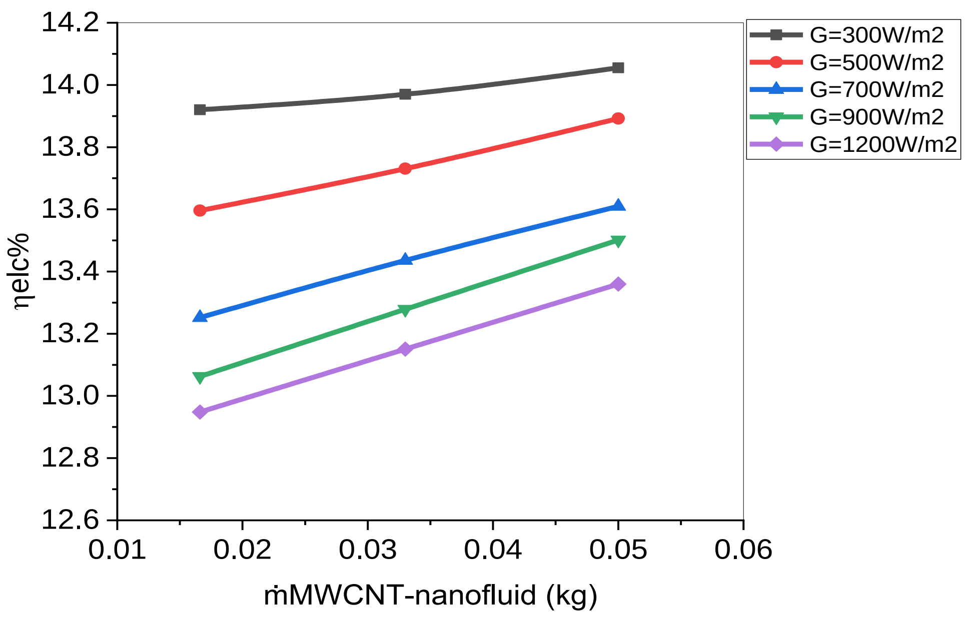

Figure5-27 Change in (ηelc) with different MWCNT -nanofluid mass flow rate

Table 5- 12Variation in base temperature (Tb) and electrical efficiency under different solar radiation and MWCNT-nanofluid mass flow

ṁ (kg/s)	300 (w/m^2)		500 (w/m^2)		700 (w/m^2)		900(w/m^2)		1200(w/m^2)	
	Tb (ºC)	η_{el} (%)	Tb (ºC)	η_{el} (%)	Tb (ºC)	η_{el} (%)	Tb (ºC)	η_{el} (%)	Tb (ºC)	η_{el} (%)
0.0166	41	13.92	45.8	13.596	48.1	13.25	50.9	13.06	55.4	12.948

0.033	40.6	13.947	43.8	13.731	46.8	13.359	49.3	13.27	52.4	13.15
0.05	39	14.055	41	13.92	42.2	13.609	45.6	13.5	49.3	13.35

a.Thermal and Overall Efficiency

Figure 5 -28 and Figure 5-29 show the increase in the total thermal efficiency ($\eta_{th,tot}$) and overall efficiency (η_{ov}) for PV/T combine system as MWCNT-nanofluid mass flow increased reaching to 0.05kg/s. After this, the increment is slight or insignificant as with water. At lower solar radiation 300w/m^2 and at (0.0166, 0.033, 0.05, 0.066, 0.0833) kg/s MWCNT-nanofluid mass flow the efficiencies values reached to **(**18.977%, 26.709%, 35.977%, 36.868%, 37.81%**)** for $\eta_{th,tot}$ and (55.644%, 63.451% ,75.018% ,76.294%,76.986%) for $\eta_{OV.}$ When the solar radiation increased to 1200W/m^2, it reached to **(**28.934%, 41.983%, 56.579%, 59.546%, 60.921%) for ηth,tot as illustrated in Figure 5-28 and specified in Table5-13 ; and (66.22%,78.869% ,92.883% ,93.756% ,94.521%) for η_{OV} as illustrated in Figure 5-29 and specified in Table 5-13 .

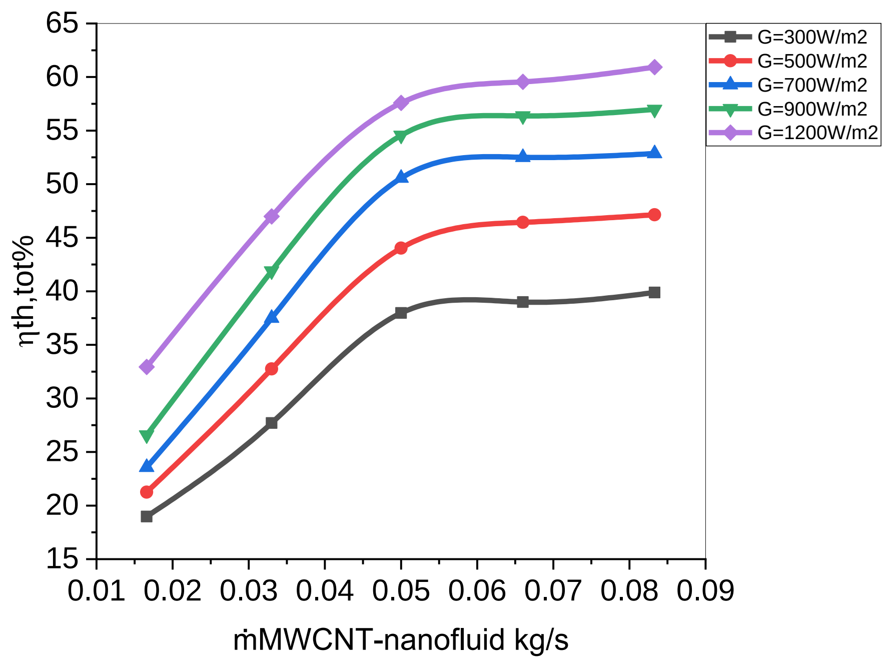

Figure5-28 Total thermal efficiency (ηth,tot) with different MWCNT-nanofluid mass flow rate

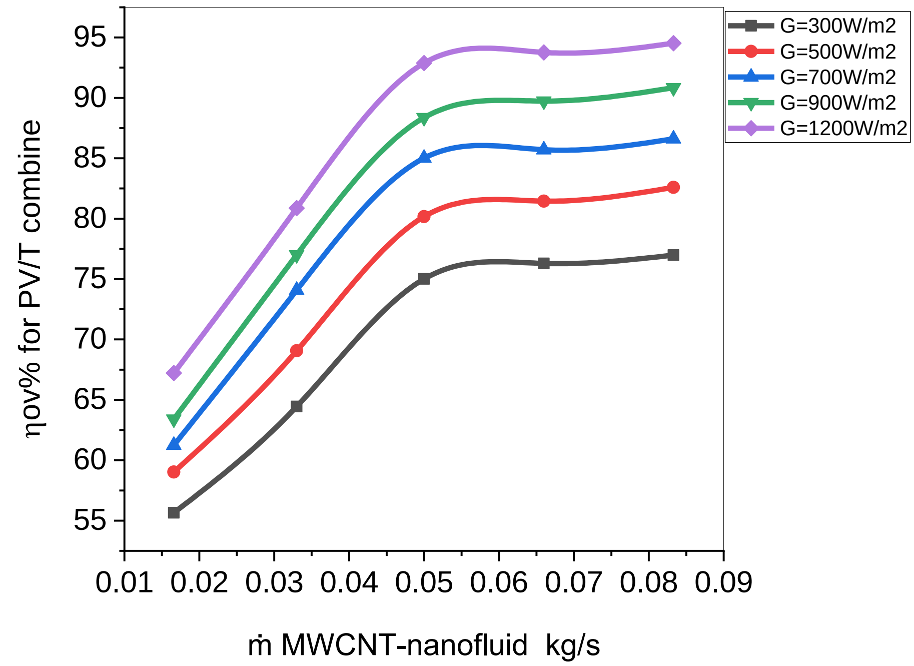

Figure5-29 Overall efficiency with different MWCNT- Nanofluid mass flow rate

Table 5- 13 Performance of PV/T combine system under different solar radiation and at constant ṁmwcnt = 0.05kg/s

Property	Case				
	Solar Radiation (w/m^2)				
	300	**500**	**700**	**900**	**1200**
Electrical efficiency η_e (%)	14.055	13.92	13.839	13.5015	13.359
Total thermal efficiency $\eta_{th,tot}$ (%)	35.977	44.028	50.571	54.558	56.579
Overall efficiency η_{ov}(%)	75.018	80.169	85.013	88.362	92.883

5.3.5.2 Influence of Air Mass Flow Rate Change

Studying the effect of changing the mass of the air passing on the electrical and thermal performance for PV/T combine system with maintaining the mass of the MWCNT-nanofluid passing.

a.Base Temperature (Tb)

Figure 5-30 shown the decreased in electrical efficiency at 300 W/m^2 reached to (14.055 %, 13.886%, 13.852%) with (0.0244, 0.03167, 0.0504) kg/s air mass flow rate . At higher solar raidation 1200 W /m^2 the electrical efficiency reached to (13.359%, 13.049%, 13.015%) respectively as specified in Table 5-14 .

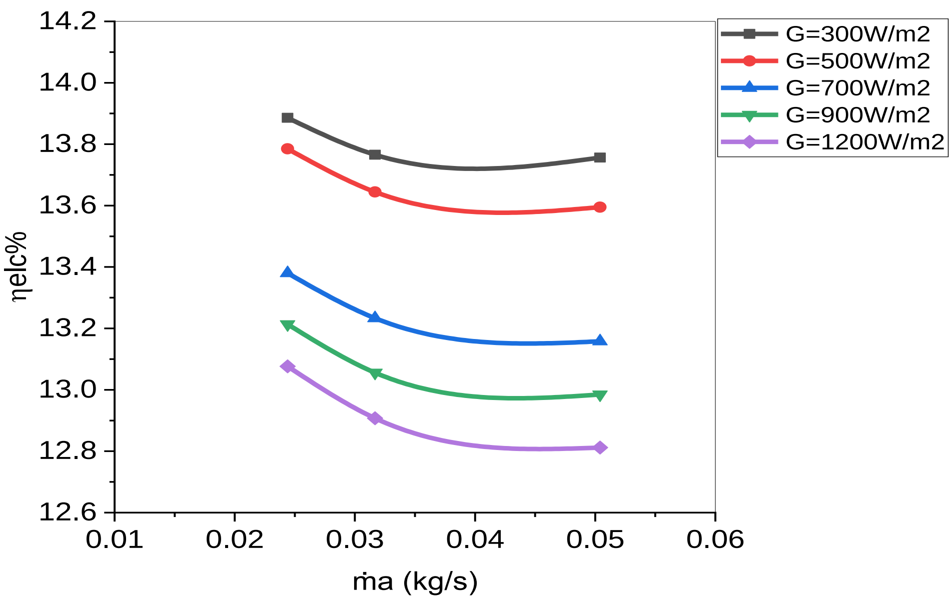

Figure5-30 Variation in (ηelc) with different air mass flow rate

Table 5- 14Performance of PV/T combine system under different solar radiation and MWCNT-nanofluid mass flow rate

ṁ (kg/s)	300 (w/m^2)		500 (w/m^2)		700 (w/m^2)		900(w/m^2)		1200(w/m^2)	
	Tb (ºC)	η_{el} (%)	Tb (ºC)	η_{el} (%)	Tb (ºC)	η_{el} (%)	Tb (ºC)	η_{el} (%)	Tb (ºC)	η_{el} (%)
0.0244	39	14.05	41	13.92	43.2	13.6	45.6	13.45	49.3	13.35
0.0317	41.5	13.88	43.6	13.74	47.7	13.38	50	13.14	53.9	13.04
0.0504	42	13.85	44	13.71	48.2	13.36	51	13.09	54.4	13

b. Thermal and Overall Efficiency

Figure 5-31 and Figure 5-32 show the reduction that occurs in both thermal and overall efficiency as air mass flow which was increased. At lower solar radiation 300w/m^2, the ($\eta_{tot,th}$) arrived to (35.977, 29.817, 14.377) and η_{ov} arrived to (75.018, 68.38, 52.856) with air mass flow (0.0244, 0.0317, 0.0504) kg/s respectively, and as explained in Table 5-15.

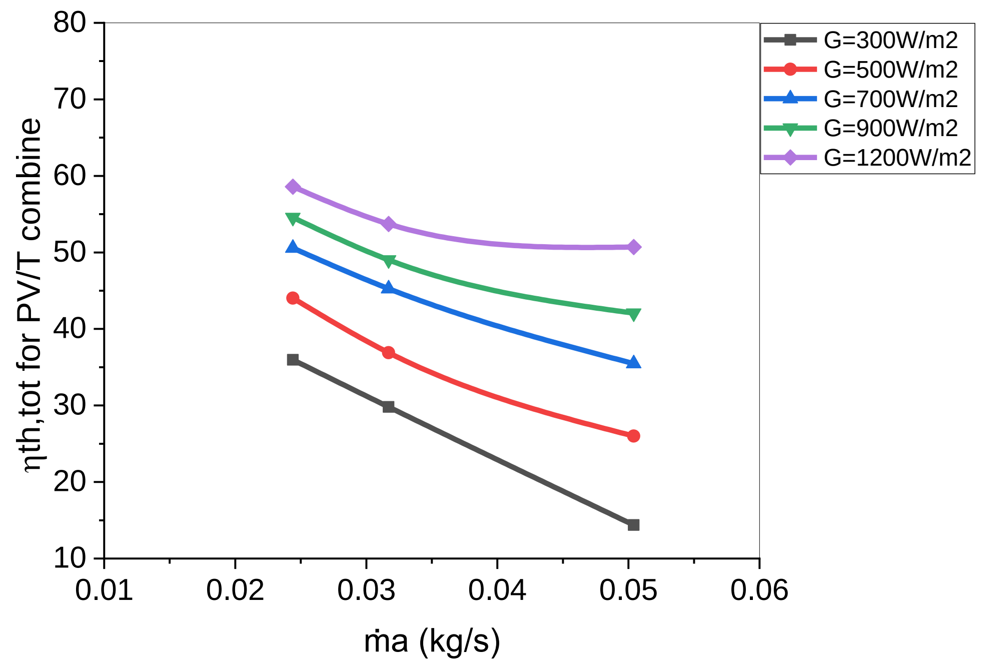

Figure5-31 Variation in (ηth,tot) with different air mass flow rate

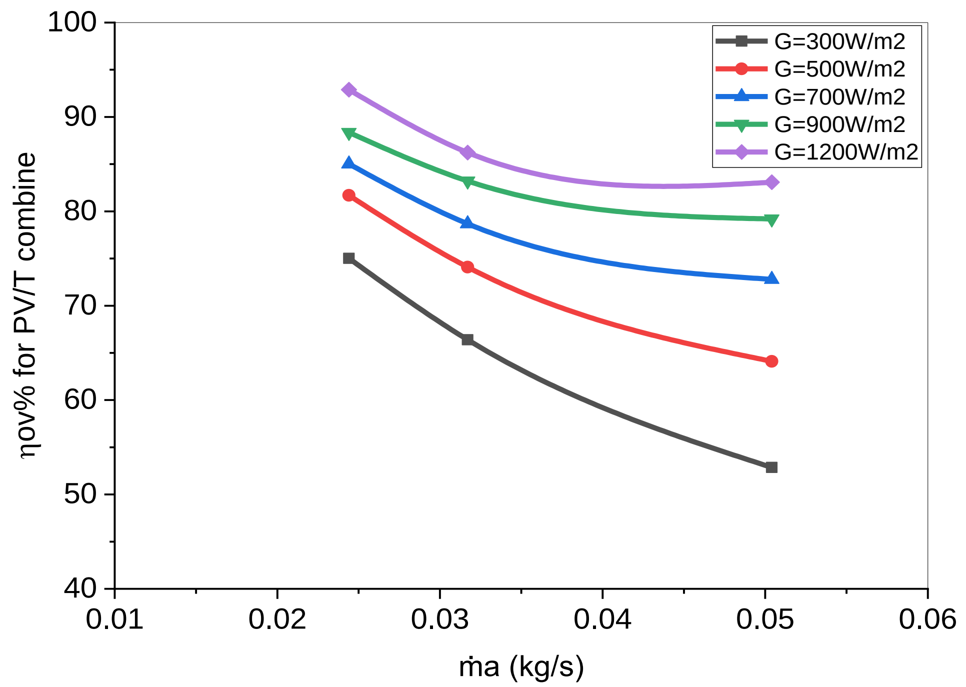

Figure5-32 Variation in (ηOV) with different air mass flow rate

When the solar radiation was raised to 1200W/m^2, both $\eta_{tot,th}$ and η_{ov} were increased and reached to (58.579%, 53.71%, 50.706%) for $\eta_{tot,th}$ as shown in Figure 5-

31 and explained in the Table 5-15, and (92.88%, 86.221%, 83.085%) for η_{ov} at (0.0244, 0.0317, 0.0504) kg/s air mass flow rate as shown in Figure 5-32 and explained in the Table 5-15.

Table 5- 15Performance of PV/T combine system under different solar radiation and constant MWCNT-nanofluid at 0.05kg/s

Property	**Case**				
	Solar Radiation (W/m^2)				
	300	**500**	**700**	**900**	**1200**
Electrical efficiency η_{elc} (%)	14.055	13.92	13.609	13.501	13.359
Total thermal efficiency $\eta_{th,tot}$ (%)	35.977	44.02	50.571	54.558	58.579
Overall efficiency η_{ov}(%)	75.018	81.695	85.013	88.362	92.88

5.4 Energy and Exergy Analyses

In thermodynamics, the greatest potential beneficial work performed during a process to put a system into thermal equilibrium is called exergy. Exergy, in other words, is the greatest ability of energy to do meaningful work. As a system approached equilibrium, it is the difference between the system's total energy and the energy that is not available (e.g. losses).

5.4.1 Effect of Change Masses Flow (Water, MWCNT-nanofluid) on Power Generation

5.4.1.1 Effect of Change Masses Flow (Water, MWCNT-nanofluid) on Power Generation at Constant Air Mass Flow

a. Electrical Power

Figure 5-33 and Figure 5-34 show the increase in electrical Power generation as the mass flow rate increased for both (water, MWCNT-nanofluid) . At lower solar radiation 300 W/m^2, the electrical Power generation reached to (17.09, 17.143, 18.938) W at (0.0166, 0.033,0.05) kg/s for PV/T combine system with water as illustrated in Figure 5-33 and specified in Table 5-16, and reached to (18.804, 19.517,20.801)W, at (0.0166 ,0.033 ,0.05) kg/s for PV/T combine system with MWCNT-nanofluid as shown in Figure 5-33 and specified in Table 5-16.

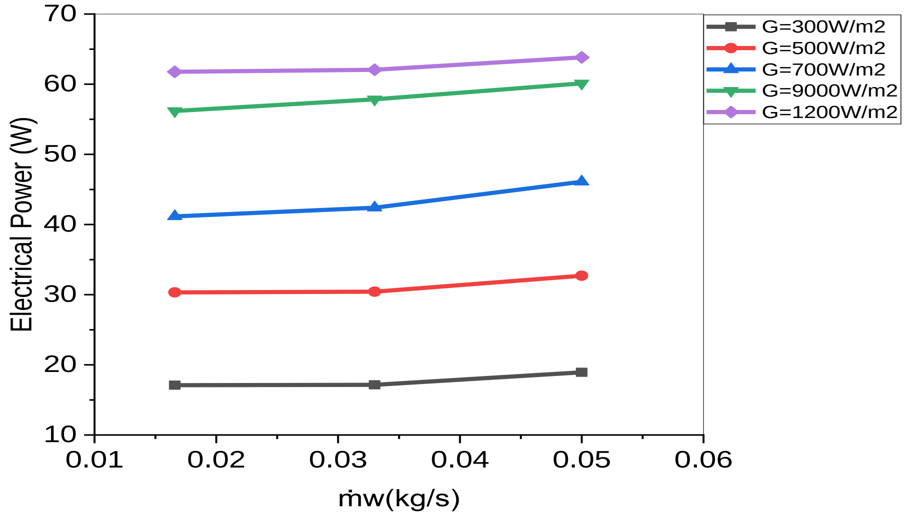

Figure5-33 Electrical power generation under different water mass flow rate

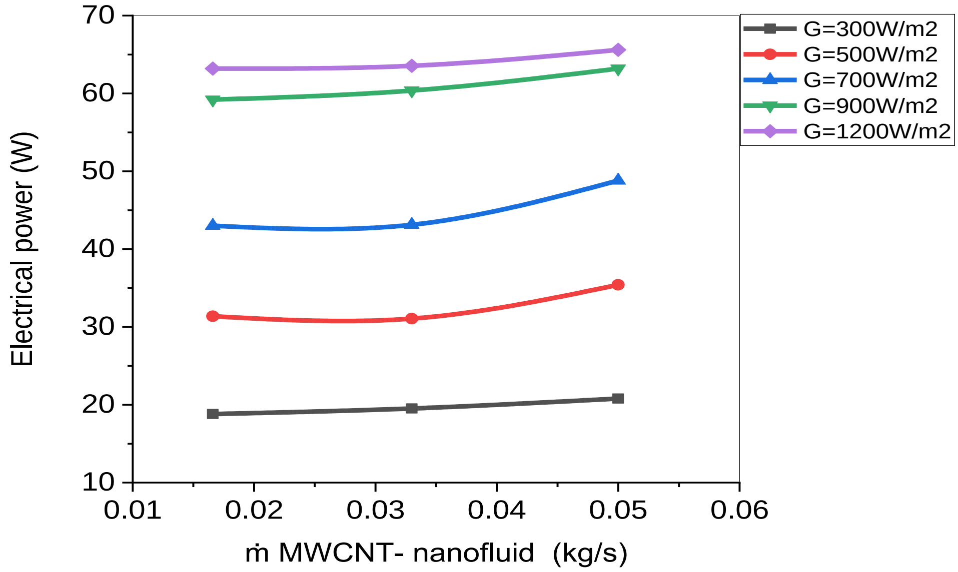

Figure5-34 Electrical power generation with different MWCNT-nanofluid mass flow rate

At 1200W/m^2, the electrical Power generation increased and arrived to (61.758, 62.054, 63.812) W at (0.0166, 0.033, 0.05) kg/s for PV/T combine system with water as shown in Figure 5-33 and specified in Table 5-16, and it reached to

(63.186, 63.543, 65.195) W at (0.0 66 ,0.033 ,0.05) kg/s for PV/T combine system with MWCNT-nanofluid as shown in Figure 5-34 and specified in Table 5-16.

b. Thermal Power

Figure 5-35 and Figure 5-36 explain the increase in the thermal energy generation as mass flow rate increased for both (water, MWCNT-nanofluid). At lower solar radiation 300 W/m^2, the thermal energy generation reached to (26.5, 45.784, 66.368, 70.149, 74.874) W at (0.0166,,0.033 0.05, 0.066, 0.0833) kg/s for PV/T combine system with water as shown in Figure 5-35 and specified in Table 5-16, and reached to (35.604, 66.088, 93.901, 100.154, 106.96) W at (0.0166,0.033,0.05,0.066,0.0833) kg/s for PV/T combine system with MWCNT-nanofluid as shown in Figure 5-36 and specified in Table 5-16.

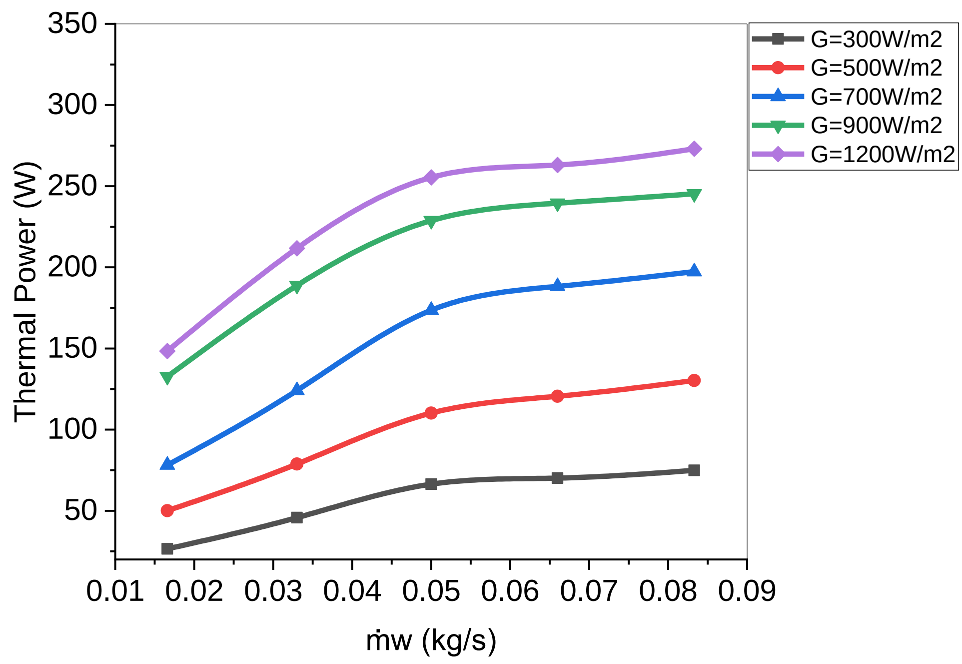

Figure5-35Thermal power generation with different water mass flow rate

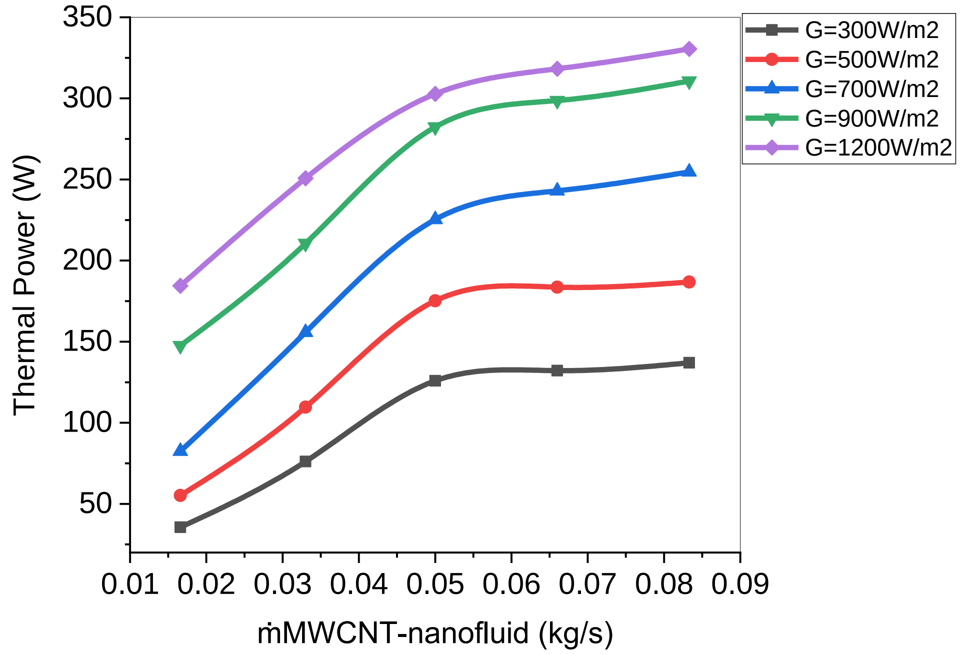

Figure5-36 Thermal power generation with different MWCNT-nanofluid mass

At higher solar radiation 1200W/m^2, the electrical energy generation raised and arrived to (148.426, 211.73, 255.403, 261.105, 273.037) W at (0.0166, 0.033, 0.05, 0.066, 0.0833) kg/s for PV/T combine system with water as shown in Figure 5-35 and specified in Table 5-16. It reached to (184.429, 250.775, 302.728, 318.288, 330.503) W at (0.0166 ,0.033 ,0.05 ,0.066, 0.0833) kg/s for PV/T combine system with MWCNT-nanofluid as shown in Figure 5-36 and specified in Table 5-16.

Table 5- 16 Power analysis for PV/T combine system with MWCNT-nanofluid and PV/T combine system with water and PV module at ṁa=0.0244kg/s and at solar radiation 1200 W/m^2

Mass flow (kg/s)	PV/T combine with MWCNT-nanofluid and air		PV/T combine with water and air		PV module	
	Thermal Power (W)	Electrical Power (W)	Thermal Power (W)	Electrical Power (W)	Thermal Power (W)	Electrical Power (W)
0.0166	184.429	63.186	148.426	61.758	-	52.742
0.033	250.775	63.543	211.73	62.054	-	52.742

0.05	302.728	65.595	255.403	63.812	-	52.742
0.066	318.288	-	261.105	-	-	52.742
0.0833	330.503	-	273.037	-	-	52.742

5.4.1.2 Effect of Air Mass Flow Change on Power Generation

a. Electrical Power

Figure 5-37 and Figure 5-38 show the decrease in the electrical energy generation as air mass flow rate increased. At 300 W/m^2, the electrical energy generation reached to (18.938, 18.057, 17.021) W at (0.0244, 0.031, 0.0504) kg/s for PV/T combine system with water as shown in Figure 5-37 and specified in Table 5-17. It reached to (20.8,19.66,18.5) W at (0.0244, 0.0317 ,0.0504) kg/s for PV/T combine system with MWCNT-nanofluid as shown in Figure 5-38 and specified in Table 5-17.

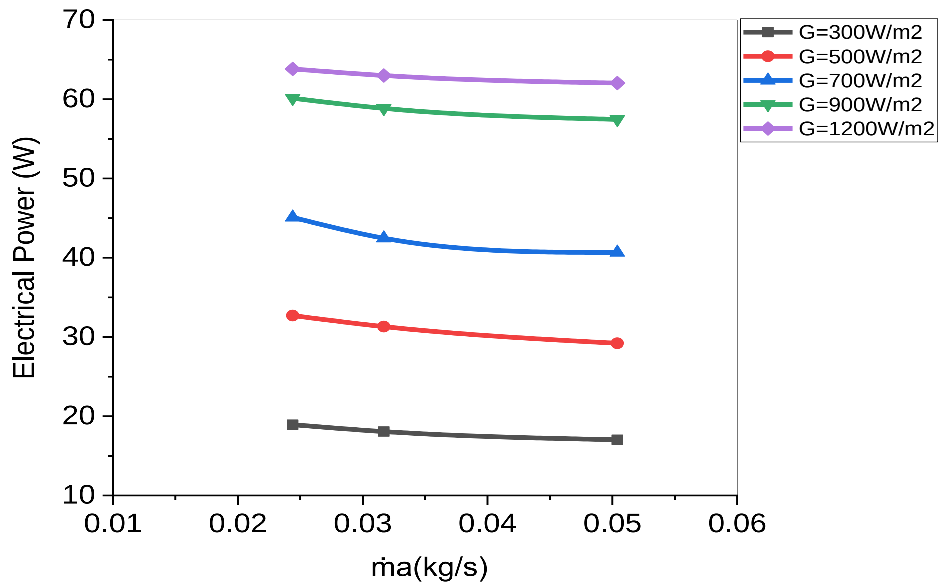

Figure5-37 Electrical power generation with different air mass flow rate

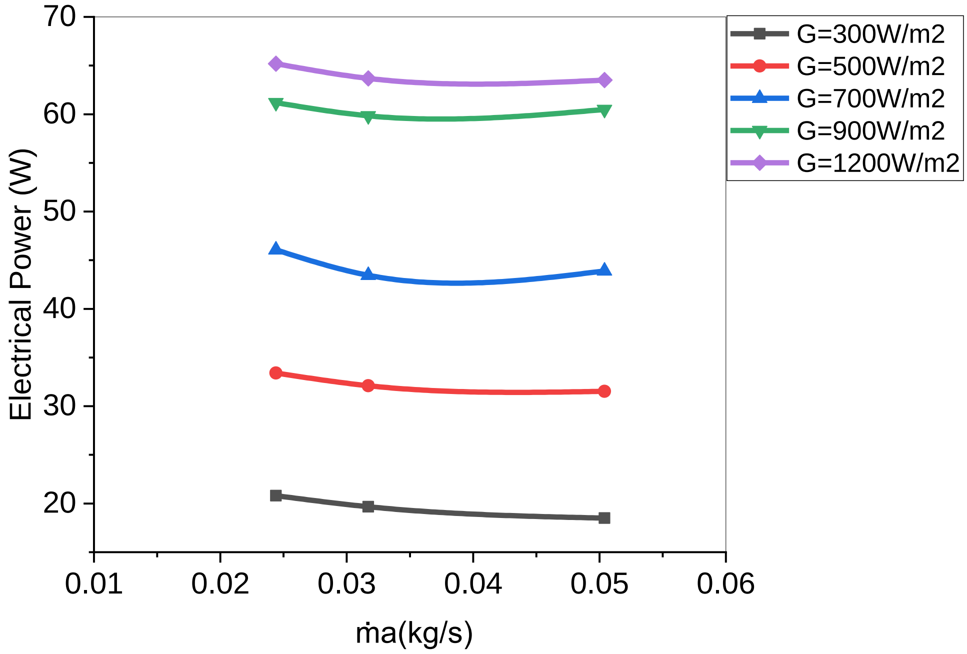

Figure5-38 Electrical Power generation with different air mass flow rate

At higher solar radiation 1200W/m^2 electrical energy generation increased and it arrived to (63.812, 62.988, 62.033) W at (0.0244 , 0.0317,0.0504) kg/s air mass flow rate for PV/T combine system with water as shown in Figure 5-37 and specified in Table 5-18. It reached to (65.195, 63.68, 63.515) W at (0.0244,0.0317,0.0504) kg/s air mass flow rate for PV/T combine system with MWCNT-nanofluid as shown in Figure 5-38 and specified in Table 5-17.

b. Thermal Power

Figure 5-39 and Figure 5-40 explain the decrease in the thermal power generation as air mass flow rate increased. At lower solar radiation 300 W/m^2, the thermal power generation reached to (66.368, 28.051, 24.263) W at (0.0244, 0.0317, 0.0504) kg/s for PV/T combine system with water as shown in Figure 5-39 and specified in Table 5-17. It reached to (93.901, 44.498, 23.924) W at (0.0244, 0.0317, 0.0504) kg/s for PV/T combine system with MWCNT-nanofluid as shown in Figure 5-40 and specified in Table 5-17.

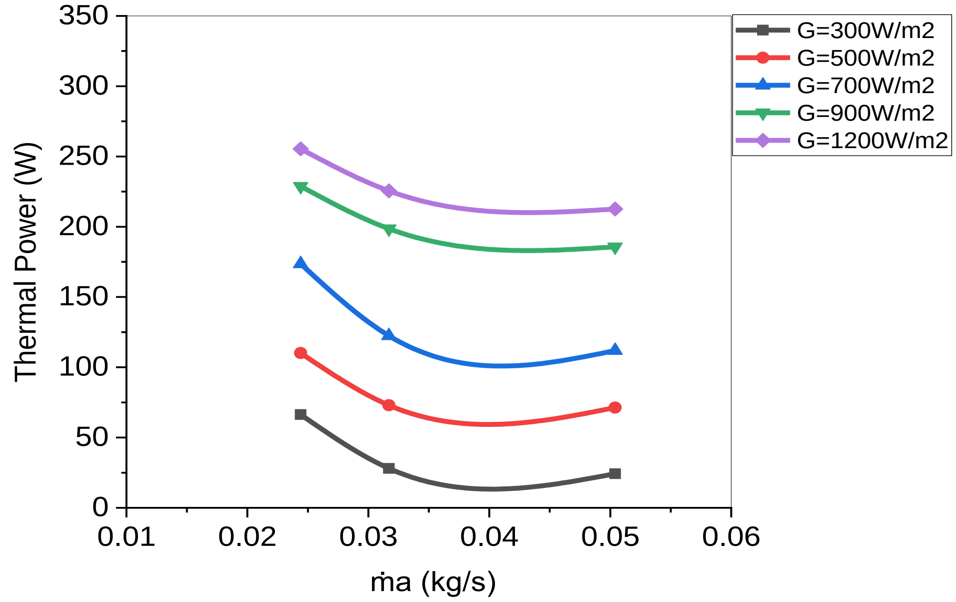

Figure5-39 Thermal power generation with air mass flow rate

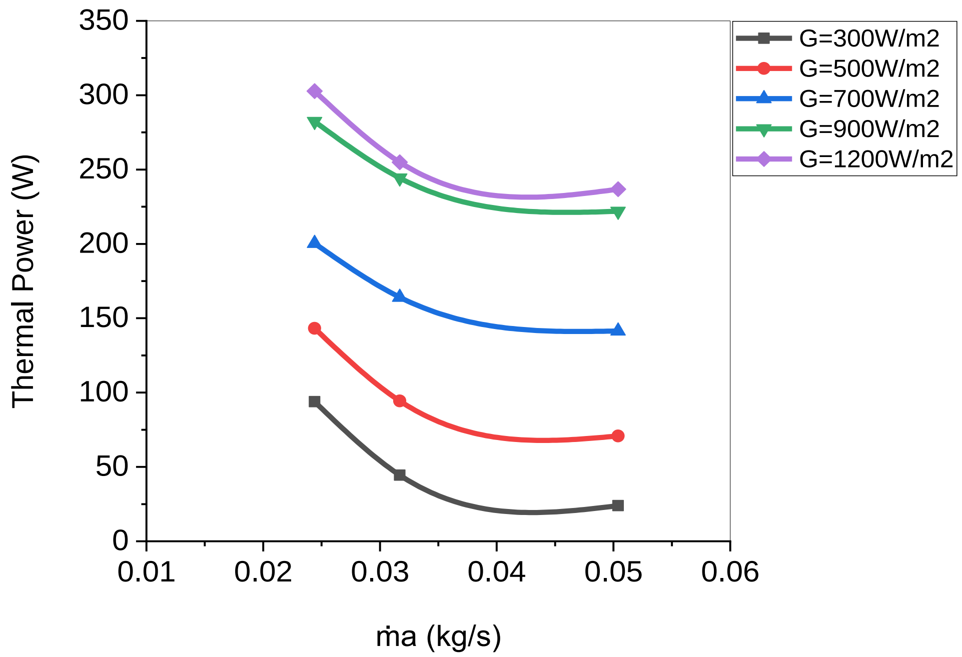

Figure5-40 Thermal power generation with different air mass flow rate

At higher solar radiation 1200W/m^2, the thermal power generation raised and it arrived to (245.403, 225.526, 212.586) W at (0.0244 ,0.0317 ,0.0504) kg/s for PV/T combine system with water as shown in Figure 5-40 and specified in Table 5-17. It reached to (302.728,254.881, 236.817) W at (0.0244, 0.0317, 0.0504) kg/s for PV/T combine system with MWCNT-nanofluid as shown in Figure 5-40 and specified in Table 5-17.

Table 5- 17Power analysis for PV/T combine system with MWCNT-nanofluid and PV/T combine system with water and PV module at ṁ = 0.05kg/s and at 1200 W/m2 solar radiation

Air mass Flow rate (kg/s)	PV/T combine with MWCNT-nanofluid		PV/T combine with Water mass		PV module	
	Thermal Power (W)	Electrical Power (W)	Thermal Power (W)	Electrical Power (W)	Thermal Power (W)	Electrical Power (W)
0.0244	302.728	65.195	255.403	63.812	-	52.777
0.0317	254.881	63.68	225.526	62.988	-	52.777
0.0504	236.817	63.515	212.586	62.033	-	52.777

5.4.2. Effect of Changing Masses Flow on Exergy Generation for PV/T Combine System

5.4.2.1 Effect of Changing (Water, MWCNT-nanofluid) Mass Flow on Exergy Generation

a. Electrical Exergy

Figure 5-41 and Figure 5-42 show the increase in the electrical exergy generation as mass flow rate increased for both (water, MWCNT-nanofluid) . At 300 W/m^2, the electrical exergy generation reached to (17.165, 17.021, 17.998) W at (0.0166, 0.033, 0.05) kg/s for PV/T combine system with water as shown in Figure 5-41 and specified in Table 5-18. It reached to (17.2, 17.392, 20.652) W at (0.0166, 0.033,0.05) kg/s for PV/T combine system with MWCNT-nanofluid as shown in Figure 5-42 and specified in Table 5-18.

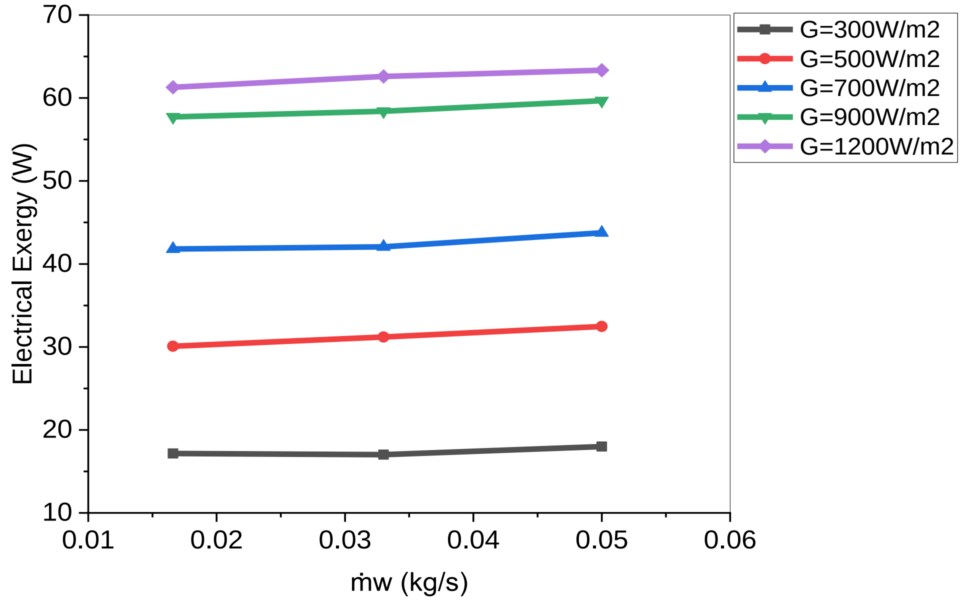

Figure5- 41 Electrical exergy generation with different water mass flow rate

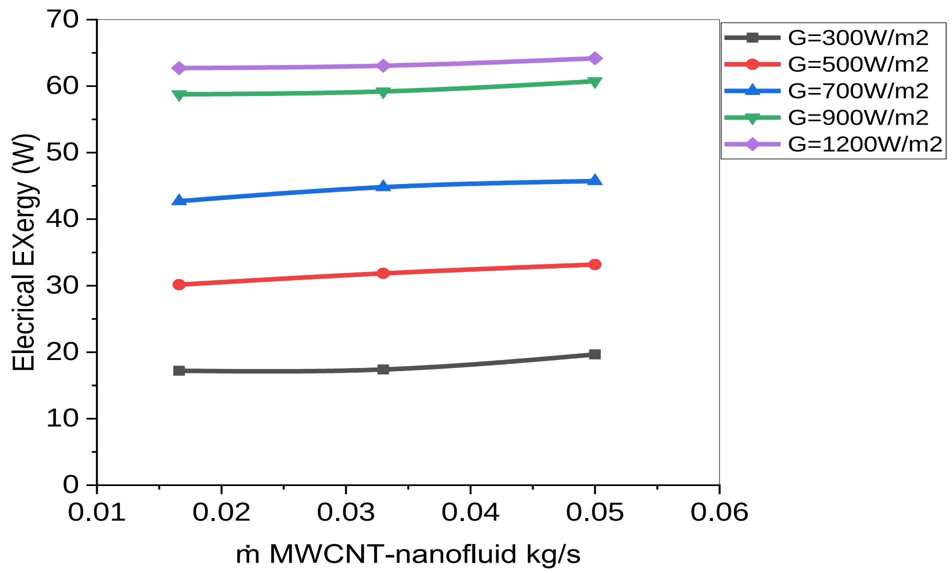

Figure5-42 Electrical exergy generation with different MWCNT-nanofluid mass flow rate

At 1200W/m^2, the electrical exergy generation raised and arrived to (61.29, 62.59, 63.344) W at (0.0166, 0.033, 0.05) kg/s for PV/T combine system with water as shown in Figure 5-41 and specified in Table 5-18. It reached to (62.715, 63.073, 64.185) W at (0.0166, 0.033, 0.05) kg/s for PV/T combine system with MWCNT-nanofluid as shown in Figure 5-42 and specified in Table 5-18.

b.Thermal Exergy

Table 5- 18 indicates that the thermal exergy of the PV/T combine system is much less than its electrical exergy, and this shows that electrical energy is of greater quality than thermal energy. The highest value of thermal exergy is reached when the solar radiation increases. At 1200 W/m^2 solar radiation, the thermal exergy reached to (-3.939, -4.373, -4.771, -6.989, -8.06) W for PV/T combine with MWCNT-nanofluid and (-3.04, -4.05, -4.068, -6.265, -7.429) for PV/T combine with water under (0.0166, 0.033, 0.05, 0.066 ,0.0833) kg/s mass flow for both MWCNT-nanofluid and water.

Allusion regarding the negative signal showing in the thermal exergy appears due to the temperature difference between the fluids circulating within the PV/T combine system and the ambient temperature. This leads to reversing the thermal losses direction from the ambient to the system, because the temperature of the fluid passing inside the pipes is lesser than the ambient temperature through the testes.

Table 5- 18Exergy analysis for PV/T combine system with MWCNT-nanofluid and PV/T combine system with water and PV module at ṁa = 0.05kg/s and at 1200 W/m2 solar radiation

Mass Flow rate (kg/s)	PV/T combine with MWCNT-nanofluid		PV/T combine with Water mass		PV module	
	Thermal Exergy (W)	Electrical Exergy (W)	Thermal Exergy (W)	Electrical Exergy (W)	Thermal Exergy (W)	Electrical Exergy (W)
0.0166	-3.939	62.715	-3.041	62.294	-	52.616
0.033	-4.373	63.073	-4.050	62.59	-	52.616
0.05	-4.771	64.716	-4.0688	63.344	-	52.616
0.066	-6.989	-	-6.265	-	-	52.616
0.0833	-8.061	-	-7.429	-	-	52.616

5.4.2.2 Effect of Air Mass Flow Change on Exergy Generation

a. Electrical Exergy

Figure 5-43 and Figure 5-44 show the decrease in the electrical exergy generation as air mass flow rate increased. At 300 W/m^2, the electrical exergy generation reached to (18.257, 17.29, 16.899) W at (0.0244, 0.0317, 0.0504) kg/s for PV/T combine system with water as shown in Figure 5-43 and specified in Table 5-19. It reached to (20.65, 19.52, 18.355) W at (0.0244, 0.0317, 0.0504) kg/s for PV/T combine system with MWCNT-nanofluid as shown in Figure 5-44 and specified in Table 5-19.

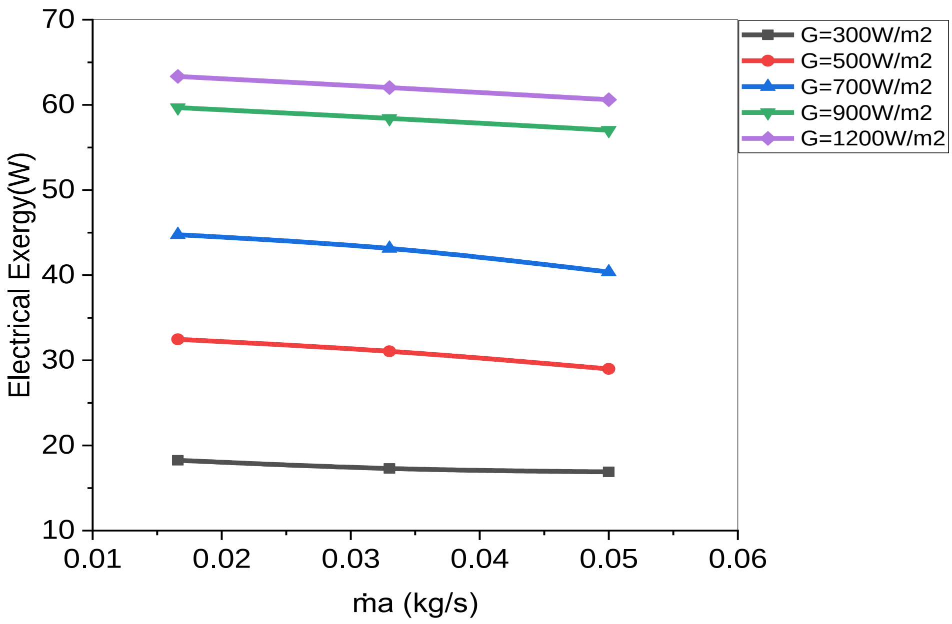

Figure5-43 Electrical exergy generation with different air mass flow rate

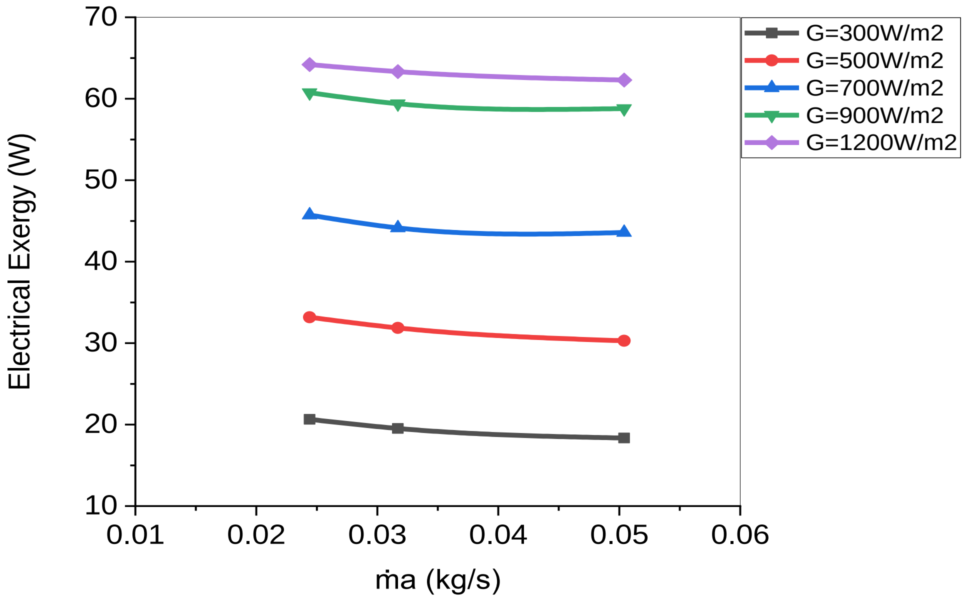

Figure5-44 Electrical exergy generation with different air mass flow rate

At 1200W/m^2, the electrical exergy generation arrived to (63.344, 62.033, 60.615) W at (0.0244, 0.0317, 0.0504) kg/s for PV/T combine system with water as shown in Figure 5-43 and specified in Table 5-19. It reached to (64.185, 63.327, 62.287) W at (0.0244, 0.0317, 0.0504) kg/s for PV/T combine system with MWCNT-nanofluid as shown in Figure 5-44 and specified in Table 5-19.

b.Thermal Exergy

Table 5-19 shows that the thermal exergy of the PV/T combine system decreased as air mass flow rate increased. At 1200 W/m^2 solar radiation, the thermal exergy reached to (-4.771, -5.504, -6.862) W for PV/T combine with MWCNT-nanofluid and (-4.068, -5.026, -6.764) for PV/T combine with water under (0.0244 ,0.0317 ,0.0504) kg/s air mass flow.

Table 5- 19 Exergy analysis for PV/T combine system with MWCNT-nanofluid and PV/T combine system with water and PV module at ṁw = 0.0504kg/s and at 1200 W/m2 solar radiation

Air mass Flow	PV/T combine with MWCNT-nanofluid	PV/T combine with Water mass	PV module

rate (kg/s)	Thermal Exergy (W)	Electrical Exergy (W)	Thermal Exergy (W)	Electrical Exergy (W)	Thermal Exergy (W)	Electrical Exergy (W)
0.0244	-4.771	64.185	-4.068	63.344	-	53.431
0.0317	-5.504	63.327	-5.026	62.033	-	53.431
0.0504	-6.862	62.287	-6.764	60.615	-	53.431

5.5 Exergy Efficiency

Figure 5-45 and Figure 5-46 illustrate the effect of various fluids mass flow rate (Water, MWCNT-nanofluid) on the exergy efficiency of the PV/T combine system. It shows that the exergy efficiency increased with the increase in fluids mass flow (Water, MWCNT-nanofluid). At lower solar radiation 300 w/m^2, the exergy efficiency reached to (13.456, 13.624, 14.061) % for PV/T combine system with water as shown in Figure 5-45, and reached to (13.625 ,13.711 14.225) % for PV/T combine system with MWCNT-nanofluid as shown in Figure 5-46, at (0.0166 , 0.033 , 0.05)kg/s mass flow rate for (Water, MWCNT-nanofluid) and constant air mass flow at 0.0244kg/s.

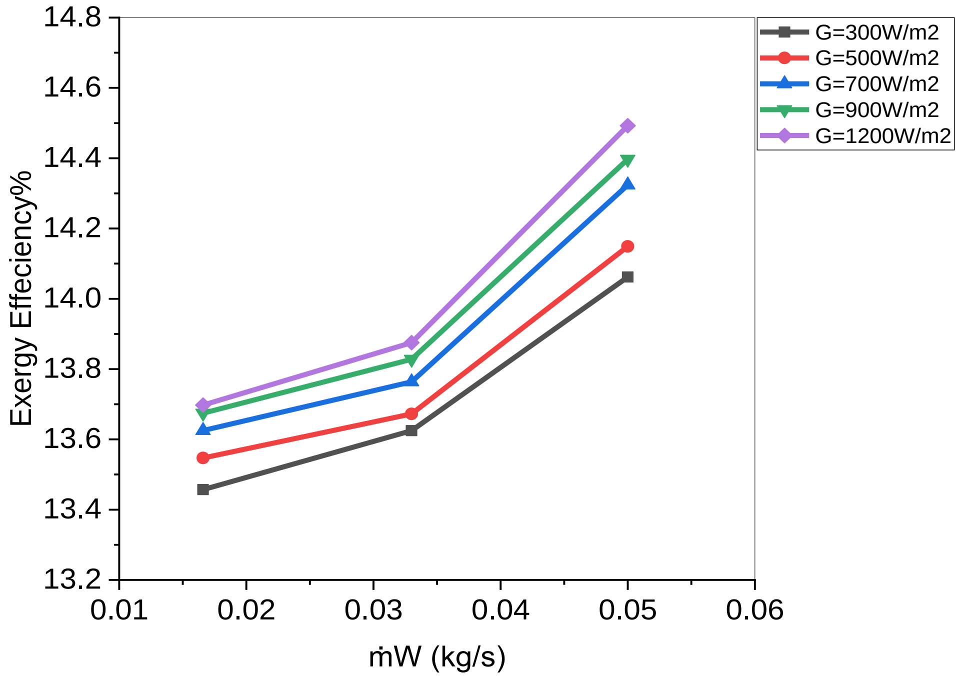

Figure5-45 Exergy efficiency variation with water mass flow rate and solar

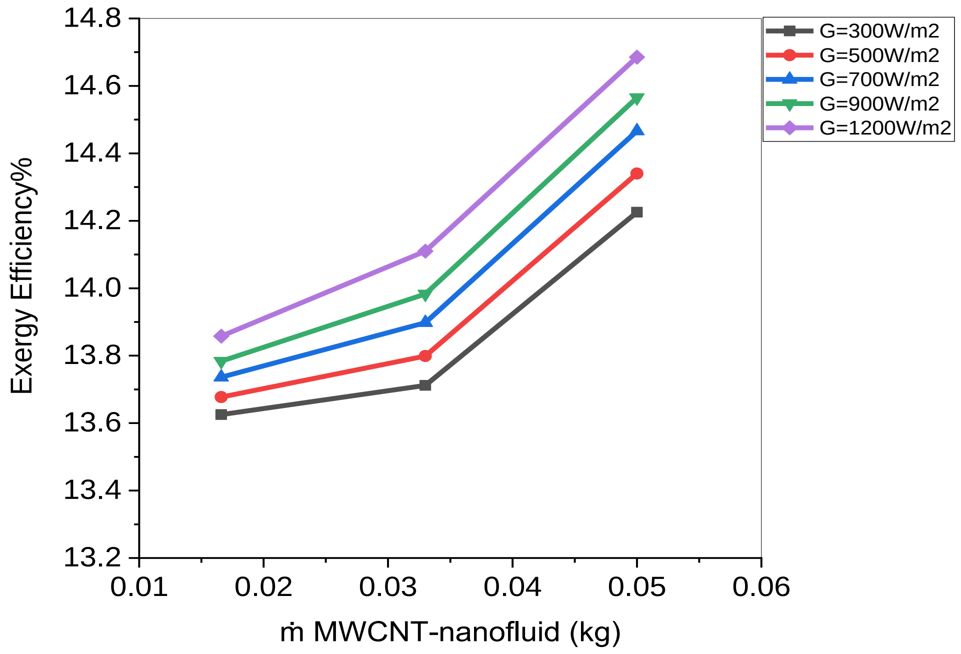

Figure546 Exergy efficiency variation with MWCNT-nanofluid mass flow rate and solar radiation

When the solar radiation increased to1200 W/m^2, the exergy efficiency increased and reached to (13.69, 13.875, 14.492) % for PV/T combine system with water as shown in Figure 5-45, and to (13.857, 14.109 ,14.685) % for PV/T combine system with MWCNT-nanofluid as shown in Figure 5-46, at (0.0166 ,0.033, 0.05) kg/s mass flow rate for (Water, MWCNT-nanofluid) and constant air mass flow at 0.0244 kg/s.

Figure 5-47 and Figure 5-48 illustrate the effect of various air mass flow on the exergy efficiency of the PV/T combine system with constant (Water, MWCNT-nanofluid) mass flow rate at 0.05 kg/s. It shows that the exergy efficiency decreased with the increase in air mass flow rate. It also shows that at lower solar radiation 300 w/m^2, the exergy efficiency reached to (14.061, 13.695, 13.654) % for PV/T combine system with water as shown in Figure 5-47, and to (14.685, 13.702, 13.693) % for PV/T combine system with MWCNT-nanofluid as shown in Figure 5-48 at (0.0244, 0.0317, 0.0504) kg/s air mass flow rate for both PV/T combine system with water and PV/T combine system with MWCNT-nanofluid .

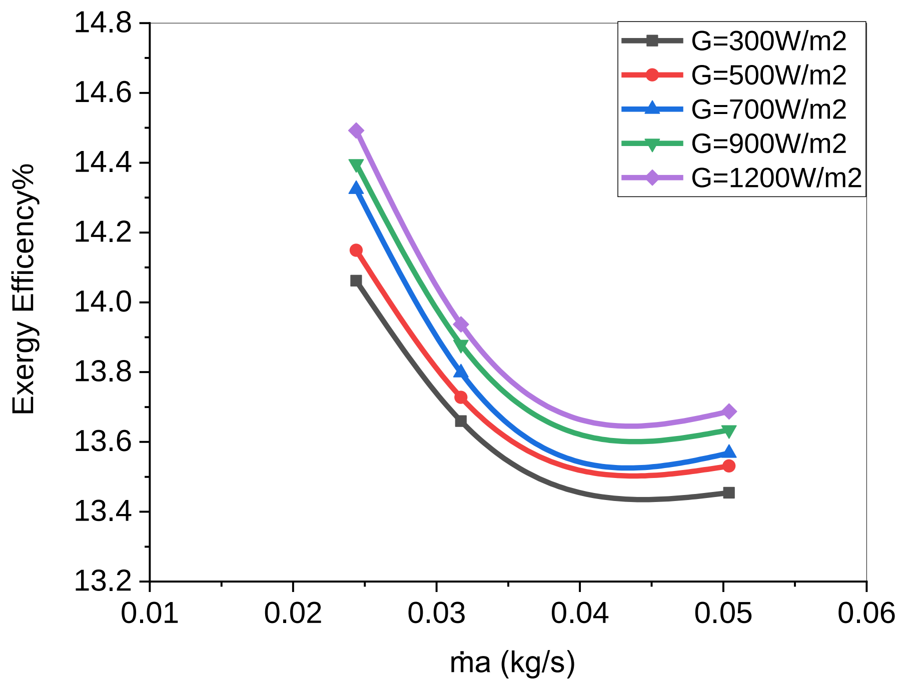

Figure5-47 Exergy efficiency variation with air mass flow rate and solar radiation

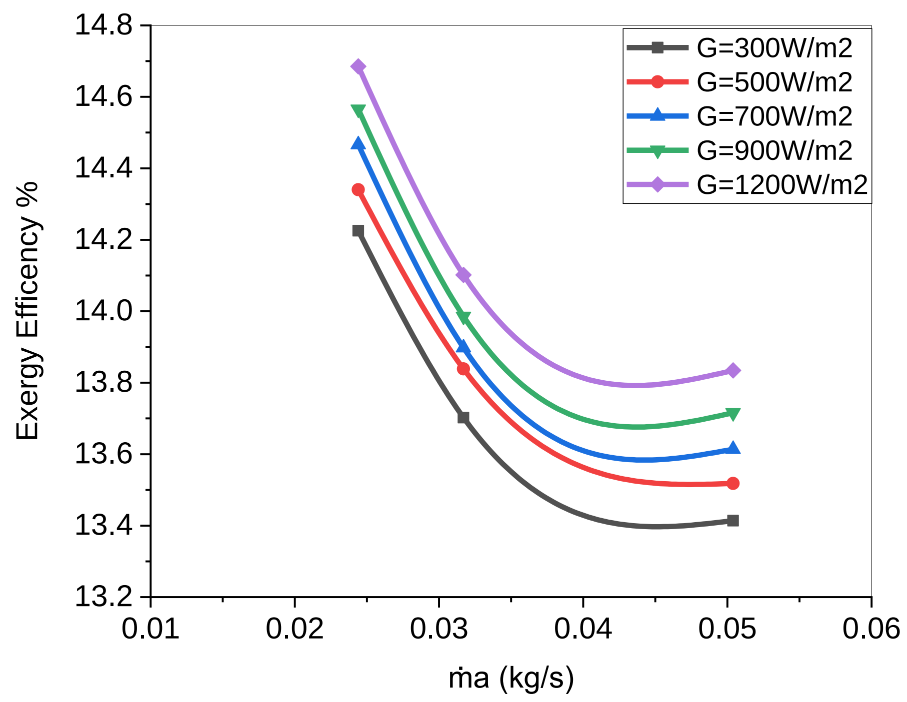

Figure5-48 Exergy efficiency variation with air mass flow rate and solar radiation

When the solar radiation increased to 1200 W/m^2, the exergy efficiency increased and reached to (14.49, 13.93, 13.85) % for PV/T combine system with water as shown in Figure 5-47, and (14.68,14.1,14.01) % for PV/T combine system with MWCNT-nanofluid as shown in Figure 5-48 at (0.0244, 0.0317, 0.0504) kg/s air mass flow rate for both PV/T combine system with water and PV/T combine system with MWCNT-nanofluid.

Chapter Six

Conclusions and Recommendations

for Future Projects

6-1 Conclusions

From numerical and practical study were conducted on the PV/T combine system, the following conclusions were obtained:

1-The diameter of the pipes works effectively by contributing to the reduction in the temperature of the PV panel, where the simulation results for a Comsol program showed the lowest distribution of base temperature for PV panel when using cupper pipe with 8mm inner diameter.

2-Increasing the number of pipes that are distributed under the PV panel contributes to increasing the contact area, which provides the largest area for heat exchange, where the simulation results showed that the best temperature distribution was achieved at 16 pipes number.

3- The mass flow rate has a significant impact on the PV/T combine system cooling, including the base temperature (Tb). Increment in air and water mass flow or air and MWCNT-nanofluid mass flow as a result of the volume entering the system will increase and take the heat away from the PV/T combine system. This also lowers the base temperature (Tb) of the PV/T combine system. The highest temperature reduction obtained was at 0.0244kg/s mass flow rate for air and 0.05kg/s for water and MWCNT-nanofluid mass flow with both PV/T combine with air and water and PV/T with air and MWCNT-nanofluid.

4- The practical tests showed that the PV/T combine system with MWCNT-nanofluid and air as cooling fluid has a higher improvement in the electrical efficiency than PV/T combine system with water and air in comparison with traditional PV panel. The amount of improvement in the electrical efficiency was 21.667% for PV/T combine with air and water as a cooling fluid when the base temperature(Tb) was lowered from 89.3℃ to 53.5℃. The electrical efficiency increased from 10.747%

to13.076 % for PV/T combine system with water and air. The rate of improvement in the electrical efficiency was 23.529% when the base temperature (Tb) was lowered from 87℃ to 49.3℃ and it increased from 10.815% to 13.359% for PV/T with air and MWCNT-nanofluid as a cooling fluid.

5- Also, the practical tests showed the improvement in the thermal performance of the PV/T combine system with MWCNT-nanofluid and air compared to the thermal performance of the PV/T combine with water and air. Each of the generated heat energy, total thermal efficiency ,overall efficiency and exergy efficiency for PV/T combine reached to 302.728W, 56.579%, 92.883%, 14.685% respectively with MWCNT-nanofluid and air and 235.403W, 49.475% 82.966%,14.492% for PV/T combine with water and air as a cooling fluid.

6- Due to the presence of phase changing materials(PCM) the difference in temperature continued for an hour after sunset for both the air and the outside water.

6-2 Recommendations for Future Projects

For future projects, the following suggestions are offered:

1- Employing other kinds of PCM with additives, where it is possible to add nanoparticles that improve heat transfer and draw the largest amount of heat from the base surface of PV solar panel for PV/T combine system.
2- Employing MWCNT with different concentrations, in addition to using other types of nanofluids such as Cuo ,Sio ,Tio.
3- Circulating the water leaving the PV/T combine system inside a heat exchanger that is placed inside a thermally insulated tank for several cycles. It works to raise the temperature of the water inside the tank and can be used later for domestic uses.
4- Using a thermally insulated hose to introduce hot air outcome from the PV/T combine system into a thermally insulated chamber, where it works to warm the air inside the room and may be utilized for drying applications.

References:

[1] R. Nasrin, N. A. Rahim, H. Fayaz, and M. Hasanuzzaman, “Water/MWCNT nanofluid based cooling system of PVT: Experimental and numerical research,” *Renew. Energy*, vol. 121, pp. 286–300, 2018, doi: 10.1016/j.renene.2018.01.014.

[2] A. I. A. AL-Musawi, A. Taheri, A. Farzanehnia, M. Sardarabadi, and M. Passandideh-Fard, “Numerical study of the effects of nanofluids and phase-change materials in photovoltaic thermal (PVT) systems,” *J. Therm. Anal. Calorim.*, vol. 137, no. 2, pp. 623–636, 2019, doi: 10.1007/s10973-018-7972-6.

[3] F. Yazdanifard and M. Ameri, “Exergetic advancement of photovoltaic/thermal systems (PV/T): A review,” *Renew. Sustain. Energy Rev.*, vol. 97, no. May, pp. 529–553, 2018, doi: 10.1016/j.rser.2018.08.053.

[4] H. Fayaz, R. Nasrin, N. A. Rahim, and M. Hasanuzzaman, “Energy and exergy analysis of the PVT system: Effect of nanofluid flow rate,” *Sol. Energy*, vol. 169, no. April, pp. 217–230, 2018, doi: 10.1016/j.solener.2018.05.004.

[5] N. S. Binti Rukman, A. Fudholi, N. F. Mohd Razali, M. Hafidz Ruslan, and K. Sopian, “Investigation of TiO2 and MWCNT Nanofluids-based Photovoltaic-Thermal (PV/T) System,” *IOP Conf. Ser. Earth Environ. Sci.*, vol. 268, no. 1, 2019, doi: 10.1088/1755-1315/268/1/012076.

[6] A. N. Al-Shamani, K. Sopian, S. Mat, H. A. Hasan, A. M. Abed, and M. H. Ruslan, “Experimental studies of rectangular tube absorber photovoltaic thermal collector with various types of nanofluids under the tropical climate conditions,” *Energy Convers. Manag.*, vol. 124, pp. 528–542, 2016, doi: 10.1016/j.enconman.2016.07.052.

[7] A. Hassan *et al.*, “Thermal management and uniform temperature regulation of photovoltaic modules using hybrid phase change materials-nanofluids system,” *Renew. Energy*, vol. 145, pp. 282–293, 2020, doi: 10.1016/j.renene.2019.05.130.

[8] M. Mustapha, A. Fudholi, C. Hoy Yen, M. Hafidz Ruslan, and K. Sopian, “Review on Energy and Exergy Analysis of Air and Water Based Photovoltaic Thermal (PVT) Collector,” *Int. J. Power Electron. Drive Syst.*, vol. 9, no. 3, p. 1367, 2018, doi: 10.11591/ijpeds.v9.i3.pp1367-1373.

[9] A. Fudholi, K. Sopian, M. Y. Othman, M. H. Ruslan, and B. Bakhtyar, “Energy analysis and improvement potential of finned double-pass solar collector,” *Energy Convers. Manag.*, vol. 75, pp. 234–240, 2013, doi: 10.1016/j.enconman.2013.06.021.

[10] S. Diwania, S. Agrawal, A. S. Siddiqui, and S. Singh, “Photovoltaic–thermal (PV/T) technology: a comprehensive review on applications and its advancement,” *Int. J. Energy Environ. Eng.*, vol. 11, no. 1, pp. 33–54, 2020, doi: 10.1007/s40095-019-00327-y.

[11] J. Ji, C. Guo, W. Sun, W. He, Y. Wang, and G. Li, “Experimental investigation of tri-functional photovoltaic/thermal solar collector,” *Energy Convers. Manag.*, vol. 88, pp. 650–656, 2014, doi: 10.1016/j.enconman.2014.09.030.

[12] X. Yang, L. Sun, Y. Yuan, X. Zhao, and X. Cao, “Experimental investigation on performance comparison of PV/T-PCM system and PV/T system,” *Renew. Energy*, vol. 119, pp. 152–159, 2018, doi: 10.1016/j.renene.2017.11.094.

[13] O. Of, “Energy and exergy analysis of a two pass photovoltaic – thermal (PV/T) air heater,” *Int. J. Energy Environ.*, vol. 4, no. 3, pp. 467–480, 2013.

[14] M. Y. H. Othman, F. Hussain, K. Sopian, B. Yatim, and H. Ruslan, “Performance study of air-based photovoltaic-thermal (PV/T) collector with different designs of heat exchanger,” *Sains Malaysiana*, vol. 42, no. 9, pp. 1319–1325, 2013.

[15] K. E. Amori and M. A. Abd-AlRaheem, “Field study of various air based photovoltaic/thermal hybrid solar collectors,” *Renew. Energy*, vol. 63, pp. 402–414, 2014, doi: 10.1016/j.renene.2013.09.047.

[16] O. K. Ahmed and Z. A. Mohammed, “Influence of porous media on the performance of hybrid PV/Thermal collector,” *Renew. Energy*, vol. 112, no. November, pp. 378–387, 2017, doi: 10.1016/j.renene.2017.05.061.

[17] “Exergy and sustainability index of photovoltaic thermal (PVT) air collector.pdf.” .

[18] S. Y. Wu, T. Wang, L. Xiao, and Z. G. Shen, “Effect of cooling channel position on heat transfer characteristics and thermoelectric performance of air-cooled PV/T system,” *Sol. Energy*, vol. 180, no. January, pp. 489–500, 2019, doi: 10.1016/j.solener.2019.01.043.

[19] Y. Zhao, T. Meng, C. Jing, J. Hu, and S. Qian, “Experimental and numerical investigation on thermal performance of PV-driven aluminium honeycomb solar air collector,” *Sol. Energy*, vol. 204, no. April, pp. 294–306, 2020, doi: 10.1016/j.solener.2020.04.047.

[20] A. A. Jadallah, M. K. Alsaadi, and S. A. Hussien, “The hybrid Photovoltaic-Thermal double-pass solar system for drying applications,” *IOP Conf. Ser. Mater. Sci. Eng.*, vol. 765, no. 1, 2020, doi: 10.1088/1757-899X/765/1/012024.

[21] A. Nahar, M. Hasanuzzaman, and N. A. Rahim, “Numerical and experimental investigation on the performance of a photovoltaic thermal collector with parallel plate flow channel under different operating conditions in Malaysia,” *Sol. Energy*, vol. 144, pp. 517–528, 2017, doi: 10.1016/j.solener.2017.01.041.

[22] A. Kazemian, M. Hosseinzadeh, M. Sardarabadi, and M. Passandideh-Fard, “Effect of glass cover and working fluid on the performance of photovoltaic thermal (PVT) system: An experimental study,” *Sol. Energy*, vol. 173, no. June, pp. 1002–1010, 2018, doi: 10.1016/j.solener.2018.07.051.

[23] H. A. Kazem, A. H. A. Al-Waeli, M. T. Chaichan, K. H. Al-Waeli, A. B. Al-Aasam, and K. Sopian, "Evaluation and comparison of different flow configurations PVT systems in Oman: A numerical and experimental investigation," *Sol. Energy*, vol. 208, no. July, pp. 58–88, 2020, doi: 10.1016/j.solener.2020.07.078.

[24] W. Pang, Q. Zhang, G. J. Wilson, Q. Yang, and H. Yan, "Empirical influence of various environmental conditions and mass flow rates on hybrid photovoltaic thermal modules," *Appl. Therm. Eng.*, vol. 171, no. December 2019, p. 114965, 2020, doi: 10.1016/j.applthermaleng.2020.114965.

[25] M. Sardarabadi, M. Hosseinzadeh, A. Kazemian, and M. Passandideh-Fard, "Experimental investigation of the effects of using metal-oxides/water nanofluids on a photovoltaic thermal system (PVT) from energy and exergy viewpoints," *Energy*, vol. 138, pp. 682–695, 2017, doi: 10.1016/j.energy.2017.07.046.

[26] A. N. Al-Shamani, M. A. Alghoul, A. M. Elbreki, A. A. Ammar, A. M. Abed, and K. Sopian, "Mathematical and experimental evaluation of thermal and electrical efficiency of PV/T collector using different water based nano-fluids," *Energy*, vol. 145, pp. 770–792, 2018, doi: 10.1016/j.energy.2017.11.156.

[27] C. L. L. Beicker, M. Amjad, E. P. Bandarra Filho, and D. Wen, "Experimental study of photothermal conversion using gold/water and MWCNT/water nanofluids," *Sol. Energy Mater. Sol. Cells*, vol. 188, no. May, pp. 51–65, 2018, doi: 10.1016/j.solmat.2018.08.013.

[28] S. Alous, M. Kayfeci, and A. Uysal, "Experimental investigations of using MWCNTs and graphene nanoplatelets water-based nanofluids as coolants in PVT systems," *Appl. Therm. Eng.*, vol. 162, no. August, p. 114265, 2019, doi: 10.1016/j.applthermaleng.2019.114265.

[29] S. Preet, B. Bhushan, and T. Mahajan, "Experimental investigation of water based photovoltaic/thermal (PV/T) system with and without phase change material (PCM)," *Sol. Energy*, vol. 155, pp. 1104–1120, 2017, doi: 10.1016/j.solener.2017.07.040.

[30] S. Mousavi, A. Kasaeian, M. B. Shafii, and M. H. Jahangir, "Numerical investigation of the effects of a copper foam filled with phase change materials in a water-cooled photovoltaic/thermal system," *Energy Convers. Manag.*, vol. 163, no. September 2017, pp. 187–195, 2018, doi: 10.1016/j.enconman.2018.02.039.

[31] J. Zhao, Z. Li, and T. Ma, "Performance analysis of a photovoltaic panel integrated with phase change material," *Energy Procedia*, vol. 158, pp. 1093–1098, 2019, doi: 10.1016/j.egypro.2019.01.264.

[32] A. H. A. Al-Waeli *et al.*, "Comparison of prediction methods of PV/T nanofluid and nano-PCM system using a measured dataset and artificial neural network," *Sol. Energy*, vol. 162, no. December 2017, pp. 378–396, 2018, doi: 10.1016/j.solener.2018.01.026.

[33] T. Maatallah, R. Zachariah, and F. G. Al-Amri, "Exergo-economic analysis of a serpentine flow type water based photovoltaic thermal system with phase change material (PVT-PCM/water)," *Sol. Energy*, vol. 193, no. May, pp. 195–204, 2019, doi: 10.1016/j.solener.2019.09.063.

[34] C. Kandilli, "Energy, exergy, and economical analyses of a photovoltaic thermal system integrated with the natural zeolites for heat management," *Int. J. Energy Res.*, vol. 43, no. 9, pp. 4670–4685, 2019, doi: 10.1002/er.4605.

[35] H. Xu, C. Zhang, N. Wang, Z. Qu, and S. Zhang, "Experimental study on the performance of a solar photovoltaic/thermal system combined with phase change material," *Sol. Energy*, vol. 198, no. December 2019, pp. 202–211, 2020, doi: 10.1016/j.solener.2020.01.064.

[36] M. N. Abu Bakar, M. Othman, M. Hj Din, N. A. Manaf, and H. Jarimi, "Design concept and mathematical model of a bi-fluid photovoltaic/thermal (PV/T) solar collector," *Renew. Energy*, vol. 67, pp. 153–164, 2014, doi: 10.1016/j.renene.2013.11.052.

[37] M. Y. Othman, S. A. Hamid, M. A. S. Tabook, K. Sopian, M. H. Roslan, and Z. Ibarahim, "Performance analysis of PV/T Combi with water and air heating system: An experimental study," *Renew. Energy*, vol. 86, no. Florschuetz 1979, pp. 716–722, 2016, doi: 10.1016/j.renene.2015.08.061.

[38] M. Y. Othman, S. A. Hamid, M. A. S. Tabook, K. Sopian, M. H. Roslan, and Z. Ibarahim, "Performance analysis of PV/T Combi with water and air heating system: An experimental study," *Renew. Energy*, vol. 86, pp. 716–722, 2016, doi: 10.1016/j.renene.2015.08.061.

[39] K. Sopian *et al.*, "Performance of double pass PV/T combi solar collector with CPC: Theoretical approach," *Energy Sustain. Small Dev. Econ. ES2DE 2017 - Proc.*, 2017, doi: 10.1109/ES2DE.2017.8015345.

[40] M. Imtiaz Hussain, J. H. Kim, and J. T. Kim, "Nanofluid-powered dual-fluid photovoltaic/thermal (PV/T) system: Comparative numerical study," *Energies*, vol. 12, no. 5, 2019, doi: 10.3390/en12050775.

[41] S. S. S. Baljit, H. Y. Chan, S. H. Zaidi, and K. Sopian, "Performance study of a dual-fluid photovoltaic thermal collector with reflection and refraction solar concentrators," *Int. J. Low-Carbon Technol.*, vol. 15, no. 1, pp. 25–39, 2019, doi: 10.1093/ijlct/ctz054.

[42] M. I. Hussain and J. T. Kim, "Outdoor testing to compare the technical and economic aspects of single-and dual-fluid photovoltaic/thermal (PV/T) systems," *Appl. Sci.*, vol. 10, no. 16, 2020, doi: 10.3390/app10165641.

[43] M. S. Hossain, A. K. Pandey, J. Selvaraj, N. A. Rahim, M. M. Islam, and V. V. Tyagi, "Two side serpentine flow based photovoltaic-thermal-phase change materials (PVT-PCM) system: Energy, exergy and economic analysis," *Renew. Energy*, vol. 136, pp. 1320–1336, 2019, doi: 10.1016/j.renene.2018.10.097.

[44] F. Mechanics and H. Machines, *rin g.n et.* .

[45] J. F. Douglas, J. M. Gasiotek, and J. A. Swaffield, *Fluid Mechanics.* 1979.

[46] A. Fudholi, K. Sopian, M. H. Yazdi, M. H. Ruslan, A. Ibrahim, and H. A. Kazem, “Performance analysis of photovoltaic thermal (PVT) water collectors,” *Energy Convers. Manag.*, vol. 78, pp. 641–651, 2014, doi: 10.1016/j.enconman.2013.11.017.

[47] S. A. Kalogirou, *Solar Energy Engineering: Processes and Systems: Second Edition*. 2014.

[48] “LECTURE NOTE, Exergy Analysis, AF (2).” .

[49] A. Kazemian, M. Hosseinzadeh, M. Sardarabadi, and M. Passandideh-Fard, “Experimental study of using both ethylene glycol and phase change material as coolant in photovoltaic thermal systems (PVT) from energy, exergy and entropy generation viewpoints,” *Energy*, vol. 162, pp. 210–223, 2018, doi: 10.1016/j.energy.2018.07.069.

[50] N. D. S. E. Materials, J. M. S. E. Materials, and S. Cells, “07 Alternative energy sources (solar energy) 02 / 02080 Network analysis of fault-tolerant solar photovoltaic arrays 02 / 02075 Calculation of the PV modules angular losses under field conditions by means of an analytical model 02 / 02081 Performance ev,” no. July, p. 2002, 2002.

[51] V. Tomar, G. N. Tiwari, T. S. Bhatti, and B. Norton, “Thermal modeling and experimental evaluation of five different photovoltaic modules integrated on prototype test cells with and without water flow,” *Energy Convers. Manag.*, vol. 165, no. November 2017, pp. 219–235, 2018, doi: 10.1016/j.enconman.2018.03.039.

[52] M. Hu *et al.*, “Performance assessment of a trifunctional system integrating solar PV, solar thermal, and radiative sky cooling,” *Appl. Energy*, vol. 260, no. October 2019, p. 114167, 2020, doi: 10.1016/j.apenergy.2019.114167.

[53] C. S. Malvi, D. W. Dixon-Hardy, and R. Crook, “Energy balance model of combined photovoltaic solar-thermal system incorporating phase change material,” *Sol. Energy*, vol. 85, no. 7, pp. 1440–1446, 2011, doi: 10.1016/j.solener.2011.03.027.

[54] P. Barnwal and G. N. Tiwari, “Life cycle energy metrics and CO2 credit analysis of a hybrid photovoltaic/thermal greenhouse dryer,” *Int. J. Low Carbon Technol.*, vol. 3, no. 3, pp. 203–220, 2008, doi: 10.1093/ijlct/3.3.203.

[55] G. Paul, J. Philip, B. Raj, P. K. Das, and I. Manna, “Synthesis, characterization, and thermal property measurement of nano-Al95Zn05 dispersed nanofluid prepared by a two-step process,” *Int. J. Heat Mass Transf.*, vol. 54, no. 15–16, pp. 3783–3788, 2011, doi: 10.1016/j.ijheatmasstransfer.2011.02.044.

[56] E. Ebrahimnia-Bajestan, M. Charjouei Moghadam, H. Niazmand, W.

Daungthongsuk, and S. Wongwises, “Experimental and numerical investigation of nanofluids heat transfer characteristics for application in solar heat exchangers,” *Int. J. Heat Mass Transf.*, vol. 92, pp. 1041–1052, 2016, doi: 10.1016/j.ijheatmasstransfer.2015.08.107.

[57] T. T. Chow, G. Pei, K. F. Fong, Z. Lin, A. L. S. Chan, and J. Ji, “Energy and exergy analysis of photovoltaic-thermal collector with and without glass cover,” *Appl. Energy*, vol. 86, no. 3, pp. 310–316, 2009, doi: 10.1016/j.apenergy.2008.04.016.

[58] M. YEŞİLYURT, M. NASİRİ, and A. OZAKIN, “Techniques for Enhancing and Maintaining Electrical Efficiency of Photovoltaic Systems,” *Int. J. New Technol. Res.*, vol. 4, no. 4, p. 263082, 2018.

[59] M. A. M. Shaltout, M. M. El-Nicklawy, A. F. Hassan, U. A. Rahoma, and M. Sabry, “Temperature dependence of the spectral and efficiency behavior of Si solar cell under low concentrated solar radiation,” *Renew. energy*, vol. 21, no. 3, pp. 445–458, 2000, doi: 10.1016/S0960-1481(00)00075-6.

[60] H. Fayaz, R. Nasrin, N. A. Rahim, and M. Hasanuzzaman, “Energy and exergy analysis of the PVT system: Effect of nanofluid flow rate,” *Sol. Energy*, vol. 169, no. May, pp. 217–230, 2018, doi: 10.1016/j.solener.2018.05.004.

LIST OF APPENDICES

APPENDIX	TITLE
A	: Specifications of the PCM
B	: Specifications of the ultrasonic water bath (Elmasonic P180H)
C	: Specifications of the data logger (model AT-4532)
D	: Specifications of the Pyranometer (model TENMARS TM 207)
E	: Calibration of the Pyranometer (Solar meter)
F	: Calibration of K-type thermocouples provided from the test with Hg-thermometer

A : Specifications of the PCM

Details	**Specifications**
Type	Paraffin wax
Melting point ,Tm (℃)	38–43
Heat of fusion/kJ kg-1	165
Quantity/kg	8.5
Density/kg m-3	880 for solid,770 for liquid
Specific heat/kJ kg-1 K-1	2
Thermal conductivity k for-liquid and solid W/m. K	0.2

B : Characteristics of the ultrasonic water bath (Elmasonic P180H)

Property	**Value**
Mains voltage	115 - 120 V / 220 - 240 V
Ultrasonic frequency	37 / 80 kHz
Power consumption total P180H	1330 W
Ultrasonic power effective	330 W
Ultrasonic peak performance max.	1320 W
Heating power	1000 W
Unit outer dimensions W/D/H	3.90 / 3.40 / 3.21 cm
Tank internal dimensions W/D/H	327 / 300 / 200 cm
Basket internal dimensions W/D/H	280 / 250 / 115 cm
Max. filling volume tank	12 liter
Weight	8.5 kg
Material tank	stainless steel V2A
Material casing	stainless steel V2A
Drain	3/8“
CE-compliant	√
Protection class	IP 20

Sound pressure level (LpAU) * (dB)	62 / 58
Ultrasonic sound level (LpZ) ** (dB)	96 / 87

C: Characteristics of the data logger (model AT-4532)

Property	Value
Thermocouple compatibility	J, K, T, E, S, N and B
Accuracy	0.2 % + 1 °C
Range	From -200 °C to 1300 °C (varies depending on thermocouple)
Resolution	0.1 °C
Channels	32-channel thermocouples
Speed	Fast: 100 ms /channel Medium: 500 ms /channel Low: 1ms /channel
Correction	Error correction for each channel
Comparator	High and low beep High and low value setting individually for each channel
Interface	U-disc interface RS232C interface Mini USB (virtual serial port)

D: Characteristics of the Pyranometer (model TENMARS TM 207)

Property	Value
Range	From 0 to ~2000 W/m^2
Temperature Error	±0.38 ºC

Drift	< ± 2% per year
Accuracy	±10 W/m^2 or ± 5 %
Sampling Time	0.25 Second
Operating Temperature	From 0 ºC to 50 ºC
Spectral response	400 nm - 1100 nm
Humidity	< 80 % RH
Weight	0.5 kg
Dimensions W/D/H	22.5 cm / 15.75 cm / 4.75 cm
Battery	1pcs 9 V

E: Characteristics of the Anemometer

Property	Value
Range of velocity	From 0.4 m/s to ~30 m/s
Range of temperature	From 0 ºC to 50 ºC
Accuracy	±2 %
Display	10mm(0.4") 4-digits LCD
Operating temperature	From 0 ºC to 50 ºC
Humidity	< 85 % RH
Weight	0.3 kg
Resolution	0.1 (m/s, km/h and ft/min)
Device screen	Large LCD display for easy viewing (4 digits of 10 mm).

Dimensions W/D/H	14.1 / 7.1 / 3.2 cm
Power Supply	1 x 9 V 6 F22
Sensor head	7.2 cm Diameter

F : Calibration curve of thermocouples

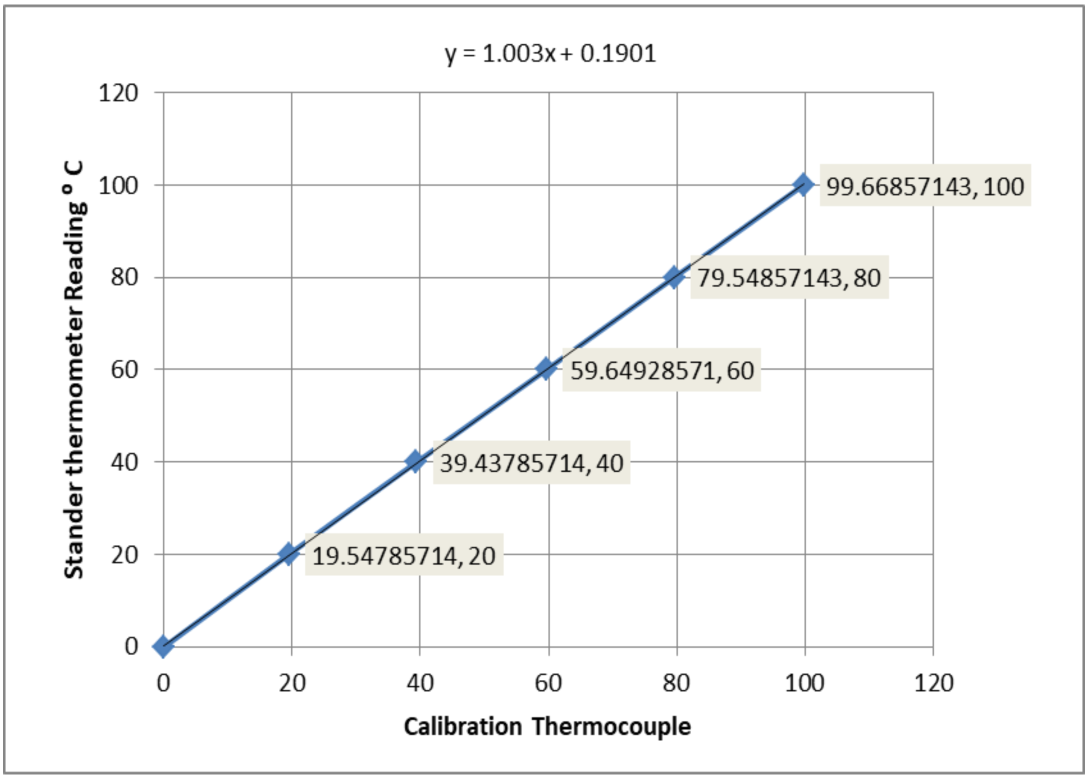

LIST OF PUBLICATIONS

1- Zainab M. Mahdi, Ali N. Al-Shamani, Hazim A. Al-zurfil and K. Sopian“ **Numerical study to determine the optimum design of PV/T water collector, pipes diameter**, **and number of pipes** “Cite as: AIP Conference Proceedings 2404, 020006 (2021); https://doi.org/10.1063/5.0069057 Published Online: 11 October 2021

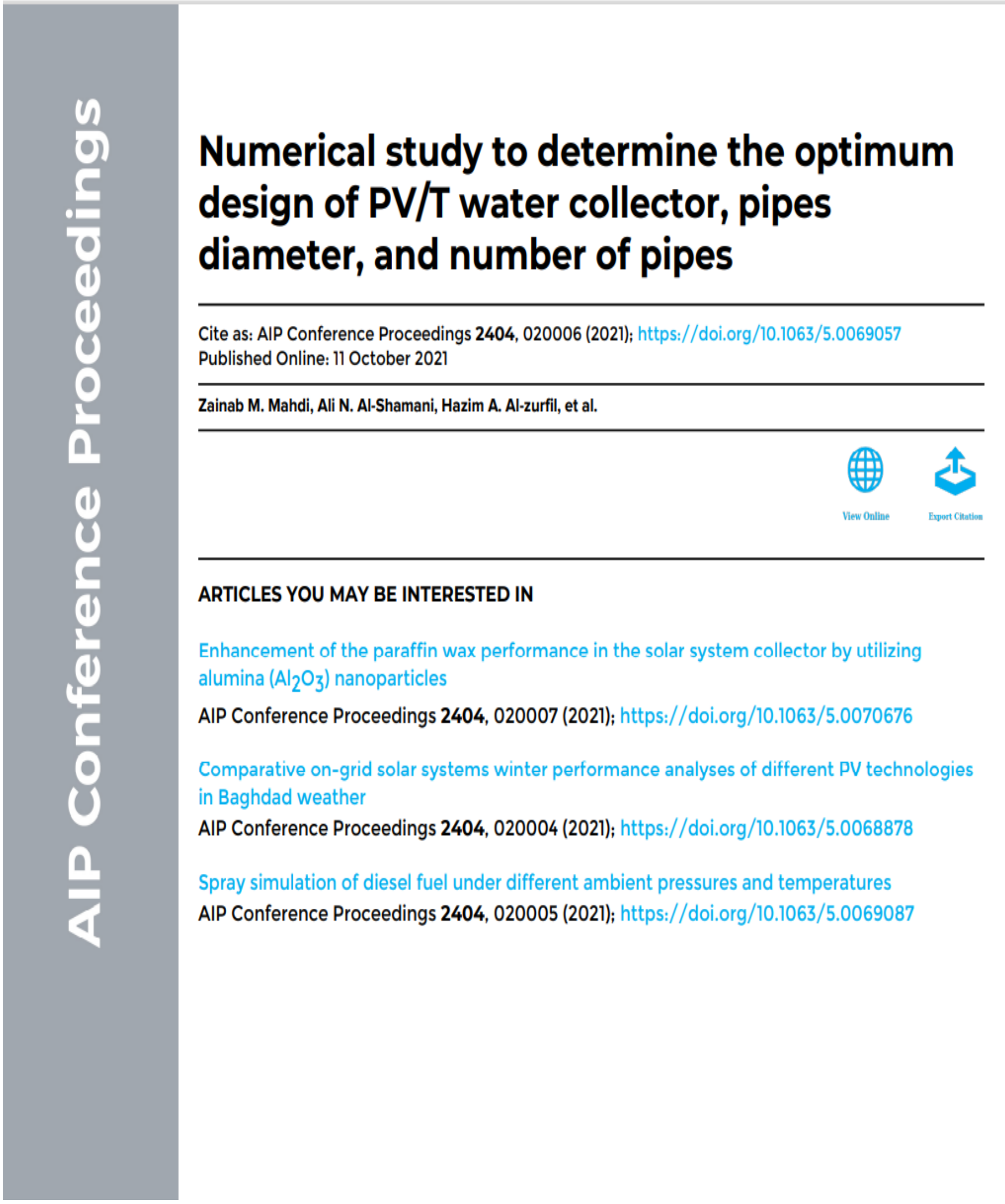

AIP Conference Proceedings

Numerical study to determine the optimum design of PV/T water collector, pipes diameter, and number of pipes

Cite as: AIP Conference Proceedings **2404**, 020006 (2021); https://doi.org/10.1063/5.0069057
Published Online: 11 October 2021

Zainab M. Mahdi, Ali N. Al-Shamani, Hazim A. Al-zurfil, et al.

View Online Export Citation

ARTICLES YOU MAY BE INTERESTED IN

Enhancement of the paraffin wax performance in the solar system collector by utilizing alumina (Al_2O_3) nanoparticles
AIP Conference Proceedings **2404**, 020007 (2021); https://doi.org/10.1063/5.0070676

Comparative on-grid solar systems winter performance analyses of different PV technologies in Baghdad weather
AIP Conference Proceedings **2404**, 020004 (2021); https://doi.org/10.1063/5.0068878

Spray simulation of diesel fuel under different ambient pressures and temperatures
AIP Conference Proceedings **2404**, 020005 (2021); https://doi.org/10.1063/5.0069087

2- Zainab M .Mahdi, Ali Najah Al-Shamani, "**Technical Employed to Rise the PV Panels Efficiency a Review**":, (Renewable and Sustainable Energy Reviews - Journal Elsevier)- Clarivate (Thomson Reuters), Scopus Q1 - (accepted).

Technical Employed to Rise the PV Panels Efficiency a Review:

Zainab M .*Mahdi*[1], Ali Najah *alShamani* [2]

[1]Affiliation1(Al-Furat Al-Awsat Technical University, Technical engineering collage/Najaf,Mechanical engineering techniques of power , 31001, Iraq. zainab.mahdi@atu.edu.iq E-mail: (10 pt)

[2] Al - Furat Al- Awsat Technical University, 31001, Iraq. ali.alshamani@yahoo.com

[*]Corresponding author E-mail: (10 pt).

Abstract

Combination sun photovoltaic energy with sun heat energy in the same system define as hybrid photovoltaic-thermal (PVT) system, this model product not only electricity but also capable to product thermal energy ,It reduces manufacturing cost, It occupies a little space , lowers the temperature of the PV and this contributes to rise its efficiency, Any rise in the PV temperature leads to a lower in the PV conversation efficiency from solar energy to electrical energy for this reason, researchers have come to find ways to cool them, Water and air play the main factors in PV cooling as heat extracting medium, uniting solar air collector with PV panel define as PV/T with air passed system, and uniting solar water collector with

3- Zainab M.Mahdi1, a) . Ali N. Al-Shamani2,b). Hazim A. Al-zurfi13,c).K.Sopian4,d) "**Exergy and Energy Analysis for Photovoltaic Thermal PV/T Combine System with many Additive , PCM , Porous Media, and MWCNT-nanofluid**". (submitted).

EXergy and Energy Analysis for Photovoltaic Thermal PV/T Combine System with many Additive , PCM , Porous Media, and MWCNT-nanofluid.

Zainab M.Mahdi[1, a)] . Ali N. Al-Shamani[2,b)]. Hazim A. Al-zurfi1[3,c)].K.Sopian[4,d)].

Al-Furat Al-Awsat Technical University, Technical engineering collage/Najaf,Mechanical engineering techniques of power , 31001, Iraq.

[2] Al - Furat Al- Awsat Technical University, 31001, Iraq

[3]Al-Najaf Technical Institute, Al-Furat Al-Awsat Technical University, Al-Najaf, Iraq.

[4]Solar Energy Research Institute (SERI), University Kebangsaan Malaysia, 43600 Bangi, Selangor, Malaysia

[a)] corresponding author: zainab.mahdi@atu.edu.iq

[b)] alshamani@atu.edu.iq

[c)] hazim.alzurfi@gmail.com

ABSTRACT

This paper presents an enhancement structure of a photovoltaic-thermal (PV/T) solar collector merged a PV panel with a sheet and tube water thermal collector and a double pass single duct air channel as the air thermal collector with a lot of additives PCM, Porous Media and MWCNT-nanofluid. In addition to the electrical power generated, this sort of collector allows both hot air and water to be produced and increasing the overall efficiency per unit area compared to the traditional PV/T separate systems. The use of both fluids (combine) allows for a larger range of thermal applications and allows for the use of hot air or water depending on energy demands and purposes. The electrical and thermal performance in additional to exergy and energy analysis of the PV/T Combine System was investigated under tow mode of fluid flow air and water and air and MWCNT-nanofluid . From the experimental result the average daily reduction in PV panel surface temperature was 22℃ and 28℃ and the average daily improvement in electrical efficiency, total thermal efficiency achieved and overall efficiency was 12.8% ,43.16% ,79.9% and 16.488% ,56.25%, 93.644% respectively, for PV/T combine system with water and air and PV/T combine system with MWCN-nanofluid and air as a cooling fluid. the total thermal energy gained reached and the average daily exergy

الخلاصة

ينتج النظام الكهروضوئي الحراري المزدوجPV/T combine system الطاقة الكهربائية بالإضافة الى الطاقه الحراريه على شكل هواء وماء ساخن .حيث تهدف هذه الدراسه الى الجمع بين الالواح الشمسية الكهروضوئيه PV panel ونوعين من المجمعات الشمسيه الحراريه للهواء والماء اللذان يعملان على سحب اكبر كميه من الطاقه الحراريه وخفض درجة حرارة اللوح PV وهذا يؤدي الى زيادة انتاجيته الكهربائية مع وجود العديد من الاضافات مثل المواد متغيرة الطور , والاوساط المساميه والسوائل النانويه حيث تم استخدام جزيئات الكاربون النانويه MWCNT بتركيز 1%. تم بناء العمل التجريبي في الكلية التقنية الهندسية بالنجف ، جامعة الفرات الأوسط التقنية ، العراق. جغرافياً ، تم إجراء التجارب على النظام الكهروضوئي الحراري المزدوجPV/T combine system في ظل الظروف الجوية في النجف (32 درجة شمالاً / 44 درجة شرقاً) لأيام محدد من شهر يونيو ويوليو من الساعة 7 صباحًا حتى 8 مساءً ، وتم أخذ القراءات وتسجيلها كل 15 دقيقة . تم اختبار اداء النظام تحت وضعين من تدفق الهواء مع الماء والهواء مع MWCNT-nanofluid مع PV panel التقليدية دون أي نظام تبريد تحت معدل تدفق كتلة مختلف للهواء من 0.02 كجم / ثانية إلى 0.05 كجم / ثانية ومن 0.01 كجم / ثانية إلى 0.08 كجم / ثانية لكل من الماء والسوائل النانوية MWCNT.تم اختبارانابيب نحاسيه بثلاث اقطارمختلفه (8,10,12)mm بترتيب مختلف لعدد الانابيب اسفل PV panel يبدأ من 8 الى 16انبوب للحصول على افضل تصميم للمجمع الحراري للتبريد بالماء ,ولتحقيق الحسابات العدديه تم استخدام برنامج Comsol Multiphysics لحساب حركة السوائل, الدراسة العدديه تم اجرائها للحصول على افضل تصميم من بين التصاميم المقترحة .الخطوات العملية لتصميم الجهاز تم اجراءها بعد الحصول على افضل تصميم من حيث القطر الداخلي للانابيب وعدد الأنابيب النحاسيه للتصميم بعد الحصول عليها من النتائج العدديه , كل تصميم يتكون من لوح من مادة النحاس يتم توزيع الانابيب النحاسيه اسفل منها التي يتم تدوير الماء داخل النظام من خلالها والتي يتم وضعها لاحقا اسفل PV panel بواسطة الضغط عليها لضمان حصول التبادل الحراري .تم استخدم شمع البرافين كماده متغيرة الطور حيث تم وضعها داخل حوض يحيط بالأنابيب النحاسية.تم استخدام مجمع حراري هوائي من نوع ثنائي المسار, حيث يدخل الهواء من القناة العلوية التي تقع بين السطح العلوي PV panel والغطاء الزجاجي ويتم خروجه من القناة السفلية التي تقع اسفل حوض الشمع والذي تم ملئه بالمواد المساميه (steel wool) . حيث اثبتت التجارب العملية ان استخدام السائل الناوي-MWCNT مع الهواء كسوائل للتبريد يظهر تحسين عالي بمقدار الكفائه الكهربائية عن استخدام الماء والهواء وعن

PV panel بدون سوائل تبريد ,بلغ مقدار الزيادة بالكفائه الكهربائية %21.667. للنظام الكهروضوئي المزدوج الذي يتم تبريده بالماء والهواء حيث تم تخفيض درجة حرارة السطح السفلي للوح من 83.9 الى 53.5 ادى الى زيادة الكفائه الكهربائية من 10.747% الى% 13.076للنظام الكهروضوئي الحراري المزدوج عند تبريده بالهواء والماء بالمقارنة باللوح الكهروضوئيه بدون تبريد .بينما بلغ معدل الزيادة بالكفائه الكهربائية 23.529% حيث تم تخفيض درجه الحرارة من 87°Cالى49.3°Cادى الى زيادة الكفائه الكهربائية من 10.815% الى 13.359% للنظام الكهروضوئي الحراري المزدوج الذي تم تبريده بالسائل النانوي MWCN والهواء عند مقارنته باللوح الكهروضوئي بدون تبريد .ايضا, التجارب العملية اظهرت تحسين عالي بالأداء الحراري عند استخدام السائل النانوي MWCNT– والهواء عن استخدام الماء والهواء كموائع للتبريد مع النظام الكهروضوئي الحراري المزدوج .حيث كل من الطاقه الحراريه المتولدة , الكفائه الحراريه الكلية , الطاقه المكافئه الكليه, وكفائه الأكسيرجي للنظام الكهروضوئي المزدوج الذي تم تبريده بالسائل النانوي-MWCNT والهواء كسوائل للتبريد بلغت W 92.883%,302.728 ,14.685%,56.579% ,وبلغت 255.403W ,49.475%,14.492%,82.966%للنظام الكهروضوئي الحراري المزدوج الذي تم تبريد بالهواء والماء. بسبب وجود مواد متغيرة الطورPCM استمر الفرق في درجة الحرارة لمدة ساعة بعد غروب الشمس لكل من الهواء والماء الخارج من النظام.

وزارة التعليم العالي والبحث العلمي

جامعة الفرات الاوسط التقنية

الكلية التقنية الهندسية / النجف

تحليل الطاقة والاداء لمجمع حراري كهروضوئي مزدوج (PV/T) مع مادة متغيرة الطور، سائل نانوي و وسط مسامي

رسالة مقدمة الى

قسم هندسة تقنيات ميكانيك القوى في الكلية التقنية الهندسية - النجف / جامعة الفرات الأوسط التقنية كجزء من متطلبات نيل شهادة الماجستير التقني في هندسة تقنيات الميكانيك

من

زينب محمد مهدي

بكالوريوس هندسة تقنيات ميكانيك القوى

2016

اشراف

الأستاذ المساعد الدكتور

علي نجاح كاظم

2022